FLÁVIA CAROLINE TORRES RODRIGUES

PHYSIOLOGICAL, BIOCHEMICAL, AND MOLECULAR ASPECTS OF SOYBEAN RESISTANCE AGAINST *Phakopsora pachyrhizi* INFECTION POTENTIATED BY SOME INDUCED RESISTANCE STIMULI

Thesis submitted to the Graduate Program in Plant Pathology of the Universidade Federal de Viçosa in partial fulfilment of the requirements for the degree of *Doctor Scientiae*.

Advisor: Fabrício de Ávila Rodrigues

VIÇOSA - MINAS GERAIS
2022

Ficha catalográfica elaborada pela Biblioteca Central da Universidade Federal de Viçosa - Campus Viçosa

T

R696p
2022

Rodrigues, Flávia Caroline Torres, 1992-
Physiological, biochemical, and molecular aspects of soybean resistance against *Phakopsora pachyrhizi* infection potentiated by some induced resistance stimuli / Flávia Caroline Torres Rodrigues. - Viçosa, MG, 2022.
1 dissertação (133 f.): il. (algumas color.).

Texto em inglês.
Orientador: Fabrício de Ávila Rodrigues.
Tese (doutorado) - Universidade Federal de Viçosa, Departamento de Fitopatologia, 2022.
Inclui bibliografia.
DOI: https://doi.org/10.47328/ufvbbt.2022.352
Modo de acesso: World Wide Web.

1. *Glycine max*. 2. Soja - Resistência a doenças e pragas. 3. Fotossíntese. 4. Ferrugem-da-soja. 5. Oxigênio - Efeito fisiológico. I. Rodrigues, Fabrício de Ávila, 1974-. II. Universidade Federal de Viçosa. Departamento de Fitopatologia. Programa de Pós-Graduação em Fitopatologia. III. Título.

CDD 22. ed. 633.3494

Bibliotecário(a) responsável: Alice Regina Pinto CRB6 2523

FLÁVIA CAROLINE TORRES RODRIGUES

PHYSIOLOGICAL, BIOCHEMICAL, AND MOLECULAR ASPECTS OF SOYBEAN RESISTANCE AGAINST *Phakopsora pachyrhizi* INFECTION POTENTIATED BY SOME INDUCED RESISTANCE STIMULI

Thesis submitted to the Graduate Program in Plant Pathology of the Universidade Federal de Viçosa in partial fulfilment of the requirements for the degree of *Doctor Scientiae*.

APPROVED: May 16, 2022

Assent:

Flávia Caroline Torres Rodrigues
Author

Fabrício de Ávila Rodrigues
Advisor

I dedicate it to my mother and grandmother, Luzia Torres Nascimento and Aurelina Xavier Torres Nascimento, for the love and unconditional support in all stages of my life.

ACKNOWLEDGMENTS

First of all, I thank God for the blessings and opportunities.

I want to express my sincere thanks to:

My mother Luzia Torres Nascimento and my grandmother Aurelina Xavier Torres Nascimento for their support, trust, love, words of encouragement, understanding, and all their efforts for the accomplishment of my professional life.

Professor Fabrício Ávila Rodrigues, a great professor and researcher, for his great guidance, support, and understanding.

My colleagues from the Laboratory of Host-Pathogen Interaction for their friendship, knowledge sharing, and contribution to this research.

All my friends that support me during this journey.

A special thanks to my friends: Valdeir, Marcela, Renata, Luisa, and Lillian for all the support, friendship, time, and experiences lived together for all those years in Viçosa.

The Women in Plant Pathology Group.

UFV employees, especially Mr. Mário, Mr. Bruno, and Mrs. Sara.

Thanks are due to Universidade Federal de Viçosa (UFV), Department of Plant Pathology, Laboratory of Host-Pathogen Interaction, and the Postgraduate Program in Plant Pathology for providing me with all the necessary conditions for my study and to the development of this research.

This study was financed in part by the Coordenação de Aperfeiçoamento de Pessoal de Nível Superior – Brasil (CAPES) – Finance Code 001.

The Coordenação de Aperfeiçoamento de Pessoal de Nível Superior (CAPES), to granting the scholarship.

BIOGRAPHY

FLÁVIA CAROLINE TORRES RODRIGUES, daughter of Luzia Torres Nascimento and Osvaldo Rodrigues da Silva, was born on July 17, 1992, in Januária, Minas Gerais, Brazil. In March 2016, she graduated from Instituto Federal do Norte de Minas Gerais with a Bachelor in Agronomy. In February 2018, she obtained the *Master Scientiae* in Plant Pathology at Universidade Federal de Viçosa (UFV). In March 2018, she started the doctoral degree in the Plant Pathology Program at UFV under the guidance of Professor Fabrício Ávila Rodrigues defending her Thesis on May, 2022

ABSTRACT

RODRIGUES, Flávia Caroline Torres, D.Sc., Universidade Federal de Viçosa, May, 2022. **Physiological, biochemical, and molecular aspects of soybean resistance against *Phakopsora pachyrhizi* infection potentiated by some induced resistance stimuli.** Adviser: Fabrício de Ávila Rodrigues.

Asian soybean rust (ASR), caused by *Phakopsora pachyrhizi*, is a destructive disease affecting soybean production and has been controlled mainly by using different fungicide molecules. The finding of new environmentally-friendly control strategies to minimize fungicide sprays must be prioritized. In this scenario, induced resistance using an array of abiotic or biotic inducers of resistance becomes a very promising alternative. The study investigated the potential of using azelaic acid (AzA), hexanoic acid (HxA) and Mantus® (copper (20%) and polyphenolic (10%)) to reduce SR symptoms by boosting defense responses. In the first study, the factors studied were plants sprayed with water (control), acibenzolar-S-methyl (ASM), AzA or HxA that were non-inoculated or inoculated with *P. pachyrhizi*. Both AzA and Hxa significantly inhibited urediniospores germination *in vitro*. The area under disease progress curve significantly decreased by 95, 93, 92, 82, and 92% for ASM, HxA 5 mM, HxA 20 mM, AzA 0.1 mM, and AzA 1 mM, respectively, compared to control treatment. Hyphae of *P. pachyrhizi* colonized less abundantly the leaflet tissues of plants sprayed with ASM, HxA (20 mM), and AzA (1 mM) in comparison to water-sprayed plants. Infected and AzA and HxA-sprayed plants showed less impairment on their photosynthesis and a more robust antioxidative metabolism in contrast to infected and water-sprayed plants. In general, host genes associated with general defense as well as with systemic acquired resistance or induced systemic resistance were strongly up-regulated for infected plants sprayed with AzA, ASM and HxA in comparison to water-sprayed plants. Interestingly, most of the genes were expressed earlier for infected and HxA-sprayed plants than for infected and AzA-sprayed plants, and more expressively in comparison to infected and ASM-sprayed plants. In the second study, the factors studied were plants sprayed with water or Mantus® (referred to as induced resistance (IR) stimulus thereafter) that were non-inoculated or inoculated with *P. pachyrhizi*. Urediniospores germination was reduced by 97% by the IR stimulus *in vitro*. The SR severity and area under disease progress curve decreased by 68 and 35%, respectively, for IR stimulus-sprayed plants compared to water-sprayed plants. Defense-related genes were up-regulated for IR stimulus-sprayed plants compared to water-sprayed plants during the infection process of *P. pachyrhizi*. Infected and IR stimulus-sprayed plants showed less impairment in their photosynthesis and a more robust

antioxidative metabolism in contrast to infected and water-sprayed plants. The results reported here highlight the potential of using AzA and HxA and this IR stimulus for SR management considering its fungistatic effect against urediniospores and by priming soybean resistance more efficiently to cope against *P. pachyrhizi* infection.

Keywords: *Glycine max*. Disease management. Induced resistance. Plant defense mechanisms. Photosynthesis. Rust. Reactive oxygen species.

RESUMO

RODRIGUES, Flávia Caroline Torres, D.Sc., Universidade Federal de Viçosa, maio de 2022. **Aspectos fisiológicos, bioquímicos e moleculares da resistência da soja em resposta à infecção por Phakopsora pachyrhizi potencializada por indutores de resistência.** Orientador: Fabrício de Ávila Rodrigues.

A ferrugem asiática da soja (FAS), causada por *Phakopsora pachyrhizi*, é uma doença destrutiva que afeta a produção de soja e tem sido controlada principalmente pelo uso de diferentes moléculas fungicidas. Entretanto a busca por estratégias de controle mais sustentáveis deve ser priorizada. Nesse cenário, a indução de resistência usando indutores bióticos e abióticos é uma alternativa promissora. Esse estudo investigou o potencial do uso do ácido azeláico (AzA) e do ácido hexanóico (HxA) e Mantus® (cobre (20%) a polifenóis (10%)) em reduzir os sintomas da FS através da potencialização do seu sistema de defesa. No primeiro estudo, os fatores estudados foram plantas pulverizadas previamente (24h antes da inoculação) com água (controle), acibenzolar-S-methyl (ASM), AzA, ou HxA que foram inoculadas ou não com *P. pachyrhizi*. Aza e Hxa inibiram significativamente a germinação de urediniósporos *in vitro*. A área abaixo da curva de progresso da doença reduziu significativamente em 95, 93, 92, 82, e 92% para ASM, HxA 5 mM, HxA 20 mM, AzA 0.1 mM, and AzA 1 mM, respectivamente, comparado com o controle. Hifas de *P. pachyrhizi* colonizaram os folíolos de forma menos abundante em plantas pulverizadas com ASM, HxA (20 mM), e AzA (1 mM) em comparação com o controle. Plantas infectadas e pulverizadas com Aza e HxA mostraram menos danos na fotossíntese e um metabolismo antioxidativo mais robusto em comparação com plantas infectadas e pulverizadas com água. No geral, a expressão de genes associados com a defesa basal e com a resistência sistêmica adquirida aumentaram significativamente para as plantas infectadas e pulverizadas com AzA, ASM e HxA em comparação com as plantas pulverizadas com água. A maioria dos genes foi expressa mais cedo para as plantas infectadas e pulverizadas com HxA do que para as plantas infectadas e pulverizadas com AzA, e de forma mais expressiva em comparação com as plantas infectadas e pulverizadas com ASM. No segundo experimento, os fatores estudados foram plantas pulverizadas com água ou Mantus® (referido como estímulo de indução de resistência - IR), que foram inoculadas ou não com *P. pachyrhizi*. Germinação de urediniósporos foi reduzida em 97% pelo estímulo IR *in vitro*. A severidade e a área abaixo da curva de progresso da doença foram reduzidas em 68 e 35% respectivamente, para o estímulo IR comparado com o controle. A expressão de genes relacionados a defesa aumentou significativamente quando comparado ao controle durante o

processo de infecção de *P. pachyrhizi*. Plantas infectadas e pulverizadas com estímulo IR mostraram menos dano na fotossíntese e um metabolismo antioxidativo mais robusto em comparação ao controle. Esses resultados mostram o potencial do uso do AzA, HxA e do Mantus® no manejo da FS considerando o seu efeito fungicida e seu efeito priming, tornando a planta de soja mais eficiente para resistir a infecção.

Palavras-chave: *Glycine max*. Manejo de doenças. Resistência induzida. Mecanismo de defesa das plantas. Fotossíntese. Ferrugem. Espécies reativas de oxigênio

SUMMARY

CHAPTER I

INDUCTION OF RESISTANCE IN SOYBEAN AGAINST *Phakopsora pachyrhizi* INFECTION BY AZELAIC AND HEXANOIC ACIDS

Abstract

Asian soybean rust (ASR), caused by *Phakopsora pachyrhizi*, has mainly been controlled using different fungicide molecules. This non-eco-friendly strategy pinpoints the use of inducers of resistance as a very promising alternative to reduce fungicides spraying. This study investigated the potential of using azelaic acid (AzA) and hexanoic acid (HxA) to reduce ASR symptoms by boosting defense responses. A 4 × 2 factorial experiment was arranged in a completely randomized design with four replications per sampling time. The factors studied were plants sprayed with water (control), acibenzolar-S-methyl (ASM), AzA, or HxA that were non-inoculated or inoculated with *P. pachyrhizi*. Both AzA and HxA significantly inhibited urediniospores germination *in vitro*. The area under disease progress curve significantly decreased by 95, 93, 92, 82, and 92% for ASM, HxA 5 mM, HxA 20 mM, AzA 0.1 mM, and AzA 1 mM, respectively, compared to control treatment. Hyphae of *P. pachyrhizi* colonized the leaflet tissues of plants sprayed with ASM, HxA (20 mM), and AzA (1 mM) less abundantly in comparison to water-sprayed plants. Infected and AzA and HxA-sprayed plants showed less impairment on photosynthesis (moderate changes in chlorophyll *a* fluorescence parameters and great concentrations of total chlorophyll *a*+*b* and carotenoids) and a more robust antioxidative metabolism (great activities of superoxide dismutase, ascorbate peroxidase, catalase, peroxidase, and glutathione reductase resulting in reduced deposition of hydrogen peroxide and anion superoxide and less concentration of anion superoxide) in contrast to infected and water-sprayed plants. In general, host genes associated with host defense responses were strongly up-regulated for infected plants sprayed with AzA (*PAL1.1*, *PAL1.3*, *PR1-A*, *PR10*, *MMP2*, *CHIB1*, *ACS*, *NAC19*, and *URE*) ASM (*PAL2.1*, *URE*, *ETR1*, *MMP2*, *ACS*, *SABATH2*, and *NAC19*) and HxA (*PAL1.1*, *PAL2.1*, *PAL3.1*, *PR1-A*, *SABATH2*, *JAR1*, *PR10*, *MMP2*, *NAC19*, *URE*, *ICS2*, *CHIB1*, *ETR1*, and *OPR3*) in comparison to water-sprayed plants. Most of these genes were expressed earlier for infected and HxA-sprayed plants than for infected and AzA-sprayed plants, and more expressively than infected and ASM-sprayed plants (*PAL2.1*, *URE*,

ETR1, *MMP2*, *ACS*, *SABATH2*, and *NAC19*). Collectively, the physiological, biochemical, and molecular responses obtained for infected and AzA and HxA-sprayed plants were comparable to that obtained with ASM, a well-known inducer of resistance. In short, this study provides a global picture of the potential of using AzA and HxA for ASR management considering their fungicide effect and the capacity to prime soybean plants towards a more efficient defense to cope against *P. pachyrhizi* infection.

Keywords: *Glycine max*. Antioxidant enzymes. Induced systemic resistance. Photosynthesis. Reactive oxygen species. Systemic acquired resistance.

Introduction

Among the cash crops grown worldwide, soybean (*Glycine max* (L.) Merril) stands out as one of the most important considering the remarkable contents of protein and oil used for human consumption, livestock, and biodiesel (Hymowith, 2008; Singh, 2010). Epidemics of soybean rust, caused by the biotrophic fungus *Phakopsora pachyrhizi* H. Sydow & P. Sydow, have dramatically threatened soybean production (Hartman et al., 2011; Pagano and Miransari, 2016). As a result of high levels of soybean rust severity, plants show reduced growth, intense defoliation, and impairment of their photosynthetic machinery that culminates in significant yield losses (Goellner et al., 2010; Li et al., 2010; Rios et al., 2018). Although some cultural practices (*e.g.*, the use of early-maturing cultivars, the anticipation of sowing dates, early detection of disease symptoms and pathogen signs, and fulfilling a period without growing soybean in the off-season to avoid early inoculum production) have been used by the farmers to manage soybean rust, they still rely on the abundant spraying of fungicide to minimize yield losses (Langenbach et al., 2016; Kashiwa et al., 2020). The reduced efficacy of most fungicide molecules available for soybean rust control owing to the arising of *P. pachyrhizi* populations resistant to them (Scherm et al., 2009; Klosowski et al., 2018) supports research for more sustainable agricultural practices. The efficacy of different resistance inducers to activate (*e.g.*, eliciting or priming) the defense mechanisms of plants from pathogen attack (Kesel et al., 2021; Vlot et al., 2021; Zeier, 2021) place them as an environmentally-friendly alternative for soybean rust management.

Plants use multiple facets of defense mechanisms (*e.g.*, physical or biochemical strategies that can be constitutive or induced) to defend themselves against infection by pathogens of different lifestyles as efficiently as possible in terms of speed, duration, and intensity (Kaur et al., 2022). Interestingly, the basal level of resistance of plants from highly productive cultivars, but susceptible to major diseases, can be raised by using resistance inducers (Lyon, 2007; Reignault and Walters, 2007; Siah, 2018). In this regard, the well-studied phenomena of

systemic acquired resistance (SAR) and induced systemic resistance (ISR) take place to hamper pathogen infection (Pieterse et al., 2012; Vlot et al., 2021; Zeier, 2021). Several studies have demonstrated that the innate immune system of plants exhibiting SAR, signaled by salicylic acid (SA), is rapidly boosted and becomes more efficient against infection mainly by biotrophic and hemibiotrophic pathogens (Pieterse et al., 2012; Kesel et al., 2021; Vlot et al., 2021; Zeier, 2021). On the other hand, plants exposed to nonpathogenic microorganisms or some resistance inducers are prone to develop ISR signaled by jasmonic acid (JA) and ethylene (ET) to cope against infection by necrotrophic pathogens (Pieterse et al., 2012; Vlot et al., 2021). The cross-talk between the signaling pathways mediated by SA or JA/ET can overlap or be interconnected synergistically or antagonistically for a prompt activation of host defense reactions against pathogen infection (Pieterse et al., 2012; Kesel et al., 2021).

The C18 fatty acids are non-enzymatic and enzymatically cleaved (*e.g.*, oleic acid (18:1) or their unsaturated derivatives, linoleic acid (18:2) and linolenic acid (18:3)) to produce azelaic acid (AzA), a C9 dicarboxylic acid that is found in the endoplasmic reticulum, plasm membrane, plasmodesmata, plastid envelopes, and possibly thylakoid membranes of plants exposed to biotic stress (Zoeller et al., 2012; Yu et al., 2013; Shah and Zeier, 2013). Yu et al. (2013) demonstrated an intricate feedback regulatory loop among phosphorylated sugar derivative glycerol-3-phosphate (G3P) and two lipid transfer proteins known as defective in induced resistance 1 (*DIR1*) and azelaic acid induced 1 (*AZI1*) for the establishment of SAR and that AzA functions upstream of G3P in this pathway. According to the authors, the free unsaturated fatty acids released in plant tissues infected by pathogens are important sources of AzA precursors and after increasing in concentration acts increasing the levels of G3P and work together for a prompt SAR establishment.

Interestingly, the levels of AzA in plant tissues may be raised through lipid peroxidation due to the action of lipoxygenases, hydroperoxide lyase, and reactive oxygen species as well as

non-enzymatic galactolipids (Aranega-Bou et al., 2014; Singh et al., 2017). Many plant species exogenously exposed to AzA, which become mobile in the phloem, are primed for SA signaling pathway (*e.g.*, favoring glycerol-3-phosphate biosynthesis to modulate primary and secondary metabolic pathways that can be involved in host defense reactions) with the involvement of G3P biosynthesis for an efficient response against infection caused by a plethora of pathogens (Chanda et al., 2008; Jung et al., 2009; Aranega-Bou et al., 2014; Camañes et al. 2015; Cecchini et al., 2015, 2019; Singh et al., 2017; Adam et al., 2018).

An increasing body of evidence suggests that hexanoic acid (HxA), a short-chain monocarboxylic acid derived from hexane, is also able to reduce the symptoms of many diseases affecting different plant species by boosting defense response mainly by inducing callose deposition, increasing the pool of phenolics (*e.g.*, caffeic acid and chlorogenic acids), priming both SA and JA signaling pathways, and promoting a more robust antioxidative metabolism (Flors et al., 2003; Leyva et al., 2008; Vicedo et al., 2009; Kravchuk et al., 2011; Aranega-Bou et al., 2014; Finiti et al., 2014; Llorens et al., 2015a,b; Fernández-Crespo et al., 2017; Caccalano et al., 2021).

Taking into consideration the economic importance of soybean and the potential of Asian soybean rust to reduce yield, the present study hypothesized that HxA and AzA could potentiate defense reactions along with fine adjustments in the photosynthetic performance and a more robust antioxidative metabolism to cope with *P. pachyrhizi* infection. It is expected that the use of these resistance inducers could become a promising alternative to help farmers to face the demand of society for a more environmentally friendly global food production and security.

Material and Methods

In vitro assay

The sensitivity of urediniospores from *P. pachyrhizi* to AzA and HxA was evaluated *in vitro*. Melted water-agar (AA) medium was amended with different concentrations of AzA (0.1 and 1 mM L/AA medium) and HxA (5 and 20 mM L/AA medium) and a total of 20 mL was poured into each Petri dish. Petri dishes containing only AA medium served as the control treatment. A total of 100 µl of urediniospores suspension (10^5 urediniospores/mL) was transferred to the center of each Petri dish and homogeneously distributed using a Drigalski glass handle. The urediniospores were collected from soybean plants (cv. 'TMG 135') previously inoculated with the monouredinial isolate UFV-DFP *Pp*25. Petri dishes were transferred to a growth chamber (25°C and photoperiod of 12 h of light and 12 h of dark). After 24 h, a total of 5 µl of lactophenol was added to each dish to stop urediniospores germination. One hundred urediniospores were randomly examined in each Petri dish under a light microscope (Carl Zeiss AxioImager A1) at 40 × magnification. Urediniospore with germ tube larger than its diameter was considered germinated. The percentage of urediniospores germination was calculated for the replication of each treatment.

Plant growth

A total of six soybean seeds (cultivar TMG 135, susceptible to SR) (Einhardt et al., 2020), were sown in each plastic pot containing 2 kg of substrate (Tropstrato®, Vida Verde, Mogi Mirim, São Paulo, Brazil). After germination, a total of four seedlings were left per pot. Plants were fertilized with nutrient solution (80 mL per pot weekly) prepared according to Picanço et al. (2021). The nutrient solution was prepared using deionized water. Plants were grown in a greenhouse (temperature of 25 ± 3°C, relative humidity of 80 ± 5%, and natural photosynthetically active radiation) and watered when needed.

Application of AzA, HxA, and ASM

Plants at the V4 growth stage (≈ 30 days after seedling emergence) were sprayed (5 mL per plant) with solutions of AzA (0.1 and 1 mM), HxA (5 and 20 mM), and ASM (0.5 g L^{-1}; Bion® 500 WG Syngenta Crop Protection Inc., São Paulo, Brazil) using a VL Airbrush atomizer (Paasche Airbrush Co., Chicago, IL, USA). The AzA and HxA were purchased from Sigma-Aldrich, São Paulo, Brazil (catalog numbers 11480 and 153745, respectively). Solutions of AzA, HxA, and ASM were prepared using deionized water. Plants sprayed with deionized water served as the control treatment.

Plant inoculation with *P. pachyrhizi*

At 24 h after being sprayed with water, AzA, HxA, or ASM, plants were inoculated with a suspension of 10^5 urediniospores of *P. pachyrhizi* mL^{-1} prepared with gelatine (0.5% w/v) and Tween 80 (25 µl/L) by using a VL Airbrush atomizer. The urediniospores were collected from soybean plants (cv. 'TMG 135') previously inoculated with the monouredinial isolate UFV-DFP *Pp*25. After inoculation, plants were kept in a mist chamber at 25°C for 16 h under darkness. After this period, plants were transferred to a greenhouse (temperature of 25 ± 2°C, relative humidity of 75 ± 5%, and natural photosynthetically active radiation) until the end of the experiments. Plant non-inoculated with *P. pachyrhizi* were kept in a different greenhouse under the same environmental conditions.

Experimental design

For the *in vitro* assay, the experiment was arranged in a completely randomized design with five treatments (AzA (0.1 mM and 1 mM) and HxA (5 mM and 20 mM) at different rates, including the control) and ten replications. Each replication corresponded to one Petri dish. A 4 × 2 factorial experiment, consisting of plants sprayed with water (control), AzA (1mM), HxA (20mM), and ASM and non-inoculated or inoculated plants with *P. pachyrhizi*, was arranged

in a completely randomized design with four replications, per each sampling time (5, 10, 15 and 20 dai), to evaluate ASR severity and to obtain leaf samples to determine both Chl *a* fluorescence and photosynthetic pigments concentration. Leaf samples for biochemical and gene expression analysis were obtained from another 4 × 2 factorial experiment with the same factors described above arranged in a completely randomized design with four replications per sampling time. The experiments were repeated twice.

Evaluation of ASR severity

The ASR severity was evaluated in leaflets of second and third leaves of each plant per replication of each treatment (four replications, 16 plants, and 96 leaflets per experiment) at 5, 10, 15, and 20 days after inoculation (dai) using the diagrammatic scale proposed by Franceschi et al. (2020). The area under disease progress curve (AUDPC) for each leaflet per plant from the replications of each treatment was calculated using the trapezoidal integration of disease progress curves according to Shaner and Finney (1977). At 20 dai, the second and third leaves of each plant per replication of each treatment were collected, scanned at 600 dpi resolution, and the images were processed using the software QUANT (Fagundes-Nacarath et al., 2018) to obtain the values of ASR severity.

Light microscopy

A total of 30 leaflet fragments (≈ 25 mm^2) from the second leaf of each plant per replication of each treatment (four replications, 16 plants, and 48 leaflets per experiment) were collected at 15 hai. The fragments were processed for light microscopic observations following the procedures described by Araujo et al. (2015). Four blocks of resin (two leaflets fragments per block) were obtained for each treatment. Thirty-six longitudinal and transversal serial sections (4 μm thick), which were cut from each block using a Leica RM 2245 rotary microtome (Leica Microsystems Inc., Deerfield, IL, USA), were randomly divided and placed on three

glass slides and stained with 1% toluidine blue in 2% sodium borate buffer for 1 min. Images were digitally (Axio Cam HR; Carl Zeiss) obtained using a Carl Zeiss Axio Imager A1 microscope in the bright-field mode.

Imaging and quantification of chlorophyll (Chl) *a* fluorescence parameters

Images and parameters of Chl *a* fluorescence were obtained from leaflets of the second leaf of each plant per replication of each treatment (four replications,16 plants, and 16 leaves per experiment) at 5, 10, 15, and 20 dai and also from noninoculated plants at these same evaluation times using the Imaging-PAM fluorometer and the Imaging Win software MAXI version (Heinz Walz GmbH, Effeltrich Germany). Plants were adapted to darkness for 30 min and then placed individually in a support at a distance of 18.5 cm from the CCD ("charge-coupled device") camera to obtain images at the resolution of 640 × 480 pixels. The leaflets were exposed to a light pulse intensity of 0.5 μmol m^{-2} s^{-1}, 100 μs, 1 Hz to obtain the initial fluorescence (F_0). Next, a saturating white light pulse of 2,400 μmol m^{-2} s^{-1} (10 Hz) was emitted for 0.8 s to determine the maximum fluorescence emission (F_m). Based on these initial measurements, the maximum PS II photochemical efficiency of dark-adapted leaflets was estimated through the variable-to-maximum Chl *a* fluorescence ratio as follows: $F_v/F_m = [(F_m - F_0)/F_m)]$. Next, the leaflets were exposed to actinic photon irradiance (100 μmol m^{-2} s^{-1}) for 300 s to obtain the steady-state fluorescence yield (F_s), after which a saturating white light pulse (2,400 μmol m^{-2} s^{-1}; 0.8 s) was applied to achieve the light-adapted maximum fluorescence (F_m'). The light-adapted initial fluorescence (F_0') was estimated according to Oxborough and Baker (1997). Based on Kramer et al. (2004), the energy that was absorbed by the PS II for the following three yield components for dissipative processes was calculated as follows: the photochemical yield [$Y(II) = (F_m' - F_s)/F_m')$], the yield for dissipation by down-regulation [$Y(NPQ) = (F_s/F_m') - (F_s/F_m)$], and the yield for other non-photochemical (non-regulated) losses [$Y(NO) = F_s/F_m$]. The apparent electron transport rate was calculated as ETR = Y(II) × PPFD

× f × α according to Baker (2008). The parameters of Chl *a* fluorescence were determined on each leaflet (area of ≈ 0.5 cm^2) by selecting the circular option on the Imaging Win software.

Determining photosynthetic pigments concentration

Five leaf discs (1 cm^2 each) obtained from leaflets of the second leaves used for imaging and quantification of Chl *a* fluorescence parameters were immersed in glass tubes containing 5 ml of saturated dimethyl sulfoxide solution and calcium carbonate (5 g/L), kept in the dark at room temperature for 24 h, and the absorbance of the extracts was read at 480, 649, and 665 nm to determine the concentrations of Chl *a*, Chl *b*, and carotenoids according to Santos et al. (2008).

Histochemical detection of H_2O_2 and $O_2^{\bullet-}$

The leaflets of the second leaf of each plant per replication of each treatment (four replications, 8 plants, and 16 leaves per experiment) were collected at 15 dai. For H_2O_2 detection, 24 leaflets were randomly placed in glass vials containing 50 mL of a 3,3'-diaminobenzidine tetrahydrochloride (1 mg/mL) solution (Sigma-Aldrich, São Paulo, Brazil) and kept in the darkness at 25°C for 12 h. For $O_2^{\bullet-}$ detection, 24 leaflets were randomly placed in glass vials containing 50 mL of 0.1% solution of nitro blue tetrazolium solution (Sigma-Aldrich, São Paulo, Brazil) in 10 mM potassium phosphate buffer (pH 6.8) and infiltrated for 24 h. Leaflets were cleared in 80% of boiling aqueous ethanol solution for 60 min until brown and blue spots were noticed as an indication of H_2O_2 and $O_2^{\bullet-}$ depositions, respectively.

Biochemical assays and genes expression using quantitative real-time PCR

The second and third leaves of each plant per replication of each treatment (four replications, 16 plants, and 32 leaves per experiment) were collected at 5, 10, 15, and 20 dai

from both non-inoculated and inoculated plants. Leaf samples were kept in liquid nitrogen during sampling and then stored at -80ºC until further analysis.

Malondialdehyde (MDA) concentration: oxidative damage in leaflet tissue was estimated as the concentration of total 2-thiobarbituric acid (TBA) reactive substances and expressed as equivalents of MDA (Cakmak and Horst, 1991). A total of 0.1 g of leaflet tissues was ground into a fine powder using a vibration ball mill (Retsch, Haan, Germany) with liquid nitrogen and homogenized in 2 ml of 0.1% (w/v) trichloroacetic acid (TCA) solution in an ice bath. The homogenate was centrifuged at 12,000 *g* for 15 min at 4°C. After centrifugation, a total of 250 µl of the supernatant was reacted with 750 µl of TBA solution (0.5% in 20% TCA) for 60 min in a boiling water bath at 95°C. After this period, the reaction was stopped in an ice bath. The samples were centrifuged at 10,000 *g* for 10 min and the specific absorbance was determined at 532 nm. The non-specific absorbance was estimated at 600 nm and subtracted from the specific absorbance value. The extinction coefficient of 155 mM^{-1} cm^{-1} (Heath and Packer, 1968) was used to calculate MDA concentration.

Concentrations of H^2O^2 and $O^{2\bullet-}$: a total of 0.1 g of leaflet tissue was ground into a fine powder as described above and homogenized in 2 ml of 0.1% (w/v) of TCA. The homogenate was centrifuged at 12,000 *g* for 15 min at 4°C. The supernatant was added to a reaction mixture containing 10 mM potassium buffer (pH 7.0) and 1 M of iodide solution and incubated for 10 min. The H_2O_2 concentration was determined based on the oxidized product formed at 390 nm (Velikova et al., 2000). A standard curve of H_2O_2 (Sigma-Aldrich, São Paulo, Brazil) was used to determine H_2O_2 concentration. A total of 0.2 g of leaf tissues was ground as described above and homogenized in 2 ml of a solution containing 100 mM sodium phosphate buffer (pH 7.2) and 1 mM sodium diethyldithiocarbamate. The homogenate was centrifuged at 22,000 *g* for 20 min at 4°C and the supernatant was used to determine $O_2^{\bullet-}$ concentration according to Chaitanya and Naithani (1994).

Activities of antioxidant enzymes: a total of 0.2 g of leaflet tissues was ground into a fine powder as described above. The fine powder was homogenized in 2 ml of a solution containing 50 mM of potassium phosphate buffer (pH 6.8), 0.1 mM EDTA, 1 mM phenylmethylsulfonyl fluoride (PMSF), and 2% (w/v) polyvinylpyrrolidone (PVP), centrifuged at 12,000 *g* for 15 min at 4°C, and the supernatant was used as the crude enzyme extract to determine ascorbate peroxidase (APX) (EC 1.11.1.11), catalase (CAT) (EC 1.11.1.6), peroxidase (POX) (EC 1.11.1.7), superoxide dismutase (SOD) (EC 1.15.1.1), and glutathione reductase (GR) (EC 1.8.1.7) activities. The SOD activity was determined by measuring its ability to photochemically reduce nitroblue tetrazolium (NBT) as described by Beauchamp and Fridovich (1971). The reaction was initiated by adding the crude enzyme extract to a mixture containing 50 mM potassium phosphate buffer (pH 7.8), 14 mM methionine, 75 μM NBT, 0.1 mM EDTA, and 2 μM riboflavin. Samples were light-exposed for 7 min, and the production of formazan blue, resulting from the photoreduction of NBT, was measured at 560 nm with a spectrophotometer (Giannopolitis and Ries, 1977). Samples kept in the dark for 7 min served as a blank. One unit of SOD was defined as the amount of enzyme necessary to inhibit NBT photoreduction by 50%. The CAT activity was determined by adding the crude enzyme extract to a reaction mixture containing 50 mM potassium phosphate buffer (pH 7.0) and 20 mM H_2O_2. The determination of CAT activity was based on the rate of H_2O_2 decomposition measured in the spectrophotometer at 240 nm for 1 min at 25°C (Cakmak and Marschner, 1992). An extinction coefficient of 36 M^{-1} cm^{-1} was used to calculate CAT activity (Anderson et al., 1995). The POX activity was assayed by determining the pyrogallol oxidation as proposed by Kar and Mishra (1976). The reaction was started after the addition of the crude enzyme extract to a reaction mixture containing 25 mM potassium phosphate (pH 6.8), 20 mM pyrogallol, and 20 mM H_2O_2. The POX activity was determined by the absorbance of colored purpurogallin recorded for 1 min at 420 nm at 25°C. The extinction coefficient of 2.47 mM^{-1} cm^{-1} (Chance

and Maehley, 1955) was used to calculate POX activity. The APX activity assay followed that described by Nakano and Asada (1981). The crude enzyme extract was added to a mixture containing 50 mM phosphate buffer (pH 7.0), 0.5 mM ascorbic acid, and 0.1 mM H_2O_2. The rate of ascorbate oxidation was measured by recording the absorbance at 290 nm for 1 min. The extinction coefficient of 2.8 mM^{-1} cm^{-1} (Nakano and Asada, 1981) was used to calculate APX activity. In order to determine GR activity, the reaction was started after the addition of the crude enzyme extract to a mixture containing 50 mM potassium phosphate (pH 7.8), 1 mM oxidized glutathione (GSSG), and 0.75 mM NADPH prepared in 0.5 mM Tris-HCl buffer (pH 7.5) according to Carlberg and Mannervik (1985). The decrease in absorbance was determined at 340 nm for 1 min at 30°C. The extinction coefficient of 6.22 mM^{-1} cm^{-1} was used to calculate GR activity (Foyer and Halliwell, 1976). The activities of these enzymes were expressed in a protein-basis whose concentration was determined according to Bradford (1976).

Activities of defense-related enzymes: a total of 0.2 g of leaflet tissue was ground into a fine powder as described above. The fine powder was homogenized in 2 ml of a solution containing 50 mM potassium phosphate buffer (pH 6.8), 1 mM EDTA, 1 mM PMSF, and 2% (w/v) PVP, centrifuged at 12,000 *g* for 15 min at 4°C, and the supernatant was used to determine chitinase (CHI) (EC 3.2.1.14), *β*-1,3-glucanase (GLU) (EC 3.2.1.39), phenylalanine ammonia-lyase (PAL) (EC 4.3.1.5), polyphenoloxidase (PPO), and lipoxygenase (LOX) (EC 1.13.11.12) activities. The CHI activity was determined by adding the crude enzyme extract to a reaction mixture containing 50 mM sodium acetate buffer (pH 5.0) and 0.1 mM *p*-nitrophenyl-β-*D*-*N*-*N*′-diacetylchitobiose (Harman et al., 1993). The reaction mixture was incubated in a water bath at 37°C for 2 h and the reaction was terminated by the addition of 0.2 M sodium carbonate. For the control samples, the sodium carbonate was added soon after the addition of the crude enzyme extract to the reaction mixture. The absorbance of the product released by CHI was measured at 410 nm. The extinction coefficient of 7×10^3 mM^{-1} cm^{-1} was used to calculate CHI

activity. The GLU activity was determined after adding the crude enzyme extract to a reaction mixture containing 50 mM sodium acetate buffer (pH 5.0) and laminarin (1 mg/mL) (Lever, 1972). The reaction mixture was incubated in a water bath for 30 min at 45°C. Afterward, this mixture was added to a reaction mixture of dinitrosalicylic acid (DNS). This reaction mixture was then incubated in a water bath for 10 min at 90°C and then cooled in an ice bath until it reached 25°C. The absorbance was measured at 540 nm. A similar procedure was used for the control samples except that the first incubation was excluded. For PAL activity, the crude enzyme extract reacted with a reaction mixture containing 25 mM Tris-HCl buffer (pH 8.8) and 25 mM *L*-phenylalanine. The reaction mixture was incubated at 40°C for 3 h. For the control samples, the extract was replaced by the Tris-HCl buffer. The reaction was stopped by adding 6 N HCl. The absorbance of *trans*-cinnamic acid derivatives was recorded at 290 nm. The extinction coefficient of 100 M^{-1} cm^{-1} was used to calculate PAL activity (Guo et al., 2007). The PPO activity was determined using the same procedure as for POX, but H_2O_2 was omitted from the reaction mixture. The LOX activity was determined by adding the crude enzyme extract to a reaction mixture containing 50 mM sodium phosphate buffer (pH 6.5) and 50 μM sodium linoleate. The reaction mixture was incubated at 25°C, and the absorbance of the product released by LOX for 1 min was measured at 234 nm. The extinction coefficient of 25000 M^{-1} cm^{-1} was used to calculate LOX activity (Axelrod et al., 1981). These enzyme activities were expressed on a protein basis and protein concentration was determined according to Bradford (1976).

Concentrations of total soluble phenols (TSP) and lignin-thioglycolic acid (LTGA) derivatives: a total of 0.1 g of leaflet tissue was ground into a fine powder as described above. The fine powder was homogenized in 1 mL of 80% (v/v) methanol solution. The crude extract was shaken at 300 rpm at 25°C for 2 h and the mixture was centrifuged at 17,000 *g* for 30 min.

The TSP concentration was determined in the methanolic extract and the pellet was used to determine the LTGA derivatives concentration according to Tatagiba et al. (2014).

Genes expression: a total of 75 mg of leaflet tissue was ground into a fine powder as described above. The fine powder was used for RNA extraction using Trizol (Invitrogen®). Contamination by DNA was removed with RQ1 RNase-Free DNase (Promega). The quality and integrity of the RNA were verified by 1.2% agarose gel electrophoresis and the amount of RNA was measured in a Qubit fluorometer using Qubit RNA HS Assay Kit (Invitrogen, São Paulo, Brazil). Single-stranded cDNAs were synthesized by reverse transcription using 5 µg of total RNA with oligo(dT) primers in a final volume of 20 µL using the SuperScript First Strand Synthesis System for RT-PCR (Invitrogen®). The qRT-PCR was performed on a Bio-Rad CFX Real Time Thermal Cycler using SYBR Green PCR Master Mix according to the manufacturer's recommendations. All reactions were performed in duplicate and the relative expression values for each gene studied were calculated using the $2^{-\Delta\Delta Ct}$ method (Livak and Schmittgen, 2001). Expression analysis of genes encoding for phenylalanine ammonia-lyase (*PAL1.1*, *PAL1.3*, *PAL2.1*, and *PAL3.1*), pathogenesis-related protein 1 (*PR1-A*), pathogenesis-related protein 10 (*PR10*), metalloproteinase (*MMP2*), urease (*URE*), isochorismate synthase (*ICS1* and *ICS2*), chalcone isomerase (*CHIB1*), 1-aminocyclopropane-1-carboxylic acid oxidase (*ACO*), 1-aminocyclopropane-1-carboxylic acid synthase (*ACS*), ethylene receptor 1 (*ETR1*), salicylic acid methyltransferase (*SABATH2*), 12-oxophytodienoic acid reductase 3 (*OPR3*), jasmonic acid-amino synthetase (*JAR1*), and NAC transcriptional factor (*NAC19*) was performed using specific primer sequences (Table 1). Expression of *TEF-1α*, corresponding to the translation elongation factor 1α of *P. pachyrhizi*, was quantified to confirm fungal infection in leaflet tissues. The Ubiquitin-3 (*UBIQ*) and glyceraldehyde-3-phosphate dehydrogenase (*GAPDH*) genes were used as references for normalization according to Mortel et al. (2007).

Data analysis

Data from the variables and parameters evaluated from the repeated experiments were combined following the procedures described by Moore and Dixon (2015). Data from urediniospores germination was submitted to analysis of variance (ANOVA) and means were compared by Tukey test ($P \leq 0.05$). Data from genes expression was submitted to analysis of variance (ANOVA) and means for ASM, AzA, HxA treatments were compared to means from control by Dunett's test ($P \leq 0.05$). For other variables and parameters, data was subjected to ANOVA and means for control, AzA, HxA, and ASM treatments as well as non-inoculated and inoculated plants were compared by Tukey test ($P \leq 0.05$). Data was checked for normality and homogeneity of variance before ANOVA. Data from variables and parameters from control, AzA, HxA, and ASM treatments for non-inoculated and inoculated plants at 10 dai was used for principal components analysis. The Minitab Statistical software was used for the statistical analysis (Minitab, Inc., 2021).

Results

Analysis of variance

The factor products (P) was significant for severity, AUDPC, Y(II), Chl *a*+*b*, Car, MDA, SOD, POX, CAT, GR, PAL, *PAL1.1*, *PAL3.1*, and *URE*. The factor plant inoculation (PI) was significant for Y(II), Y(NPQ), Y(NO), ETR, Chl *a*+*b*, Car, MDA, H_2O_2, $O_2^{\bullet-}$, and for most of enzymes and genes evaluated. The interaction P × PI was significant for most of the variables and parameters evaluated (Table 2).

In vitro assay

Germination of *P. pachyrhizi* urediniospores was significantly reduced by 92 and 94% on WA medium amended with HxA at 5 and 20 mM, respectively (Fig. 1A), and by 91% on WA medium amended AzA at 1 mM (Fig. 1b) in comparison to the control treatment.

Symptoms, AUDPC, and severity of ASR and histopathology of *P. pachyrhizi* infection

On leaflets of water-sprayed plants, there were many necrotic lesions containing several uredinia (Fig. 2A) while on leaflets of plants from ASM, HxA (5 and 20 mM), and AzA (0.1 and 1 mM) treatments, lesions were much less developed (Fig. 2B-F). Hyphae of *P. pachyrhizi* colonized more abundantly the palisade and spongy parenchyma cells and caused intense tissues degradation in leaflet tissue of plants from control treatment (Fig. 2G, arrowheads) compared to leaflet tissues of plants from ASM, HxA (20 mM), and AzA (1 mM) treatments (Fig. 2H-J, arrowheads). Moreover, in leaflets of plants from control treatment (Fig. 2B), uredinia were very well developed than those formed in leaflets of plants from ASM, HxA (20 mM), and AzA (1 mM) treatments (Fig. 2H-J).

For AUDPC, there were significant reductions of 95, 93, 92, 82, and 92% for ASM, HxA 5 mM, HxA 20 mM, AzA 0.1 mM, and AzA 1 mM, respectively, compared to control treatment (Fig. 3A). Final severity (20 dai) obtained with the QUANT software was significantly reduced

by 93, 76, 88, 87, and 91% for ASM, HxA 5 mM, HxA 20 mM, AzA 0.1 mM, and AzA 1 mM, respectively, compared to control treatment (Fig. 3B).

Imaging and quantification of Chl *a* fluorescence parameters

Notable damage to the photosynthetic apparatus occurred for plants from control treatment compared to those from ASM, HxA, and AzA treatments from 10 to 20 dai based on darker areas in the images for F_v/F_m, Y(II), Y(NPQ), and Y(NO) parameters (Fig. 4). The parameters F_v/F_m, Y(II), Y(NPQ), Y(NO), and ETR for NI plants and F_v/F_m for I plants were affected by none of the treatments regardless of the evaluation time (Fig. 5A, B, C, E, G, and I). For I plants, Y(II) significantly increased by 36 and 36% at 5 dai and by 38 and 18% at 10 dai for HxA and AzA treatments, respectively, compared to control treatment (Fig. 5D). The Y(II) was significantly higher by 39 and 39% at 5 dai for HxA and AzA treatments, respectively, and by 27% at 10 dai for HxA treatment compared to ASM treatment (Fig. 5D). Significant increases of 78, 71, and 92% for Y(II) occurred for I plants from ASM, HxA, and AzA treatments, respectively, compared to I plants from control treatment at 20 dai (Fig. 5D). For I plants, Y(NPQ) was significantly lower by 18, 24, and 32% at 15 dai for control, ASM, and HxA treatments, respectively, compared to AzX treatment (Fig. 5F). For I plants at 20 dai, Y(NPQ) significantly increased by 86, 87, and 50% for ASM, HxA, and AzA treatments, respectively, compared to control treatment (Fig. 5F). For I plants, Y(NO) significantly decreased by 12% at 5 dai for HxA treatment and by 32, 31, and 18% at 20 dai for ASM, HxA, and AzA treatments, respectively, compared to control treatment (Fig. 5H). Significant decreases of 17 and 15% at 20 dai for Y(NO) were obtained for I plant of ASM and HxA treatments, respectively, compared to AzA treatment (Fig. 5H). For I plants, ETR was significantly lower by 28, 21, and 17% at 10 dai for control, ASM, and AzA treatments, respectively, compared to HxA treatment (Fig. 5J). Regarding ETR for I plants at 20 dai, there were significant increases of 86, 67, and 85% for ASM, HxA, and AzA treatments, respectively,

compared to control treatment (Fig. 5J). In general, Y(II) and ETR were significantly higher, while Y(NPQ) and Y(NO) were significantly lower for NI plants compared to I plants for most of treatments during the time-course evaluated (Fig. 5A-J).

Concentrations of photosynthetic pigments

For NI plants, Chl *a*+*b* concentration was significantly higher by 36% at 10 dai for HxA treatment compared to control treatment and by 29 and 35% at 15 dai for HxA and AzA treatments, respectively, compared to ASM treatment (Fig. 6A). Carotenoids concentration for NI plants was significantly higher by 21 and 26% at 15 dai for HxA and AzA treatments, respectively, compared to ASM treatment (Fig. 6C). For I plants, concentration of Chl *a*+*b* was significantly higher for AzA treatment (24% at 5 dai), HxA and AzA treatments (53 and 55%, respectively, at 10 dai), ASM, HxA, and AzA treatments (61, 65, and 77%, respectively, at 15 dai), and for HxA and AzA treatments (49 and 64%, respectively, at 20 dai) compared to control treatment (Fig. 6B). Concentration of Chl *a*+*b* for I plants was significantly higher for HxA and AzA treatments (81 and 85%, respectively, at 10 dai) compared to ASM treatment, HxA and AzA treatments (43 and 60%, respectively, at 20 dai) compared to ASM treatment, and AzA treatment (44% at 20 dai) compared to HxA treatment (Fig. 6B). For I plants, carotenoids concentration significantly increased for ASM, HxA, and AzA treatments (22, 28, and 31%, respectively, at 5 dai), HxA and AzA treatments (by 51 and 56%, respectively, at 10 dai), HxA and AzA treatments (59 and 79%, respectively, at 15 dai), and HxA and AzA treatments (32 and 79%, respectively, at 20 dai) compared to control treatment (Fig. 6D). Carotenoids concentration for I plants significantly increased for HxA and AzA treatments (78 and 71%, respectively, at 10 dai) compared to ASM treatment, HxA and AzA treatments (53 and 65%, respectively, at 20 dai) compared to ASM treatment, and AzA treatment (35% at 20 dai) compared to HxA treatment (Fig. 6D). Concentrations of Chl *a*+*b* and carotenoids were

significantly higher for NI plants compared to I plants for most of the treatments during the time-course evaluated (Fig. 6A-D).

Histochemical localization of H_2O_2 and $O_2^{\bullet-}$

The leaflets of NI plants sprayed with ASM, HxA, or AzA showed absence or weak staining used to detect H_2O_2 and $O_2^{\bullet-}$ depositions compared to leaflets from plants of the control treatment (Figs. 7A-D and 8A-D). Depositions of H_2O_2 (brown color) and $O_2^{\bullet-}$ (blue color) were less remarkably intense in leaflets of I plants from ASM, HxA, and AzA treatments (Figs. 7F-H and 8F-H) compared to control treatment (Figs. 7E and 8E).

Concentrations of MDA, H_2O_2, and $O_2^{\bullet-}$

Concentrations of MDA, H_2O_2, and $O_2^{\bullet-}$ for NI plants and H_2O_2 for I plants were not affected by none of treatments regardless of evaluation time (Fig. 9A, C, D, and E). For I plants, MDA concentration was significantly lower for ASM, HxA, and AzA treatments (36, 50, and 31%, respectively, at 5 dai), HxA and AzA treatments (32 and 45%, respectively, at 10 dai), HxA and AzA treatments (40 and 34%, respectively, at 15 dai), ASM, HxA, and AzA treatments (40, 14, and 29%, respectively, at 20 dai) compared to control treatment (Fig. 9B). The MDA concentration for I plants was significantly lower for AzA treatment (70% at 10 dai) compared to ASM treatment, HxA and AzA treatments (37 and 30%, respectively, at 15 dai) compared to ASM treatment, and ASM and AzA treatments (30 and 17%, respectively, at 20 dai) compared to HxA treatment (Fig. 9B). For I plants, $O_2^{\bullet-}$ concentration was significantly lower for HxA and AzA treatments (35 and 36%, respectively, at 10 dai), ASM, HxA, and AzA treatments (75, 76, and 79%, respectively, at 15 dai), and HxA and AzA treatments (67 and 65%, respectively, at 20 dai) compared to control treatment (Fig. 9F). The concentration of $O_2^{\bullet-}$ for I plants was significantly lower for HxA and AzA treatments (53 and 49%, respectively, at 10 dai) and significantly higher for HxA and AzA treatments (69 and 71%, respectively, at 20

dai) compared to ASM treatment (Fig. 9F). Concentrations of MDA, H_2O_2, and $O_2^{\bullet-}$ were significantly higher for I plants compared to NI plants for most of treatments during the time-course evaluated (Fig. 9A-F).

Activities of antioxidant enzymes

Activities of SOD, POX, CAT, APX, and GR for NI plants were affected by none of treatments regardless of evaluation time (Fig. 10A, C, E, G, and I). For I plants, SOD activity was significantly higher for ASM, HxA, and AzA treatments (31, 35, and 55%, respectively, at 10 dai) compared to control treatment at 10 dai (Fig. 10B). The SOD activity for I plants was significantly lower for ASM and HxA treatments (35 and 31%, respectively, at 10 dai) compared to AzA treatment and for control, ASM, and AzA treatments (61, 43, and 47%, respectively, at 15dai) compared to HxA treatment (Fig. 10B). For I plants, POX activity was significantly higher by 52% for AzA treatment compared to control treatment at 10 dai and significantly lower by 53 and 45% for HxA and AzA treatments, respectively, compared to ASM treatment at 20 dai (Fig. 10D). For I plants, CAT activity was significantly higher by 60% for HxA treatment compared to ASM treatment at 10 dai and by 57, 44, and 42% for control, ASM, and AzA treatments, respectively, compared to HxA treatment at 20 dai, but significantly lower by 51, 71, and 49% for control, ASM, and AzA treatments, respectively, compared to HxA treatment at 15 dai (Fig. 10F). For I plants, APX activity significantly increased for ASM, HxA, and AzA treatments (49, 55, and 44%, respectively, at 15 dai) and significantly decreased for HxA and AzA treatments (35 and 31%, respectively, at 20 dai) compared to control treatment (Fig. 10H). For I plants, GR activity was significantly lower by 67% for ASM treatment compared to HxA treatment at 5 dai, but significantly increased for HxA treatment (63% at 15 dai) and HxA and AzA treatments (83 and 77%, respectively, at 20 dai) compared to control treatment (Fig. 10J). Activities of SOD, POX, CAT, APX, and GR were significantly

higher for I plants compared to NI plants for most of treatments during the time-course evaluated (Fig. 10A-J).

Activities of defense enzymes

Activities of CHI, GLU, PAL, PPO, and LOX for NI plants and PPO for I plants were affected by none of treatments regardless of evaluation time (Fig. 11A, C, E, G, H, and I). For I plants, CHI activity was significantly higher for ASM and HxA treatments (9 and 5%, respectively, at 15 dai) and for ASM and AzA treatments (36 and 29%, respectively, at 20 dai) compared to control treatment (Fig. 11B). The CHI activity for I plants was significantly higher for ASM and HxA treatments (50 and 47%, respectively, at 15 dai) compared to AzA treatment and for ASM and AzA treatments (49 and 43%, respectively, at 20 dai) compared to HxA treatment (Fig. 11B). For I plants, GLU activity was significantly higher by 36% for AzA treatment compared to HxA treatment at 10 dai, by 50 and 45% for HxA and AzA treatments, respectively, compared to control treatment at 15 dai, and by 45 and 40% for HxA and AzA treatments, respectively, compared to ASM treatment at 15 dai (Fig. 11D). For I plants, PAL activity was significantly higher by 72% for AzA treatment compared to control treatment at 15 dai and significantly lower by 64, 87, and 74% for control, HxA and AzA treatments, respectively, compared to ASM treatment at 20 dai (Fig. 11F). For I plants, LOX activity was significantly higher by 52 and 50% for ASM and HxA treatments, respectively, compared to control treatment at 15 dai (Fig. 11F). Activities of CHI, GLU, PAL, PPO, and LOX were significantly higher for I plants compared to NI plants for most of treatments during the time-course evaluated (Fig. 11A-J).

Concentrations of TSP and LTGA derivatives

For NI plants, concentrations of TSP and LTGA derivatives were not affected by none of treatments regardless of evaluation time (Fig. 12A and C). For I plants, TSP concentration

significantly increased for ASM and HxA treatments (34 and 34%, respectively, at 5 dai), ASM treatment (23% at 10 dai), and ASM and HxA treatments (26 and 22%, respectively, at 15 dai) compared to control treatment (Fig. 12B). For I plants, LTGA derivatives concentration was significantly lower by 40, 39, and 39% for ASM, HxA, and AzA treatments, respectively, compared to control treatment at 5 dai, by 45 and 40% for ASM and AzA treatments, respectively, compared to HxA treatment at 10 dai, by 40 and 45% for control and HxA treatments, respectively, compared to ASM treatment at 15 dai, by 33 and 38% for control and HxA treatments, respectively, compared to AzA treatment at 15 dai, and by 35 and 47% for control and ASM treatments, respectively, compared to HxA treatment at 20 dai (Fig. 12D). Concentrations of TSP and LTGA derivatives were significantly higher for I plants compared to NI plants for most of treatments during the time-course evaluated (Fig. 12A-D).

Genes expression

Comparing NI *vs.* I plants for control, ASM, HxA, and AzA treatments

Expressions of *PAL1.1*, *PAL1.3*, *PAL2.1*, *PR10*, *URE*, *ICS2*, *CHIB1*, *ACO*, *ETR1*, and *NAC19* at 5 dai, *PR1-A*, *PR10*, and *MMP2* at 10 dai, *PR1-A*, *PR10*, *CHIB1*, *ACO*, and *OPR3* at 15 dai, and *PAL1.1*, *PAL2.1*, *PR1-A*, *CHIB1*, *OPR3*, and *NAC19* at 20 dai were significantly up-regulated for I plants compared to NI plants for control treatment. Expressions of *ICS1* and *ICS2* at 10 and 15 dai were significantly down-regulated for I plants compared to NI plants for control treatment (Fig. 13A and E). Expressions of *PAL1.3*, *PR1-A*, and *MMP2* at 5 dai, *PAL1.1*, *PR10*, and *ACS* at 10 dai, *PAL1.3*, *PR1-A*, *PR10*, *MMP2*, and *OPR3* at 15 dai, and *PAL1.3*, *PAL3.1*, *ICS2*, *CHIB1*, and *OPR3* at 20 dai were significantly up-regulated for I plants compared to NI plants for ASM treatment. Expressions of *URE* and *ICS1* at 10 dai and *URE* at 15 dai were significantly down-regulated for I plants compared to NI plants for ASM treatment (Fig. 13B and F). Expressions of *PAL1.1*, *PAL3.1*, *PR1-A*, *ICS2*, *OPR3*, and *JAR1* at 5 dai, *PAL1.1*, *PAL3.1*, *PR1-A*, *PR10*, and *ACO* at 10 dai, *PAL1.1* and *CHIB1* at 15 dai, and *PAL1.1*,

PAL2.1, *PAL3.1*, *PR1-A*, *PR10*, *CHIB1*, *ACO*, *ETR1*, and *SABATH2* at 20 dai were significantly up-regulated for I plants compared to NI plants for HxA treatment. Expressions of *ICS1* and *ICS2* at 10 dai were significantly down-regulated for I plants compared to NI plants for HxA treatment (Fig. 13C and G). Expressions of *MMP2* at 5 dai, *PAL1.3*, *PAL2.1*, *PR10*, and *ACS* at 10 dai, *PR10* and *OPR3* at 15 dai, and *PAL1.3*, *PAL2.1*, *PAL3.1*, *PR1-A*, *PR10*, *URE*, *CHIB1*, and *OPR3* at 20 dai were significantly up-regulated for I plants compared to NI plants for control treatment. Expressions of *ICS2* at 5 dai and *ICS1* and *ICS2* at 10 dai were significantly down-regulated for I plants compared to NI plants for control treatment (Fig. 13D and H).

Comparing ASM, HxA, and AzA treatments with control treatment for NI and I plants

Noninoculated plants

Expression of *ACO* was significantly up-regulated at 5 dai while *ICS2* at 10 dai and *URE* at 15 dai were significantly down-regulated for ASM treatment compared to control treatment (Fig. 13A-B). Expressions of *PAL1.1* and *MMP2* at 5 dai, *PR10* at 15 dai, and *PAL2.1* at 20 dai were significantly up-regulated while *ICS2* and *ACS* at 10 dai, *PR10* at 15 dai, and *PAL2.1* at 20 dai were significantly down-regulated for HxA treatment compared to control treatment (Fig. 13A and C). Expressions of *ICS1*, *ICS2*, *ETR1*, *OPR3*, and *NAC19* at 5 dai, *MMP2* at 10 dai, *PAL2.1* at 15 dai as well as *PAL3.1* and *PR10* at 20 dai were significantly up-regulated while *ICS1* and *ICS2* at 15 dai and *ACO* and *ACS* at 20 dai were significantly down-regulated for AzA treatment compared to control treatment (Fig. 13A and D).

Inoculated plants

Expressions of *PAL2.1* and *URE* at 5 dai as well as *MMP2* and *NAC19* at 20 dai were significantly up-regulated while *ETR1* at 5 dai, *ACS* at 10 dai, *MMP2* at 15 dai, and *SABATH2* at 20 dai were significantly down-regulated for ASM treatment compared to control treatment (Fig. 13E-F). Expressions of *PAL1.1*, *PAL3.1*, *PR1-A*, *MMP2*, *CHIB1*, and *JAR1* at 5 dai,

CHIB1 at 10 dai, *URE*, *ICS2*, *CHIB1*, and *ETR1* at 15 dai were significantly up-regulated while *PAL2.1*, *URE*, *ICS2*, *ETR1*, and *NAC19* at 5 dai, *PR10* at 15 dai as well as *MMP2*, *OPR3*, and *NAC19* at 20 dai were significantly down-regulated for HxA treatment compared to control treatment (Fig. 13E and G). Expressions of *PAL1.3* at 10 dai and *PAL1.1*, *PR10*, *CHIB1*, and *ACS* at 20 dai were significantly up-regulated while *URE* and *ETR1* at 5 dai as well as *PR1-A*, *MMP2*, and *NAC19* at 20 dai were significantly down-regulated for AzA treatment compared to control treatment (Fig. 13E and H). Expression of *TEF-1α* was significantly down-regulated at 5 dai for ASM treatment, at 5 and 10 dai for HxA treatment, and at 5 dai for AzA treatment compared to control treatment (Fig. 13E-H).

PCA analysis

One principal component (PC) explained most of data variation (PC1 = 40.9% and PC2 = 26.5%) (Fig. 14A-B). According to cluster analysis with complete linkage and Pearson distance, one cluster was generated for NI for all treatments (control, ASM, HxA, and AzA) and other three other clusters (C2 - control treatment; C3 - ASM and AzA treatments; and C4 - HxA treatment) for I plants (Fig. 14A). The first PC resulted in negative scores for photosynthetic parameters (F_v/F_m, Y(II), and Y(NO)), Chl *a*+*b*, Car, and *ETR1* and positive scores for other variables and parameters evaluated (Fig. 14A-B).

Discussion

Nowadays, the ability of resistance inducers to efficiently boost different metabolic pathways involved in the defense responses of crops challenged by pathogens is of outstanding importance toward sustainable agriculture. In this regard, the present study brings novel pieces of information related to the physiological, biochemical, and molecular aspects involved in the increasing soybean resistance against *P. pachyrhizi* infection provided by HxA and AzA. In fact, soybean rust symptoms were less developed in HxA and AzA-sprayed plants due to reduced cellular damage (lower MDA concentration and less striking accumulation of H_2O_2 and $O_2^{\bullet-}$) associated with more impediment of leaf tissues colonization (based on lower transcript levels for *TEF-1α*) by *P. pachyrhizi*. Interestingly, lower soybean rust severity for HxA and AzA-sprayed plants was comparable to that obtained with ASM, a well-known resistance inducer of SAR in different host-pathogen interactions (Lyon, 2007). The HxA and AzA showed a direct antifungal activity against demonstrated by the reduction of germination of *P. pachyrhizi* urediniospores *in vitro*. The literature reports an direct effect of HxA against the development of some pathogens (*e.g.*, *Botrytis cinerea*, *Xanthomonas citri* subsp. *citri*, and *Meloidogyne javanica*) *in vitro* rather than just inducing host defense reactions (Leyva et al., 2008; Aranega-Bou et al., 2014; Llorens et al., 2015b; Ntalli et al., 2020; Caccalano et al., 2021). On the contrary, the effect of AzA on the physiology of pathogens, to the best of our knowledge, has not been reported in the literature.

The potential of HxA and AzA to affect the progress of soybean rust goes beyond their direct antifungal activity against urediniospores of *P. pachyrhizi* at the leaf surface level. At the physiological level, photosynthesis was greatly preserved in infected leaves of ASM, HxA, and AzA-sprayed plants based on Chl *a* fluorescence analysis. In general, values for energy destined for photochemical process (Y(II)), dissipation by down-regulation energy (Y(NPQ)), and ETR were higher and intrinsically linked to lower values for energy destined for other non-regulated

losses (Y(NO)) in leaves of ASM, HxA, or AzA-sprayed plants at advanced stage (20 dai) of *P. pachyrhizi* infection. Considering the pattern of these three yield components for dissipative processes, including the ETR, it is reasonable to assume that photoprotection mechanisms were efficient and photooxidative damages were greatly prevented due to sufficient thermal dissipation of energy at the photosynthetic machinery level as the infection process of *P. pachyrhizi* took place. Interestingly, damage to the reaction centers associated with the photosystems based on F_v/F_m values was similar among water, ASM, HxA, and AzA-sprayed plants regardless of *P. pachyrhizi* infection. Moreover, non-infected leaves of ASM, HxA, and AzA-sprayed plants did not show any sign of perturbation at the photosynthetic level irrespective of the Chl *a* parameter evaluated. The pool of photosynthetic pigments (Chl *a*+*b* and carotenoids) was greatly preserved in infected leaves of HxA and AzA-sprayed plants and, to a less extent, for ASM-sprayed plants, due to less soybean rust symptoms (more discreet chlorosis surrounding the smaller necrotic lesions). This finding reflects a better performance of the photosynthetic machinery of these plants since light energy was used more efficiently for photochemical reactions. It is well known that infection of soybean leaves by *P. pachyrhizi* remarkably impairs their photosynthetic apparatus due to profound limitations of biochemical and diffusional nature (Rios et al., 2018). Attempts to alleviate the stress imposed by *P. pachyrhizi* infection on photosynthesis of soybean plants (*e.g.*, spray of ASM and JA and enhanced plant nutrition with boron, nickel, and silicon) have been made (Cruz et al., 2014; Rios et al., 2018; Einhardt et al., 2020; Paula et al., 2021; Picanço et al., 2021) and the use of HxA and AzA seems to fit well in this context considering the physiological findings outlined above.

Plants submitted to different types of stress conditions rely on oxidative burst and redox signaling as key cellular components for their better development (González-Bosch, 2018). In the context of stress as a consequence of pathogen infection, a very coordinated enzymatic

system (SOD converts $O_2^{\bullet-}$ into H_2O_2 and O_2, whereas H_2O_2 can be subsequently scavenged by APX, CAT, and POX activities; GR uses NADPH as a reductant to reduce glutathione disulfide (GSSH) to reduced glutathione (GSH)) occurs in plant tissues to scavenge the excess of ROS generated (Vellosillo et al., 2010; Das and Roychoudhury, 2014). A tight balance between the production and accumulation of ROS in infected tissues of plants exposed to some resistance inducers has been associated with their increased resistance against diseases but not disregarding that the initial oxidative burst may act against the pathogen, reinforce the cell wall, and also triggers signaling hormonal networks (Resende et al., 2012; González-Bosch, 2018; Mohammadi et al., 2021). In the present study, the antioxidative metabolism of non-infected leaves was strikingly similar among water, ASM, HxA, and AzA-sprayed plants taking into consideration the histochemical detection of H_2O_2 and $O_2^{\bullet-}$ and the temporal pattern of activities of antioxidative enzymes evaluated indicating, therefore, no disturbance of cellular homeostasis. Interestingly, stimulation of the antioxidative metabolism for ASM, HxA, and AzA-sprayed and infected plants depicted by great SOD (at 10 dai for ASM, HxA, and AzA treatments and at 15 dai for HxA treatment), POX (at 10 dai for AzA treatment), CAT (at 15 dai for HxA treatment), and APX (at 15 dai for ASM, HxA, and AzA treatments) was closely linked to their increased resistance against *P. pachyrhizi* infection. On top of that, reduced symptoms of soybean rust for ASM, HxA, and AzA-sprayed plants resulted in the undermost depositions of H_2O_2 and $O_2^{\bullet-}$ along with lower $O_2^{\bullet-}$ concentration (at 10 dai for HxA and AzA treatments; at 15 and 20 dai for ASM, HxA, and AzA treatments) indicating the robustness of their antioxidant machinery toward less cellular oxidative damage. Particularly regarding GR, it is reasonable to assume that its higher activity for HxA (at 15 and 20 dai) and AzA-sprayed plants (at 20 dai) was of great importance in alleviating the oxidative stress imposed by *P. pachyrhizi* infection since adequate levels of GSH and protein synthesis were maintained for an improved redox cellular homeostasis. Higher GR activity in plant tissues infected by

pathogens helps raise the pool of GSH (Foyer et al., 1994; Kuzniak and Sklodowska, 1999). Beyond that, optimal protein synthesis in plant tissues is dependent on an elevated GSH:GSSG ratio (Das and Roychoudhury, 2014). According to Finiti et al. (2014), ROS accumulation was reduced and more restricted around infection sites of *B. cinerea* in leaves of tomato plants treated with HxA and linked with higher ratios of reduced to oxidized glutathione and ascorbate that helped to prevent the harmful effect of oxidative stress caused by fungal infection. The HxA also contributed to a less oxidized cellular environment in leaves of tomato plants coping against *Pseudomonas syringae* infection (Camañes et al., 2015). The systemic movement of *Melon necrotic spot virus* in the leaves of melon plants exposed to HxA was associated with callose deposition, reduction in the oxidative damage caused by virus infection through an efficient activation of the antioxidant machinery that kept lower levels of H_2O_2, and increased levels of oxylipin 12-oxo-phytodienoic acid (OPDA), SA, JA-isoleucine, and ferulic acid (Fernández-Crespo et al., 2017).

The resistance inducers operate through a prominent state of elicitation or priming for readily, robust, and extensive defense reactions (increased production of pathogenesis-related proteins (*e.g.*, CHI, GLU, PR1, and PR10) and antimicrobial compounds (*e.g.*, phenolics, quinones, phytoalexins, and some peptides), stimulating the oxidative burst (rapid ROS production), and cell wall strengthening with depositions of callose and lignin polymers) in different plant species coping against pathogens infection (van Loon et al., 2006; González-Bosch, 2018; Vlot et al., 2021; Kesel et al., 2021). In the present study, plants not challenged with *P. pachyrhizi* were greatly elicited by HxA and AzA taking into account the expression of several genes (8 genes for HxA (*PAL1.1* and *MMP2* at 5 dai; *PAL2.1* at 20 dai; *PR10*, *URE*, and *ICS1* at 15 dai; *ICS2* and *ACS* at 10 dai) and 13 genes for AzA (*PAL2.1* at 15 dai; *PAL3.1*, *PR10*, *ACO*, and *ACS* at 20 dai; *MMP2* at 10 dai; *ICS1* and *ICS2* at 5 and 15 dai; *ETR1*, *OPR3*, and *NAC19* at 5 dai) while the ASM elicited only three genes (*URE*, *ICS2*, and *ACO* at 15, 10,

and 5 dai, respectively) in comparison to water-sprayed plants. By contrast, many genes were strongly up-regulated for infected plants that were sprayed with ASM (7 genes - *PAL2.1*, *URE*, and *ETR1* at 5 dai; *MMP2* at 15 and 20 dai; *ACS* at 10 dai; *SABATH2* and *NAC19* at 20 dai), HxA (14 genes - *PAL1.1* at 5 and 10 dai; *PAL2.1*, *PAL3.1*, *PR1-A*, *SABATH2*, and *JAR1* at 5 dai; *PR10* at 15 dai; *MMP2* and *NAC19* at 5 and 20 dai; *URE* and *ICS2* at 5 and 15 dai; *CHIB1* at 5, 10, and 15 dai; *ETR1* at 5 and 15 dai; *OPR3* at 20 dai), and AzA (10 genes - *PAL1.1*, *PR1-A*, *PR10*, *MMP2*, *CHIB1*, *ACS*, and *NAC19* at 20 dai; *PAL1.3* at 10 dai; *URE* at 5 dai) in closely contrast to water-sprayed plants what must have contributed to their increased resistance against soybean rust. Particularly concerning HxA-sprayed and infected plants, most of the genes mentioned above were expressed earlier in contrast to AzA-sprayed and infected plants, and more expressively than ASM-sprayed plants, during the time-course evaluated.

Many resistance inducers can increase soybean resistance against diseases caused by a plethora of pathogens through SAR or ISR (Cruz et al., 2020; Paula et al., 2021; Santos et al., 2021). In infected tissues of plants exhibiting SAR, SA can be originated from either phenylpropanoid or isochorismate pathways in which *PAL* and *ICS*, respectively, play a pivotal role (Vlot et al., 2009). In the present study, a close look at the comparison between non-inoculated and inoculated plants indicated that genes were most strongly up-regulated for infected plants, and among them, *ICS1* and *ICS2* were down-regulated for infected plants than for non-infected ones. Moreover, based on *PAL1.1*, *PAL1.3*, *PAL2.1*, *PAL3.1*, *SABATH2*, *ICS1*, and *ICS2* expressions, the possible role played by HxA and AzA in SAR was more prone to occur for the former carboxylic acid. On top of that, *PR1-A* expression was up-regulated for HxA and AzA-sprayed and infected plants earlier (5 dai) and late (20 dai), respectively, confirming its importance as a marker for SAR as reported by van Loon and Pieterse (2006). On the other hand, some genes involved in ISR were up-regulated for plants sprayed with HxA (*ETR1*, *OPR3*, and *JAR1*) and AzA (*ACS* and *ETR1*) in response to *P. pachyrhizi* infection.

Notably, soybean plants exposed to HxA or AzA were more prone to be primed to establish either SA or JA/ET pathway, but their co-participation at some stage of *P. pachyrhizi* infection process must be taken into consideration. In different host-pathogen interactions, the SA and JA/ET pathways can act independently or have a joint action at some point on the signal transduction pathways (Pieterse et al., 2012). The literature sheds light on the involvement of HxA and AzA in the SA and JA/ET pathways in different host-pathogen interactions. Differential changes in the transcript levels of *Defensin* and *PR1-A*, which were more responsive to HxA and AzA, respectively, indicated a distinct activation of SA and JA/ET signaling pathways depending on the carboxylic acid involved (Djami-Tchatchou et al., 2017). The AzA was important for Arabidopsis plants to mount a faster and/or stronger defense response against *P. syringae* pv. *maculicola* infection that included a remarkable increase in SA biosynthesis and up-regulation of *PR1* (Jung et al., 2009). According to the authors, AzA *per se* did not induce defenses but was probably involved in priming of defenses of Arabidopsis plants against bacterial infection. Moreover, AzA did not induce resistance in SAR-defective SA pathway mutants but did confer resistance to plants from *sfd1* and *fad7* mutants, which lack an unidentified glycerolipid needed as a signal for SAR (Jung et al., 2009). Susceptible and resistant cultivars of olive trees to *Xylella fastidiosa* showed increased AzA concentration in leaf petioles and differential expression of *OeLTP1* and *OeLTP2* encoding lipid transport proteins (LTPs) that share a specific domain with the LTPs involved in the role played by AzA during SAR (Nicoli et al., 2019). Plants of sweet orange receiving HxA application as a soil drench or foliar spray showed reduced citrus canker symptoms due to callose deposition and increasing *PR2* expression (Llorens et al., 2015b). Scalschi et al. (2014) reported that tomato plants drenched with HxA solution or grown in nutrient solution containing HxA and infected by *Pseudomonas syringae* pv. *tomato* showed up-regulation of marker genes for SA (*PR-1*, *PR-5*, and *SAMT*) and JA (*JMT*, *PIN2*, and *JAZ1*) signaling pathways and increased levels of OPDA

supporting a positive relationship between these pathways. Tomato plants receiving HxA through the roots showed reduced symptoms caused by *B. cinerea* infection as a result of intense callose deposition in papillae at the fungal infection sites, increased production of both OPDA (a JA-precursor) and JA-isoleucine, stimulation of the JA-signaling pathway (up-regulation of *LoxD*), and positive regulation by abscisic acid (Vicedo et al., 2009). Reduction of disease symptoms caused by *B. cinerea* infection in Arabidopsis plants with their roots exposed to HxA was associated with up-regulation of *PDF1.2*, *PR-4*, and *VSP1* and higher levels of JA and OPDA, highlighting the importance of the JA-signaling pathway in this pathosystem (Kravchuk et al., 2011). In the tomato-*B. cinerea* interaction, plants primed with HxA exhibited reduced disease symptoms due to signaling for JA pathway JA, OPDA, JA-isoleucine and up-regulation of *AOS, LOX, AOC*, and *OPR3* (Vicedo et al., 2009; Camañes et al., 2015). The exposition of roots from Arabidopsis plants increased their resistance to *P. syringae* infection and partially depended on *AZI1* and *EARL11*, two genes related to lipid transfer proteins (Cecchini et al., 2019). Plants of Arabidopsis treated with yeast cell wall extract showed increased production of OPDA, AzA, phenylalanine, and camalexin which explained reduction in the symptoms caused by *B. cinerea* infection (Yaguchi et al., 2017). According to Camañes et al. (2015), tomato plants primed by HxA and infected by *B. cinerea* and *P. syringae* showed changes in their primary metabolism and the pool of amino acids and seemed to be pathogen-specific. On top of that, Llorens et al. (2016) showed alterations in the metabolic profile of citrus plants exposed to HxA and infected by *Alternaria alternata* mainly related to the mevalonic and linoleic pathways and enhancement in the emission of volatile compounds that contributed to reduce disease symptoms. Tomato plants lacking dioxygenase α-DOX 2, which catalyzes oxylipins to produce fatty acids, became more susceptible to *B. cinerea* infection even with their exposition to HxA, indicating that α-DOX 2 is important for the HxA-induced resistance

(Angulo et al., 2015). Moreover, SA-deficient *nahG* tomato plants displaying lower SA levels could not increase their resistance against *B. cinerea* promoted by HxA (Angulo et al., 2015).

Besides displaying a remarkable antimicrobial effect against pathogens, phenolics polymerize to produce lignin that hampers their colonization in plant tissues after deposition in the cell wall (Daayf et al., 2012). Particularly for infected HxA-sprayed plants, great production of LTGA derivatives at 15 and 20 dai, likely originated from the pool of TSP (at 5 dai) and was linked to earlier up-regulation of *PAL1.1*, *PAL2.1*, and *PAL3.1*, contributed to reducing soybean rust symptoms. Even though TSP and LTGA derivatives concentrations did not show significant increases for AzA-sprayed and infected plants, up-regulation of *PAL1.1* and *PAL1.3* cannot be disregarded in the context of their increased resistance against *P. pachyrhizi* infection. Tobacco cells exogenously exposed to HxA and AzA showed earlier potentiation of the shikimate/phenylpropanoid pathway (up-regulation of *PAL*, *HQT*, and *HCT* and increased production of hydroxycinnamic acid derivatives (conjugates of caffeic acid and ferulic acid) and induction of *NPR1* known to be involved in SAR establishment (Djami-Tchatchou et al., 2017). In contrast to TSP or LTGA derivatives, it seems like that flavonoids were of outstanding involvement in the increased resistance of HxA and AzA-sprayed plants against *P. pachyrhizi* infection considering the up-regulation of *CHIB1*. An array of flavonoids produced by soybean (*e.g.*, coumestrol daidzein, genistein, glyceollin, quercetin, and kaempferol) are involved in the resistance against many pathogens (Kim and Chung, 2007; Agati et al., 2012; Shah and Smith, 2020). In soybean leaves infected by *P. pachyrhizi*, *CHI1* transcripts, coding for chalcone isomerase 1, was abundantly produced at 10 hai. (Park, 2010). In the present study, up-regulation of *PR10*, *MMP2*, *URE*, and *NAC19* also added their contribution to the increased resistance of HxA and AzA-sprayed plants against soybean rust. Among 40 proteins differentially expressed in the leaves of soybean plants from a susceptible cultivar infected by *P. pachyrhizi*, PR10 stood out and *PR10* transcripts significantly raised at 10 hai and at 6 and 8

days after inoculation (Park, 2010). Many antimicrobial peptides are involved in defense of plants against pathogen infection and *MMP2* expression in soybean leaves seems to be of pivotal importance for resistance against some pathogens (Liu et al., 2001; Marino and Funk, 2012; Picanço et al., 2021). Up-regulation of *URE* enhances urea conversion to ammonium resulting in an elevated pool of compounds containing nitrogen of great value in host defense reactions as reported for the soybean-*P. pachyrhizi* pathosystem (Wiebke-Strohm et al., 2012; Einhardt et al., 2020). In soybean, NAC family transcription factor has been reported to be involved in an improved response of plants exposed to some types of abiotic stress and also facing pathogen infection (So and Lee, 2019; Bian et al., 2021; Yu et al., 2022).

Increased resistance of HxA and AzA-sprayed plants against soybean rust can also be accounted for a contribution of CHI, GLU, PAL, and LOX activities, which have been reported to be necessary for a prompt defense response of plants facing pathogen infection (Ebrahim et al., 2011; Andersen et al., 2018; You et al., 2020; Kaur et al., 2022). The CHI and GLU hydrolyze chitin and *β*-1,3-glucan, respectively, in the cell wall of fungi; PAL participates in the production of an array of phenolics from the deamination of *L*-phenylalanine in the phenylpropanoid pathway; and LOX is involved in the first steps of the octadecanoid pathway, which leads to oxylipin synthesis (*e.g.*, JA), and renders various intermediate compounds with defense implications (Creelman and Mullet, 1997; Feussner and Wasternack, 2002; Ojaghian et al., 2014; Sánchez-Vallet et al., 2015; You et al., 2020).

In conclusion, the present study brings robust physiological, biochemical, and molecular shreds of evidence regarding the potential of using HxA and AzA to efficiently reduce soybean rust symptoms as a result of a boosted and well-tuned defensive strategy holistically pictured as up-regulation of genes involved in SA and JA/ET signaling pathways, a more operant antioxidative metabolism, and preservation of the photosynthetic apparatus. It must point out that the performance of plants exposed to these two carboxylic acids was greatly better at

physiological and defense reactions levels compared to plants sprayed with the well-known resistance inducer ASM. The PCA analysis illustrated this outcome well based on the isolation of the cluster of non-inoculated plants from all treatments (control, ASM, HxA, and AzA) from the other three clusters related to inoculated plants (control *vs.* ASM; AzA *vs.* HxA) considering the variables and parameters investigated. It is tempting to assume that using HxA and AzA associated with well-known control strategies may be of paramount importance as an alternative to slow the soybean rust epidemic rate under field conditions and the number and frequency of fungicides sprayings.

References

Adam AL, Nagy ZA, Katay G, Mergenthaler E, Viczian O (2018) Signals of systemic immunity in plants: progress and open questions. International Journal of Molecular Science 19:1146.

Agati G, Azzarello E, Pollastri S, Tattini M (2012) Flavonoids as antioxidants in plants: location and functional significance. Plant Science 196:67-76.

Andersen EJ, Ali S, Byamukama E, Yen Y, Nepal MP (2018) Disease resistance mechanisms in plants. Genes 9:339.

Anderson LA, Johnson AK, Simms MD, Willingham TR (1995) Comparative analysis of catalases: spectral evidence against heme-bound water for the solution enzymes. FEBBS Letters 370:97-100.

Angulo C, Leyva MDLO, Finiti I, López-Cruz J, Fernández-Crespo E, García-Agustín P, González-Bosch C (2015) Role of dioxygenase α-DOX2 and SA in basal response and in hexanoic acid-induced resistance of tomato (*Solanum lycopersicum*) plants against *Botrytis cinerea*. Journal of Plant Physiology 175:163-173.

Aranega-Bou P, Leyva MDLO, Finiti I, García-Agustín P, González Bosch C (2014) Priming of plant resistance by natural compounds. Hexanoic acid as a model. Frontiers of Plant Science 5:488.

Axelrod B, Cheesbrough TM, Laasko S (1981) Lipoxygenases from soybeans. Methods in Enzymology 71:441-451.

Baker NR (2008) Chlorophyll fluorescence: a probe of photosynthesis *in vivo.* Annual Review of Plant Biology 59:89-113.

Beauchamp C, Fridovich I (1971) Superoxide dismutase: improved assays and an assay applicable to acryl amide gels. Analytical Biochemistry 44:276-287.

Bian Z, Gao H, Wang C (2021) NAC transcription factors as positive or negative regulators during ongoing battle between pathogens and our food crops. International Journal of Molecular Science 22:81.

Bradford MN (1976) A rapid and sensitive method for the quantitation of microgram quantities of protein utilizing the principle of protein dye binding. Analytical Biochemistry 72:248-254.

Caccalano MN, Dilarri1 G, Zamuner CFC, Domingues DS, Ferreira H (2021) Hexanoic acid: a new potential substitute for copper-based agrochemicals against citrus canker. Journal of Applied Microbiology 131:2488-2499.

Cakmak I, Horst WJ (1991) Effect of aluminum on lipid peroxidation, superoxide dismutase, catalase, and peroxidase activities in root tips of soybean (*Glycine max*). Physiologia Plantarum 83:463-468.

Cakmak I, Marschner H (1992) Magnesium deficiency and high light intensity enhance activities of superoxide dismutase, ascorbate peroxidase, and glutathione reductase in bean leaves. Plant Physiology 98:1222-1227.

Camañes G, Scalschi L, Vicedo B, González-Bosch C, García-Agustín P (2015) An untargeted global metabolomic analysis reveals the biochemical changes underlying basal resistance and priming in *Solanum lycopersicum*, and identifies 1-methyl tryptophan as a metabolite involved in plant responses to *Botrytis cinerea* and *Pseudomonas syringae*. Plant Journal 84:125-139.

Carlberg I, Mannervik B (1985) Glutathione reductase. Methods in Enzymology 113:484-490.

Cecchini NM, Roychoudhry S, Speed DJ, Steffes K, Tambe A (2019) Underground azelaic acid conferred resistance to *Pseudomonas syringae* in *Arabidopsis*. Molecular Plant-Microbe Interaction 32:86-94.

Cecchini NM, Steffes K, Schläppi MR (2015) *Arabidopsis* AZI1 family proteins mediate signal mobilization for systemic defence priming. Nature Communications 6:1-12.

Chaitanya KSK, Naithani SC (1994) Role of superoxide lipid peroxidation and superoxide

dismutase in membrane perturbation during loss of variability in seeds of *Shorea robusta* Faertn. New Phytologist 126:623-627.

Chance B, Maehley AC (1955) Assay of catalases and peroxidases. Methods in Enzymology 2:764-775.

Chanda B, Venugopal SC, Kulshrestha S, Navarre DA, Downie B, Vaillancourt L (2008) Glycerol-3-phosphate levels are associated with basal resistance to the hemibiotrophic fungus *Colletotrichum higginsianum* in *Arabidopsis*. Plant Physiology 147:2017-2029.

Creelman RA, Mullet JE (1997) Biosynthesis and action of jasmonates in plants. Annual Review of Plant Physiology and Plant Molecular Biology 48:355-381.

Cruz MFA, Rodrigues FA, Diniz APC, Moreira MA, Barros EG (2014) Soybean resistance to *Phakopsora pachyrhizi* as affected by acibenzolar-S-methyl, jasmonic acid and silicon. Journal of Phytopathology 162:132-136.

Cruz MFA, Pinto MO, Barros EG, Rodrigues FA (2020) Differential gene expression in soybean infected by *Phakopsora pachyrhizi* in response to acibenzolar-S-methyl, jasmonic acid and silicon. Journal of Phytopathology 168:571-580.

Das K, Roychoudhury A (2014) Reactive oxygen species (ROS) and response of antioxidants as ROS-scavengers during environmental stress in plants. Frontiers in Environmental Science 2:53.

Daayf F, El Hadrami A, El-Bebany AF, Henriquez MA, Yao Z, Derksen H (2012) Phenolic compounds in plant defense and pathogen counter-defense mechanisms. Recent Advances in Polyphenol Research 3:191-208.

Djami-Tchatchou AT, Ncube EN, Steenkamp PA (2017) Similar, but different: structurally related azelaic acid and hexanoic acid trigger differential metabolomic and transcriptomic responses in tobacco cells. BMC Plant Biology 17:227.

Ebrahim S, Usha K, Singh B (2011) Pathogenesis related (PR) proteins in plant defense mechanism. In: Mendez-Vilas, A (Eds). Science against microbial pathogens: communicating current research and technological advances. FORMATEX pp.1043-1054.

Einhardt AM, Ferreira S, Hawerroth C, Valadares SV, Rodrigues FA (2020) Nickel potentiates soybean resistance against infection by *Phakopsora pachyrhizi*. Plant Pathology 69:849-859.

Fagundes-Nacarath IRF, Debona D, Rodrigues FA (2018) Oxalic acid-mediated biochemical and physiological changes in the common bean-*Sclerotinia sclerotiorum* interaction. Plant Physiology and Biochemistry 129:109-121.

Fernández-Crespo E, Navarro JA, Serra-Soriano M, Finiti I, García-Agustín P, Pallás V, González-Bosch C (2017) Hexanoic acid treatment prevents systemic MNSV movement in *Cucumis melo* plants by priming callose deposition correlating SA and OPDA accumulation. Frontiers of Plant Science 8:1793.

Feussner I, Wasternack C (2002) The lipoxygenase pathway. Annual Review of Plant Biology 53:275-297.

Finiti I, Leyva MO, Vicedo B, Gómez-Pastor R, López-Cru J, García-Agustín P (2014) Hexanoic acid protects tomato plants against *Botrytis cinerea* by priming defence responses and reducing oxidative stress. Molecular Plant Pathology 15:550-562.

Flors V, Miralles MC, González-Bosch C, Carda M, García-Agustín P (2003) Induction of protection against the necrotrophic pathogens *Phytophthora citrophthora* and *Alternaria solani* in *Lycopersicon esculentum* Mill. by a novel synthetic glycoside combined with amines. Planta 216:929-938.

Foyer CH, Descourvieres P, Kunert KJ (1994) Protection against oxygen radicals: an important defense mechanism studied in transgenic plants. Plant, Cell & Environment 17:507-23.

Foyer CH, Halliwell B (1976) The presence of glutathione and glutathione reductase in chloroplasts: a proposed role in ascorbic acid metabolism. Planta 133:21-25.

Franceschi VT, Alves KS, Mazaro SM, Godoy CV, Duarte HSS, Ponte EMD (2019) A new standard diagram set for assessment of severity of soybean rust improves accuracy of estimates and optimizes resource use. Plant Pathology 69:495-505.

Giannopoilis CN, Ries SK (1977) Superoxide dismutases: II. Purification and quantitative relationship with water soluble protein in seedlings. Plant Physiology 59:315-318.

Goellner K, Loehrer M, Langenbach C, Conrath U, Koch E, Schaffrath U (2010) *Phakopsora pachyrhizi*, the causal agent of Asian soybean rust. Molecular Plant Pathology 11:169-177.

González-Bosch C (2018) Priming plant resistance by activation of redox-sensitive genes. Free Radical Biology and Medicine 122:171-180.

Guo Y, Liu L, Bi Y (2007) Use of silicon oxide and sodium silicate for controlling *Trichothecium roseum* postharvest rot in Chine cantaloupe (*Cucumis melo* L.). International Journal of Food Science Technology 42:1012-1018.

Harman GE, Hayes CK, Lorito M, Broadway RM, Di Pietro A, Peterbauer C, Tronsmo A (1993) Chitinolytic enzymes of *Trichoderma harzianum*, purification of chitobiosidase and endochitinase. Phytopathology 83:313-318.

Hartman GL, West ED, Herman TK (2011) Crops that feed the world 2. Soybean-worldwide production, use, and constraints caused by pathogens and pests. Food Security 3:5-17.

Heath RL, Packer L (1968) Photoperoxidation in isolated chloroplasts I. Kinetics and stoichiometry of fatty acid peroxidation. Archives of Biochemistry and Biophysics 125:189-198.

Hymowitz T (2008) The history of the soybean. In: Johnson LA, White PJ, Galloway R (Eds). Soybeans chemistry, production, processing, and utilization. AOCS Press pp 1-31.

Jung HW, Tschaplinski TJ, Wang L, Glazebrook J, Greenberg JT (2009) Priming in systemic plant immunity. Science 324:89-91.

So HA, Lee JH (2019) NAC transcription factors from soybean (*Glycine max* L.) differentially regulated by abiotic stress. Journal of Plant Biology 62:147-160.

Kar M, Miashra D (1976) Catalase, peroxidase and polyphenoloxidase activities during rice leaf senescence. Plant Physiology 57:315-319.

Kashiwa T, Muraki Y, Yamanaka N (2020) Near-isogenic soybean lines carrying Asian soybean rust resistance genes for practical pathogenicity validation. Scientific Reports 10:13270.

Kaur S, Samota MH, Choudhary M, Choudhary M, Pandey AK, Sharma A, Thakur J (2022) How do plants defend themselves against pathogens - Biochemical mechanisms and genetic interventions. Physiology and Molecular Biology of Plants 28:485-504.

Kesel J, Conrath U, Flors V, Luna E, Mageroy MH, Mauch-Mani B, Pastor V, Pozo MJ, Pieterse CMJ, Ton J, Kyndt T (2021) The induced resistance lexicon: do's and don'ts. Trends in Plant Science 26:685-691.

Kim JA, Chung IM (2007) Change in isoflavone concentration of soybean (*Glycine max* L.) seeds at different growth stages. Journal of the Science of Food and Agriculture 87:496-503.

Klosowski AC, Castellar C, Stammler G, May de Mio LL (2018) Fungicide sensitivity and monocyclic parameters related to the *Phakopsora pachyrhizi*-soybean pathosystem from organic and conventional soybean production systems. Plant Pathology 67:1697-1705.

Kramer DM, Johnson G, Kiirats O, Edwards GE (2004) New fluorescence parameters for the determination of Q_A redox state and excitation energy fluxes. Photosynthesis Research 79:209-218.

Kravchuk Z, Vicedo B, Flors V, Camañes G, González-Bosch C, García-Agustín P (2011) Priming for JA-dependent defenses using hexanoic acid is an effective mechanism to protect *Arabidopsis* against *B. cinerea.* Journal of Plant Physiology 168:359-366.

Kuzniak E, Sklodowska M (1999) The effect of *Botrytis cinerea* infection on ascorbate glutathione cycle in tomato leaves. Plant Science 148:69-76.

Langenbach C, Campe R, Beyer SF, Mueller AN, Conrath U (2016) Fighting Asian soybean rust. Frontiers of Plant Science 7:797.

Lever M (1972) A new reaction for colorimetric determination of carbohydrates. Analytical Biochemistry 47:273-279.

Leyva MO, Vicedo B, Finiti I, Flors V, DelAmo G, Real MD (2008) Preventive and post-infection control of *Botrytis cinerea* in tomato plants by hexanoic acid. Plant Pathology 57:1038-1046.

Liu Y, Dammann C, Bhattacharyya MK (2001) The matrix metalloproteinase gene *GmMMP2* is activated in response to pathogenic infections in soybean. Plant Physiology 127:1788-1797.

Livak KJ, Schmittgen TD (2001) Analysis of relative gene expression data using Real-time quantitative PCR and the $2^{-\Delta\Delta CT}$ method. Methods 25:402-408.

Li X, Esker PD, Pan Z, Dias AP, Xue L, Yang XB (2010) The uniqueness of the soybean rust pathosystem: an improved understanding of the risk in different regions of the word. Plant Disease 94:796-806.

Llorens E, Camañes G, Lapeña L, García-Agustín P (2016) Priming by hexanoic acid induce activation of mevalonic and linolenic pathways and promotes the emission of plant volatiles. Frontiers in Plant Science 7:495.

Llorens E, Scalschi L, Fernández-Crespo E, Lapeña L, García-Agustín P (2015a) Hexanoic acid provides long-lasting protection in 'Fortune' mandarin against *Alternaria alternata*. Physiological and Molecular Plant Pathology 91:38-45.

Llorens E, Vicedo B, López MM, Lapeña L, Graham JH, García-Agustín P (2015b) Induced resistance in sweet orange against *Xanthomonas citri* subsp. *citri* by hexanoic acid. Crop Protetion 74:77-84.

Lyon G (2007) Agents that can elicit induced resistance. In: Walters D, Newton A, Lyon G (Eds). Induced resistance for plant defense: A sustainable approach to crop protection. Blackwell Publishing. pp. 9-23.

Marino G, Funk C (2012) Matrix metalloproteinases in plants: a brief overview. Physiology Plantarum 145:196-202.

Mohammadi MA, Cheng Y, Aslam M, Jakada BH, Wai MH, Ye K, He X, Luo T, Ye L, Dong C, Hu B, Priyadarshani SVGN, Wang-Pruski G, Qin Y (2021) ROS and oxidative response systems in plants under biotic and abiotic stresses: revisiting the crucial role of phosphite triggered plants defense response. Frontiers in Microbiology 12:18.

Moore KJ, Dixon PM (2015) Analysis of combined experiments revisited. Agronomy Journal 107:763-771.

Mortel M, Recknor JC, Graham MA, Nettleton D, Dittman JD, Nelson RT, Godoy CV, Abdelnoor RV, Almeida AMR, Baum TJ, Whitha SA (2007) Distinct biophasic mRNA changes in response to Asian soybean rust infection. Molecular Plant-Microbe Interactions 20:887-899.

Nakano Y, Asada K (1981) Hydrogen peroxide is scavenged by ascorbate specific peroxidase in spinach chloroplasts. Plant and Cell Physiology 22:867-880.

Nicoli F, Negro C, Nutricati E, Vergine M, Aprile A, Sabella E, Damiano G, Bellis LD, Luvisi A (2019) Accumulation of azelaic acid in *Xylella fastidiosa*-infected olive trees: a mobile metabolite for health screening. Phytopathology 109:318-325.

Ntalli N, Menkissoglu-Spiroudi U, Doitsinis K, Kalomoiris M, Papadakis EM, Boutsis G, Dimou M, Monokrousos N (2020) Mode of action and ecotoxicity of hexanoic and acetic acids on *Meloidogyne javanica.* Journal of Pest Science 93:867-877.

Ojaghian MR, Wang L, Cui Zq, Yang C, Zhongyun T, Xie GL (2014) Antifungal and SAR potential of crude extracts derived from neem and ginger against storage carrot rot caused by *Sclerotinia sclerotiorum*. Industrial Crops and Products 55:130-139.

Oxborough K, Baker NR (1997). Resolving chlorophyll *a* fluorescence images of photosynthetic efficiency into photochemical and non-photochemical components - calculation of *qP* and *Fv′*/*Fm′* without measuring *Fo′*. Photosynthesis Research 54:135-142.

Pagano MC, Miransari M (2016) The importance of soybean production worldwide. In: Miransari M (Ed.). Abiotic and biotic stresses in soybean production. 1st Edition, Academic Press. pp. 1-26.

Paula S, Holz S, Souza DHG, Pascholati SF (2021) Potential of resistance inducers for soybean rust management. Canadian Journal of Plant Pathology 43:298-307.

Park S (2010) Study of host-fungus interactions between soybean and *Phakopsora pachyrhizi* using proteomics. *Louisiana State University. Doctoral Dissertations* 3217.

Picanço BBM, Ferreira S, Fontes BA, Oliveira LM, Silva BN, Einhardt AM, Rodrigues FA (2021) Soybean resistance to *Phakopsora pachyrhizi* infection is barely potentiated by boron. Physiological and Molecular Plant Pathology 115:101668.

Pieterse CM, Van der Does D, Zamioudis C, Leon-Reyes A, Van Wees SC (2012) Hormonal modulation of plant immunity. Annual Review of Phytopathology 28:489-521.

Reignault P, Walters D (2007) Topical applications of inducers for disease control. In: Walters D, Newton A, Lyon G (Eds). Induced resistance for plant defense: A sustainable approach to crop protection. Blackwell Publishing. pp.179-200.

Resende RS, Rodrigues FA, Cavatte PC, Martins SCV, Moreira WR, DaMatta FM (2012) Leaf gas exchange and oxidative stress in sorghum plants supplied with silicon and infected with *Colletotrichum sublineolum*. Phytopathology 102:892-898.

Rios VS, Rios JA, Aucique-Pérez CE, Silveira PR, Barros AV, Rodrigues FA (2018) Leaf gas exchange and chlorophyll *a* fluorescence in soybean leaves infected by *Phakopsora pachyrhizi*. Journal of Phytopathology 166:75-85.

Sánchez-Vallet A, Mesters JR, Thomma BPHJ (2014) The battle for chitin recognition in plant-microbe interactions. FEMS Microbiology Reviews 39:171-183.

Santos IMO, Abe VY, Carvalho K, Barazetti AR, Simionato AS, Pega, GEA, Matis SH, Cano BG, Cely MVT, Marcelino-Guimarães FC, Chryssafidis AL, Andrade G (2021) Secondary metabolites of *Pseudomonas aeruginosa* Iv strain decrease Asian soybean rust severity in experimentally infected plants. *Plants 10*:1495.

Santos RP, Cruz ACF, Iarema L, Kuki KN, Otoni WC (2008) Protocolo para extração de pigmentos foliares em porta-enxertos de videira micropropagados. Ceres 55:356-364.

Scalschi L, Camañes G, Llorens E, Fernández-Crespo E, López MM, García-Agustín P (2014) Resistance inducers modulate *Pseudomonas syringae* pv. *tomato* strain DC3000 response in tomato plants. PLoS ONE 9:e106429.

Shah A, Smith DL (2020) Flavonoids in Agriculture: Chemistry and roles in, biotic and abiotic stress responses, and microbial associations. *Agronomy 10:*1209.

Shah J, Zeier J (2013) Long-distance communication and signal amplification in systemic acquired resistance. Frontiers of Plant Science 4:30.

Shaner G, Finney RE (1977) The effect of nitrogen fertilization on the expression of slow-mildewing resistance in Knox wheat. Phytopathology 67:1051-1056.

Siah A, Randoux B, Magnin-Robert M, Choma C, Rivière C, Halama P, Reignault P (2018) Natural agents inducing plant resistance against pests and diseases. In: Mérillon JM, Rivière C (Eds). Natural Antimicrobial Agents, Sustainable Development and Biodiversity series. Springer. pp. 121-159.

Scherm H, Christiano RSC, Esker PD, Del Ponte EM, Godoy CV (2009) Quantitative review of fungicide efficacy trials for managing soybean rust in Brazil. Crop Protection 28:774-782.

Singh A, Lim GH, Pradeep Kachroo P (2017) Transport of chemical signals in systemic acquired resistance. Journal of Integrative Plant Biology 59:336-344.

Singh G (2010) The soybean: botany, production and uses. In: Qui LQ, Chang RZ (Eds). The origin and history of soybean. CABI International. pp 1-23.

Tatagiba SD, Rodrigues FA, Filippi MCC, Silva GB, Silva LC (2014) Physiological responses of rice plants supplied with silicon to *Monographella albescens* infection. Journal of Phytopathology 162:596-606.

van Loon LC, Rep M, Pieterse CMJ (2006) Significance of inducible defense-related proteins in infected plants. Annual Review of Phytopathology 44:135-162.

Velikova V, Yordanov I, Edreva A (2000) Oxidative stress and some antioxidant systems in acid rain-treated bean plants: Protective role of exogenous polyamines. Plant Science 151:59-66.

Vellosillo T, Vicente J, Kulasekaran S, Hamberg M, Castresana C (2010) Emerging complexity in reactive oxygen species production and signalling during the response of plants to pathogens. Plant Physiology 154:444-448.

Vicedo B, Flors V, Leyva MD, Finiti I, Kravchuk Z, Real MD (2009) Hexanoic acid-induced resistance against *Botrytis cinerea* in tomato plants. Molecular Plant-Microbe Interactions 22:1455-1465.

Vlot AC, Dempsey DA, Klessig DF (2009) Salicylic acid, a multifaceted hormone to combat disease. Annual Review of Phytopathology 47:177-206.

Vlot AC, Sales JH, Lenk M, Bauer K, Brambilla A, Sommer A, Chen Y, Wenig M, Nayem S (2021) Systemic propagation of immunity in plants. New Phytologist 229:1234-1250.

Wiebke-Strohm B, Pasquali G, Margis-Pinheiro M, Bencke M, Bücker-Neto L, Better-Ritt AB (2012) Ubiquitous urease affects soybean susceptibility to fungi. Plant Molecular Biology 79:75-87.

Yaguchi T, Kinami T, Ishida T, Yasuhara T, Takahashi K, Matsuura H (2017) Induction of plant disease resistance upon treatment with yeast cell wall extract. Bioscience, Biotechnology, and Biochemistry 81:2071-2078.

You X, Fang H, Wang R, Wang GL, Ning Y (2020) Phenylalanine ammonia lyases mediate broad-spectrum resistance to pathogens and insect pests in plants. Science Bulletin 65:1425-1427.

Yu G, Zou J, Wang J, Zhu R, Qi Z, Jiang H, Hua Z, Yang M, Zhao Y, Wua X, Liu C, Li C, Yang X, Zhu Z, Chen Q, Fu Y, Xin D (2022) A soybean NAC homolog contributes to resistance to *Phytophthora sojae* mediated by dirigent proteins. The Crop Journal 10:332-341.

Zeier J (2021) Metabolic regulation of systemic acquired resistance. Current Opinion in Plant Biology 62:102050.

Zoeller M, Stingl N, Krischke M, Fekete A, Waller F, Berger S, Mueller MJ (2012) Lipid profiling of the *Arabidopsis* hypersensitive response reveals specific lipid peroxidation and fragmentation processes: biogenesis of pimelic and azelaic acid. *Plant Physiology* 160:365-378.

Tables and Figures

Table 1. Primer sequences for the genes phenylalanine ammonia-lyase (*PAL1.1*, *PAL1.3*, *PAL2.1*, and *PAL3.1*), pathogenesis-related protein 1 (*PR1-A*), pathogenesis-related protein 10 (*PR10*), metalloproteinase (*MMP2*), urease (*URE*), isochorismate synthase (*ICS1* and *ICS2*), chalcone isomerase (*CHIB1*), 1-aminocyclopropane-1-carboxylic acid oxidase (*ACO*), 1-aminocyclopropane-1-carboxylic synthase (*ACS*), ethylene receptor 1 (*ETR1*), salicylic acid methyltransferase (*SABATH2*), 12-oxophytodienoic acid reductase 3 (*OPR3*), jasmonic acid-amino synthetase (*JAR1*), NAC transcriptional factor (*NAC19*), ubiquitin-3 (*UBIQ*), glyceraldehyde 3-phosphate dehydrogenase (*GAPDH*), and translation elongation factor 1α (*TEF-1*α) of *Phakopsora pachyrhizi*.

Genes	GenBank Identifications	Primer Sense 5'-3'	Primer Antisense 5'-3'
PAL1.1	Glyma 19G182300	GCAAGTGCAACCATAATCATTT	AACCAAAGCTCCGGCAAA
PAL1.3	Glyma 03g181600	TTTGTACCTATGCAAGAAAAACCA	TGAAGGAACATTGAAATTAGGCT
PAL2.1	Glyma 10G058200	ATCTCCCTCCACTCACCATA	GTTCAAGGGGTCATTAGCAC
PAL3.1	Glyma 02G309300	TGCTCTTCAGAAGGAAATGGT	GTTGCTGATTTAGGCAGTGT
PR1-A	AF136636.1	GCACTACACACAGGTCGTTTGG	CCTCCGTTATCACATGTCACTTTG
PR10	Glyma 09G040500	AAATCAACTCCCCTGTGGCTC	CCACCATTTCCCTCAACGTTT
MMP2	Glyma 01G0369001	TGGGCTCTTCCCAGTGAAA	TTGCCGCACTCTCCAAGTC
URE	Glyma 11g248700	AGTTAGTCACCATTCATGACCT	CAAGTGAAGGTACTGGAAGAAAA
ICS1	Glyma 01G104100	GAAACAGTACAGTCCCTGCT	TGTGGCTGGGAAAAGAAAAC
ICS2	Glyma 03G070600	GCAACATCCTCGTACCTCTT	CTCTCTGCAACCGTTCATTG
CHIB1	Glyma 20G2416001	GTTTCCCCTGCTTTGAAAGAGA	GGATTGGCCTCTAACTCTTTGAAG
ACO	Glyma 14g05350	CCAATGCGCCATTCCATTGTTG	TGAGGCTACGGACATTCTGGTC
ACS	Glyma 05g36250	CTCTTAACCTTCATTCTTGCTAACC	TTGCTTCTGCTTCTTTGTATGC
ETR1	Glyma 19g40090	ATGGATGCCTTCAAGAAGTGG	GCACATATCTTCCCACAAGAGG
SABATH2	NM 001250193.1	GGATTCCAGCGATTGTTCGTT	GGCAAGAGGACCAAACCAAAT
OPR3	Glyma 13G109800	GTGTATCAGCCTGGTGGG	GTGTATCAGCCTGGTGGG
JAR1	LOC 100813492	AGCCGTATGGTTGTGTTGTTC	TGCAGCATTGGGATTGGAGT

NAC19	Glyma 13G030900	TCGTTCACTATCTCTGCCGC	CCAACAGGTTTCGGTTTGCC
UBIQ	Glyma 20g141600	GTGTAATGTTGGATGTGTTCCC	ACACAATTGAGTTCAACACAAACCG
GAPDH	Glyma 04G193500	AAGGGTGGTGCAAAGAAGGT	TCTGGCTTGTACTCGTGCTC
TEF-1α	EF 560586.1	ATTCGAAGCCGGTATTTCTAAAG	CCACTTGGTTGTGTCCATCTTAT

Table 2. Analysis of variance for the effects of products (P), plant inoculation (PI), and the interaction P × PI for severity (Sev), area under disease progress curve (AUDPC), parameters of chlorophyll *a* fluorescence (maximum PSII quantum yield (F_v/F_m), effective PSII quantum yield (Y(II)), quantum yield of regulated energy dissipation (Y(NPQ)), quantum yield of non-regulated energy dissipation (Y(NO), and electron transport rate (ETR)), concentrations of photosynthetic pigments (chlorophyll *a*+*b* (Chl *a*+*b*) and carotenoids (Car)), concentrations of metabolites (malondialdehyde (MDA), hydrogen peroxide (H_2O_2), and superoxide anion radical ($O_2^{\bullet-}$)), activities of antioxidant (superoxide dismutase (SOD), peroxidase (POX), catalase (CAT), ascorbate peroxidase (APX), glutathione reductase (GR)) and defense-related enzymes (chitinase (CHI), *β*-1,3-glucanase (GLU), phenylalanine ammonia-lyase (PAL), polyphenoloxidase (PPO), and lipoxygenase (LOX)) as well as expression of genes encoding for phenylalanine ammonia-lyase (*PAL1.1*, *PAL1.3*, *PAL2.1*, and *PAL3.1*), pathogenesis-related protein 1 (*PR1-A*), pathogenesis-related protein 10 (*PR10*), metalloproteinase (*MMP2*), urease (*URE*), isochorismate synthase (*ICS1* and *ICS2*), chalcone isomerase (*CHIB1*), 1-aminocyclopropane-1-carboxylic acid oxidase (*ACO*), 1-aminocyclopropane-1-carboxylic synthase (*ACS*), ethylene receptor 1 (*ETR1*), salicylic acid methyltransferase (*SABATH2*), 12-oxophytodienoic acid reductase 3 (*OPR3*), jasmonic acid-amino synthetase (*JAR1*), and NAC transcriptional factor (*NAC19*).

Variables/Parameters	P	PI	P × PI
Sev	**<0.001**	-	-
AUDPC	**<0.001**	-	-
F_v/F_m	0.156	0.975	0.110
Y(II)	**<0.001**	**<0.001**	**<0.001**
Y(NPQ)	0.352	**<0.001**	0.351
Y(NO)	0.149	**0.013**	0.076
ETR	0.160	**<0.001**	**0.036**
Chl *a*+*b*	**0.010**	**<0.001**	0.488
Car	**<0.001**	**<0.001**	**<0.005**
MDA	**<0.001**	**<0.001**	**<0.001**
H_2O_2	0.320	**0.002**	0.954
$O_2^{\bullet-}$	0.070	**0.029**	0.056
SOD	**0.014**	0.191	0.356

POX	**0.027**	**<0.001**	**0.033**
CAT	**0.004**	**0.037**	0.406
APX	0.410	0.352	0.373
GR	**0.001**	0.831	**0.001**
CHI	0.051	**<0.001**	0.251
GLU	0.871	**<0.001**	0.489
PAL	**0.010**	**0.008**	0.299
PPO	0.527	**<0.001**	0.364
LOX	0.474	0.067	0.083
PAL1.1	0.145	**<0.001**	**0.014**
PAL1.3	**0.026**	**<0.001**	0.364
PAL2.1	0.758	**0.004**	0.631
PAL3.1	**0.006**	**<0.001**	**0.014**
PR1-A	0.147	**<0.001**	0.341
PR10	0.355	**<0.001**	0.776
MMP2	0.279	**0.009**	0.407
URE	**0.015**	0.414	**0.044**
ICS1	0.428	**0.018**	0.556
ICS2	0.154	**0.001**	0.335
CHIB1	0.191	**<0.001**	**0.002**
ACO	0.172	**<0.001**	0.637
ACS	0.175	0.107	**<0.001**
ETR1	0.228	0.260	0.464
SABATH2	0.136	**<0.001**	0.110
OPR3	0.694	**<0.001**	0.891
JAR1	0.072	0.362	0.522
NAC19	0.514	0.916	0.232

Bold values are significant at $P \leq 0.05$.

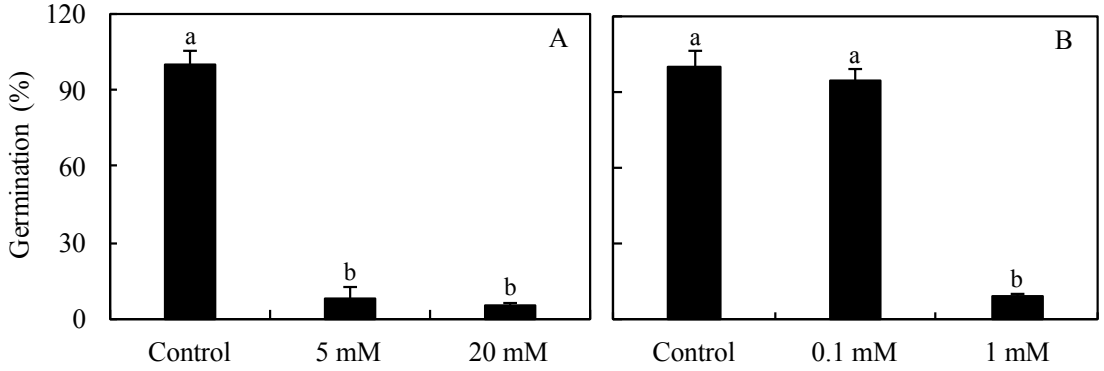

Figure 1. Germination of urediniospores from *Phakopsora pachyrhizi* in Petri dishes containing water-agar medium amended with hexanoic acid (5 and 20mM) (A) and azelaic acid (0.1 and 1 mM) (B). Water-agar medium non-amended with azelaic acid or hexanoic acid served as the control treatment. Treatments followed by the same letter (graphics A and B) do not differ significantly at $P > 0.05$ as determined by the Tukey's test. Standard error of means is represented for each bar.

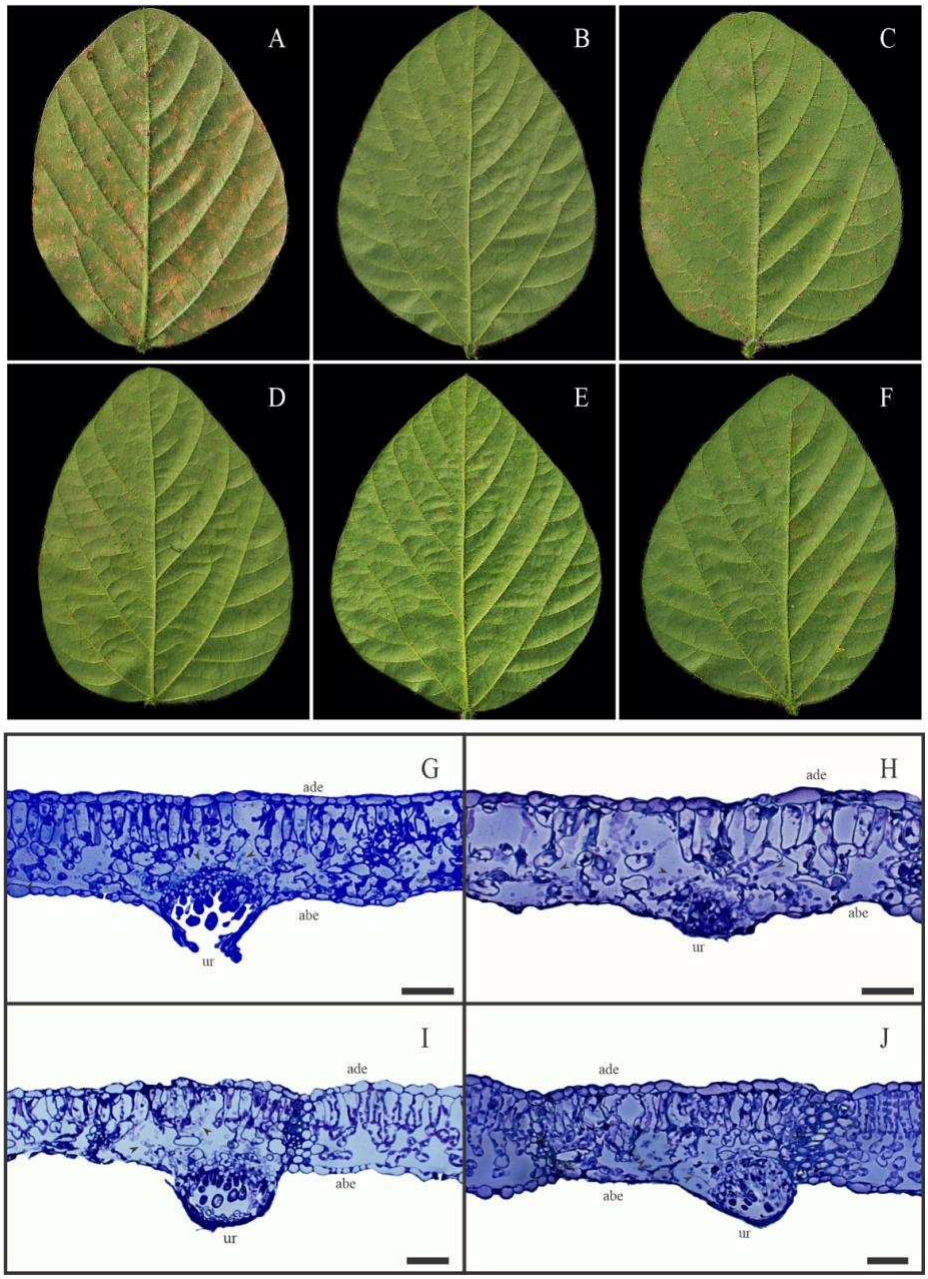

Figure 2. Symptoms of soybean rust (chlrosis and necrosis) and sporulation of *Phakopsora pachyrhizi* in the abaxial surface of leaflets from soybean plants sprayed with water (control) (A), Acibenzolar-S-Methyl (ASM) (B), hexanoic acid (HxA) (5 and 20 mM; C and D, respectively), and azelaic acid (AzA) (0.1 and 1 mM; E and F, respectively). Light micrographs of transverse sections of leaflet tissue from soybean plants sprayed with water, ASM, HxA (20 mM), and AzA (1 mM) (G, H, I, and J, respectively) at 15 days after inoculation with *P. pachyrhizi*. ade = adaxial epidermis, abe = abaxial epidermis, ur = uredinia, and arrowheads = fungal cells. Scale bars = 50 μm.

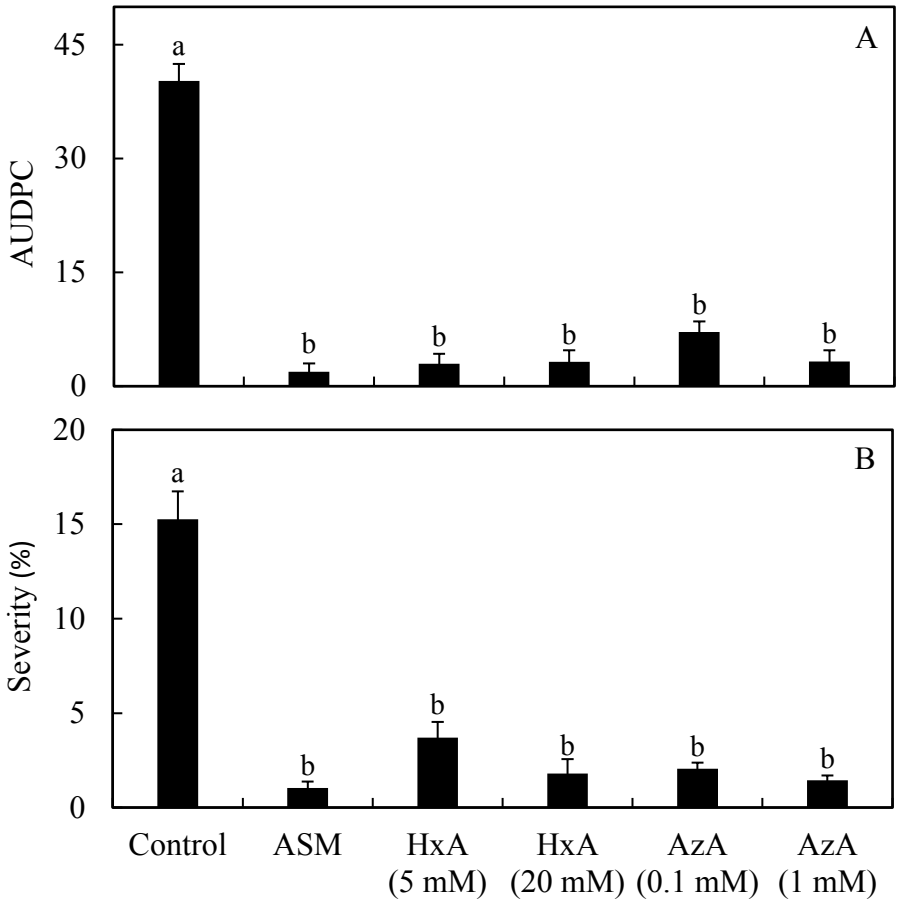

Figure 3. Area under disease progress curve (AUDPC) (A) and final severity (20 dai) of soybean rust estimated by using the software QUANT (B) for soybean plants sprayed with water (control), Acibenzolar-S-Methyl (ASM), hexanoic acid (HxA) (5 and 20 mM), and azelaic acid (AzA) (0.1 and 1 mM). Treatments followed by the same letter (graphics A and B) do not differ significantly at $P > 0.05$ as determined by the Tukey's test. Standard error of means is represented in each bar.

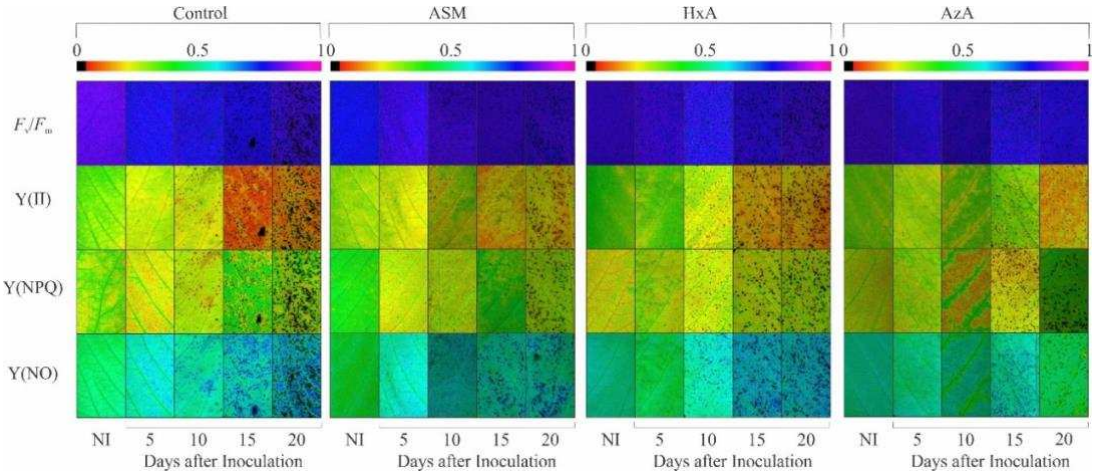

Figure 4. Images of chlorophyll *a* fluorescence parameters maximum PSII quantum yield (F_v/F_m), effective PSII quantum yield (Y(II)), quantum yield of regulated energy dissipation (Y(NPQ)), and quantum yield of non-regulated energy dissipation (Y(NO)) obtained from leaflets of soybean plants sprayed with water (control), Acibenzolar-S-Methyl (ASM), hexanoic acid (HxA), and azelaic acid (AzA) and non-inoculated (NI) or at 5, 10, 15, and 20 days after inoculation with *Phakopsora pachyrhizi*.

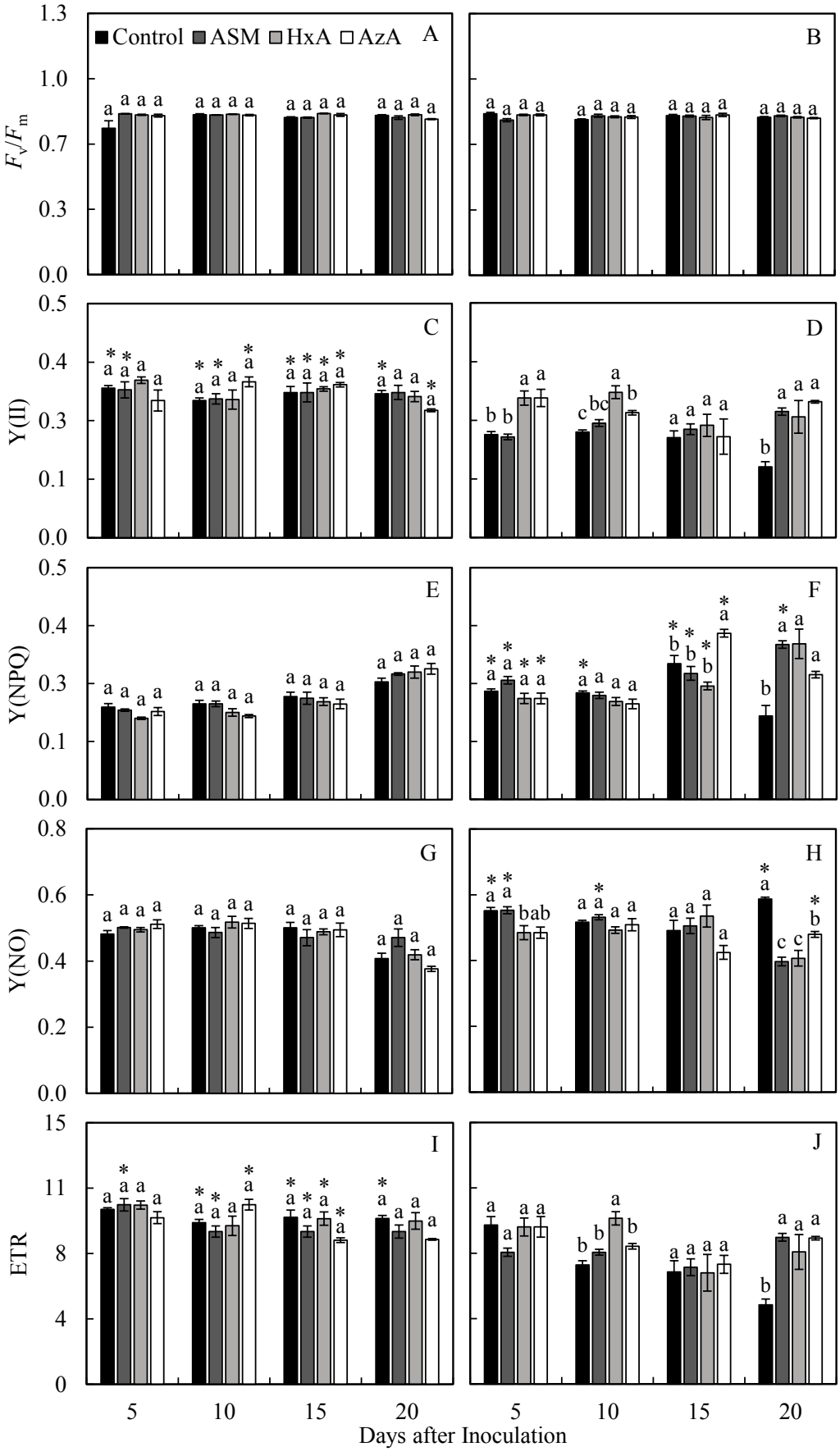
Control
ASM
HxA
AzA
A
B
C
D
E
F
G
H
I
J
F_v/F_m
Y(II)
Y(NPQ)
Y(NO)
ETR
Days after Inoculation
5
10
15
20

Figure 5. Quantification of chlorophyll *a* fluorescence parameters maximum PSII quantum yield (F_v/F_m) (A and B), effective PSII quantum yield (Y(II)) (C and D), quantum yield of regulated energy dissipation (Y(NPQ)) (E and F), quantum yield of non-regulated energy dissipation (Y(NO)) (G and H), and electron transport rate (ERT) (I and J) determined on the leaflets of soybean plants non-inoculated (A, C, E, G, and I) or inoculated (B, D, F, H, and J) with *Phakopsora pachyrhizi* and sprayed with water (control), Acibenzolar-S-Methyl (ASM), hexanoic acid (HxA), and azelaic acid (AzA). Means from non-inoculated and inoculated plants followed by an asterisk (*), at each evaluation time, are significantly different according to the *F* test ($P \leq 0.05$). Means from control, ASM, HxA, and AzA treatments followed by different letters, at each evaluation time, are significantly different according to the Tukey's test ($P \leq 0.05$). Bars represent the standard deviation of the means.

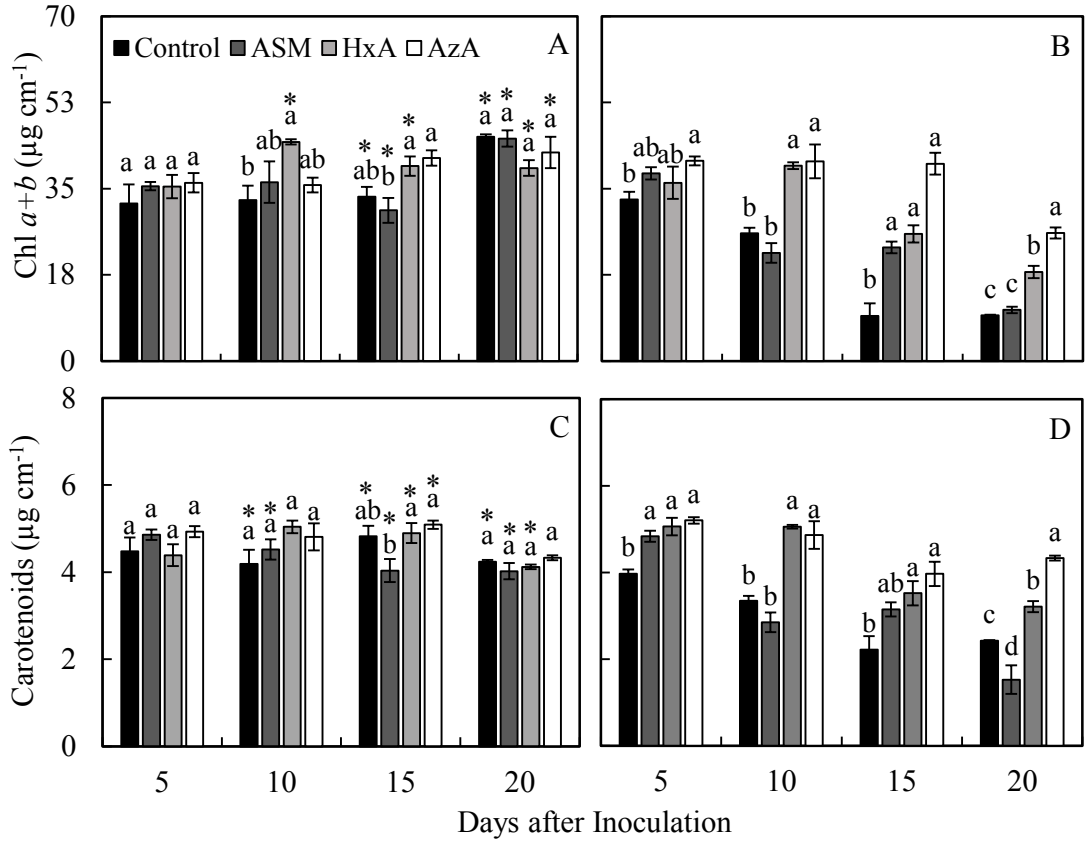

Figure 6. Concentrations of chlorophyll *a*+*b* (Chl *a*+*b*) (A and B) and carotenoids (C and D) determined on the leaves of soybean plants non-inoculated (A and C) or inoculated (B and D) with *Phakopsora pachyrhizi* and sprayed with water (control), Acibenzolar-S-Methyl (ASM), hexanoic acid (HxA), and azelaic acid (AzA). Means from non-inoculated and inoculated plants followed by an asterisk (*), at each evaluation time, are significantly different according to the *F* test ($P \leq 0.05$). Means from control, ASM, HxA, and AzA treatments followed by different letters, at each evaluation time, are significantly different according to the Tukey's test ($P \leq 0.05$). Bars represent the standard deviation of the means.

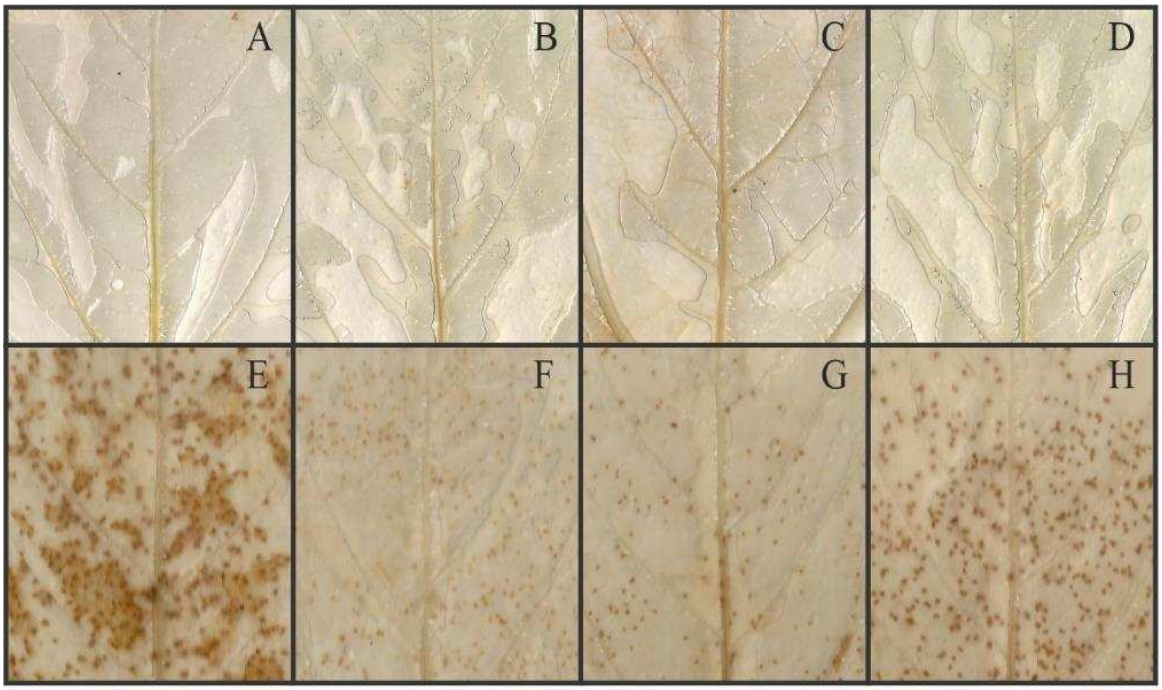

Figure 7. Histochemical detection of hydrogen peroxide on leaflets of soybean plants non-inoculated (A, B, C, and D) or inoculated (E, F, G, and H) with *Phakopsora pachyrhizi* and sprayed with water (control) (A and E), Acibenzolar-S-Methyl (B and F), hexanoic acid (C and G), and azelaic acid (D and H). The leaflets were sampled at 20 days after non-inoculation or inoculation of plants with *P. pachyrhizi*.

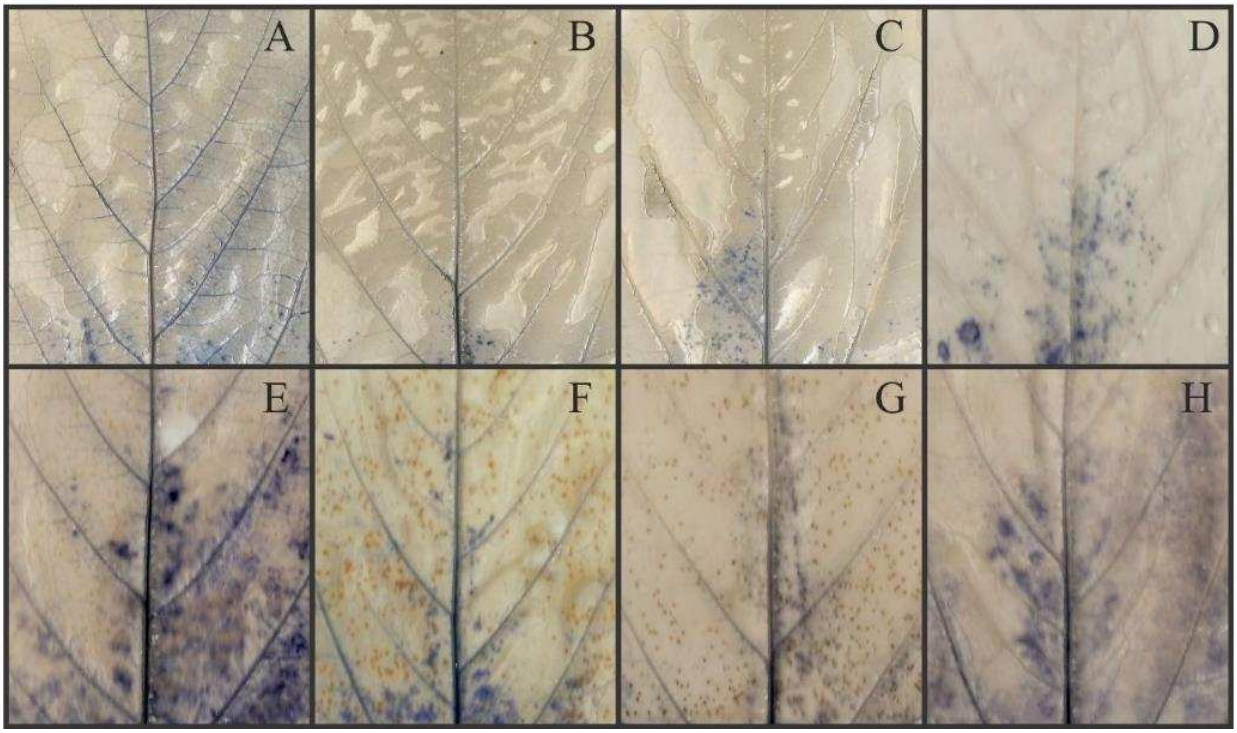

Figure 8. Histochemical detection of superoxide anion radical on the leaflets of soybean plants non-inoculated (A, B, C, and D) or inoculated (E, F, G, and H) with *Phakopsora pachyrhizi* and sprayed with water (control) (A and E), Acibenzolar-S-Methyl (B and F), hexanoic acid (C and G), and azelaic acid (D and H). The leaflets were sampled at 20 days after non-inoculation or inoculation of plants with *P. pachyrhizi*.

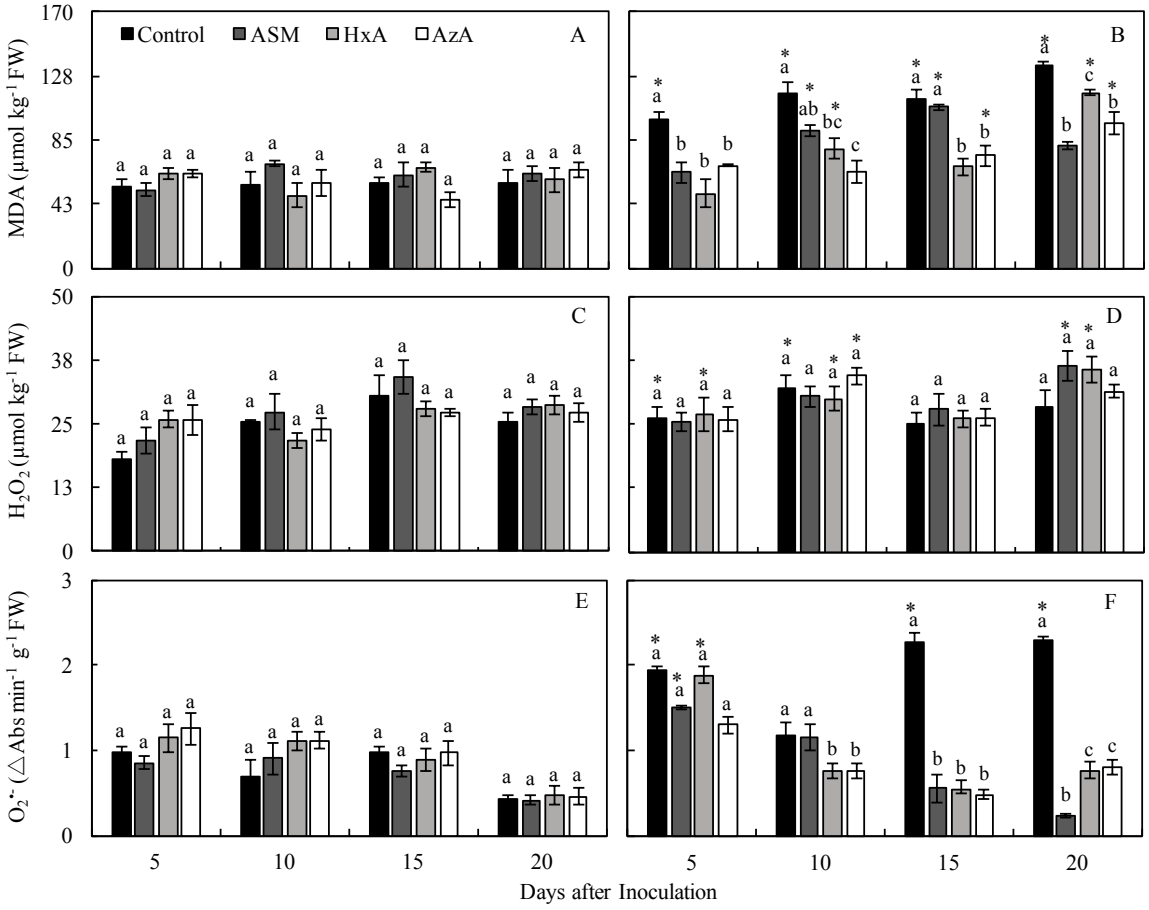

Figure 9. Concentrations of malondialdehyde (MDA) (A and B), hydrogen peroxide (H_2O_2) (C and D), and superoxide anion radical ($O_2^{\bullet-}$) (E and F) determined on leaves of soybean plants non-inoculated (A and C) or inoculated (B and D) with *Phakopsora pachyrhizi* and sprayed with water (control), Acibenzolar-S-Methyl (ASM), hexanoic acid (HxA), and azelaic acid (AzA). Means from non-inoculated and inoculated plants followed by an asterisk (*), at each evaluation time, are significantly different according to the *F* test ($P \leq 0.05$). Means from control, ASM, HxA, and AzA treatments followed by different letters, at each evaluation time, are significantly different according to the Tukey's test ($P \leq 0.05$). Bars represent the standard deviation of the means. FW = fresh weight.

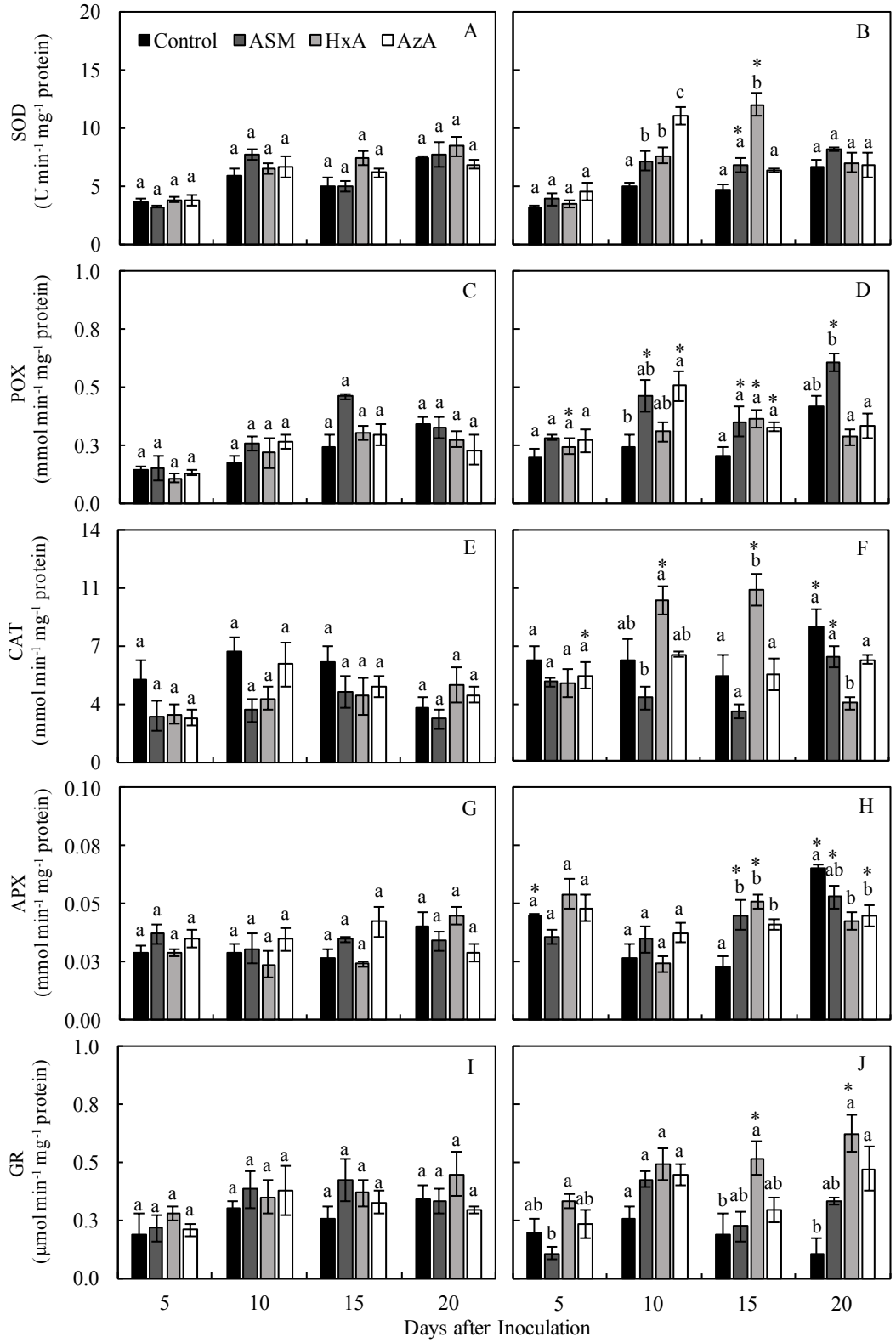
Control
ASM
HxA
AzA
A
B
C
D
E
F
G
H
I
J
SOD (U min-1 mg-1 protein)
POX (mmol min-1 mg-1 protein)
CAT (mmol min-1 mg-1 protein)
APX (mmol min-1 mg-1 protein)
GR (μmol min-1 mg-1 protein)
Days after Inoculation

Figure 10. Activities of superoxide dismutase (SOD) (A and B), peroxidase (POX) (C and D), catalase (CAT) (E and F), ascorbate peroxidase (APX) (G and H), and glutathione reductase (GR) (I and J) determined on leaves of soybean plants non-inoculated (A, C, E, G, and I) or inoculated (B, D, F, H, and J) with *Phakopsora pachyrhizi* and sprayed with water (control), Acibenzolar-S-Methyl (ASM), hexanoic acid (HxA), and azelaic acid (AzA). Means from non-inoculated and inoculated plants followed by an asterisk (*), at each evaluation time, are significantly different according to the *F* test ($P \leq 0.05$). Means from control, ASM, HxA, and AzA treatments followed by different letters, at each evaluation time, are significantly different according to the Tukey's test ($P \leq 0.05$). Bars represent the standard deviation of the means.

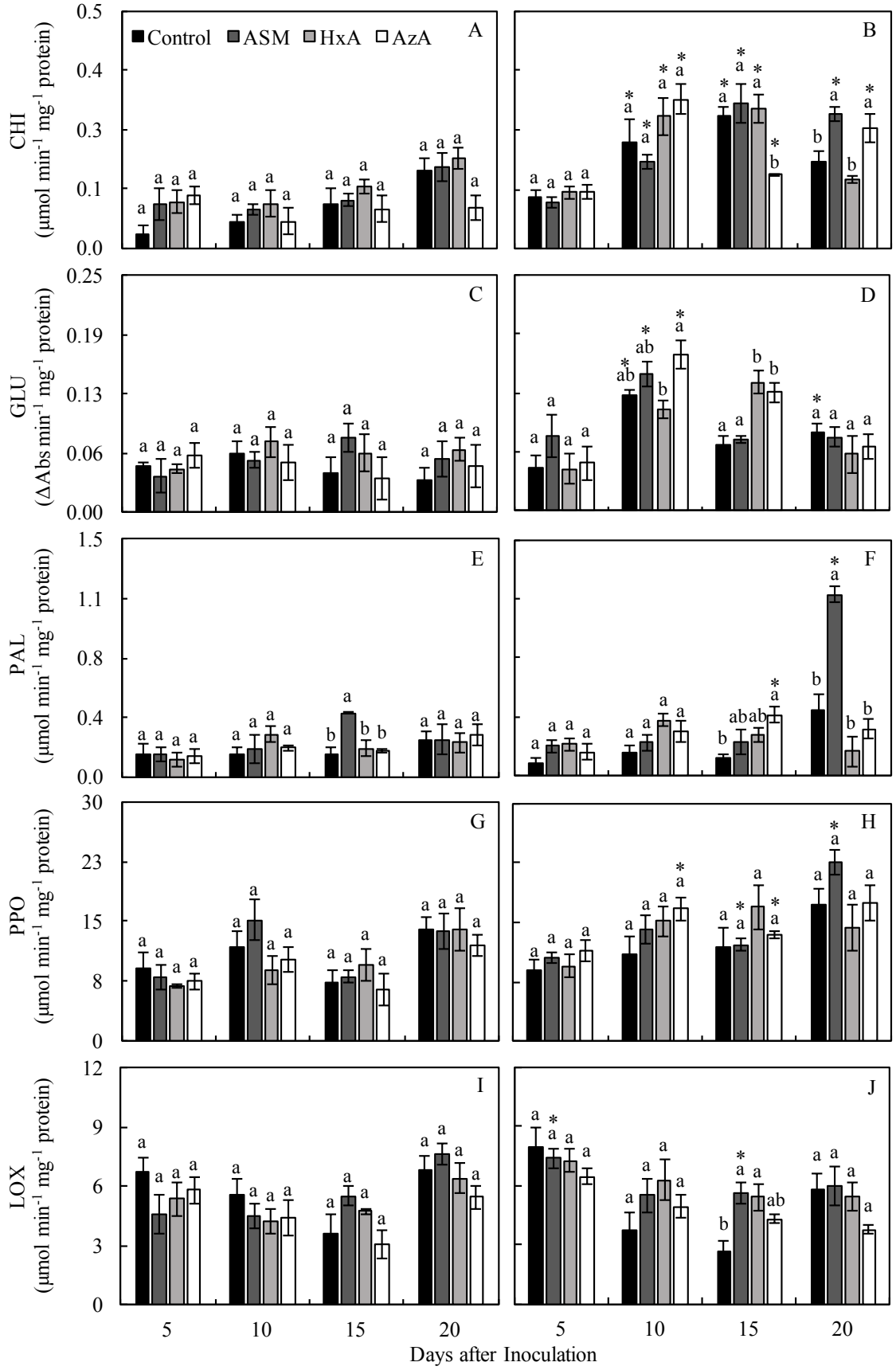
Control
ASM
HxA
AzA
A
B
C
D
E
F
G
H
I
J
CHI (μmol min-1 mg-1 protein)
GLU (ΔAbs min-1 mg-1 protein)
PAL (μmol min-1 mg-1 protein)
PPO (μmol min-1 mg-1 protein)
LOX (μmol min-1 mg-1 protein)
0.5
0.4
0.3
0.1
0.0
0.25
0.19
0.13
0.06
0.00
1.5
1.1
0.8
0.4
0.0
30
23
15
8
0
12
9
6
3
0
5
10
15
20
Days after Inoculation

Figure 11. Activities of chitinase (CHI) (A and B), *β*-1,3-glucanase (GLU) (C and D), phenylalanine ammonia-lyase (PAL) (E and F), polyphenoloxidase (PPO) (G and H), and lipoxygenase (LOX) (I and J) determined on leaves of soybean plants non-inoculated (A and C) or inoculated (B and D) with *Phakopsora pachyrhizi* and sprayed with water (control), Acibenzolar-S-Methyl (ASM), hexanoic acid (HxA), and azelaic acid (AzA). Means from non-inoculated and inoculated plants followed by an asterisk (*), at each evaluation time, are significantly different according to the *F* test ($P \leq 0.05$). Means from control, ASM, HxA, and AzA treatments followed by different letters, at each evaluation time, are significantly different according to the Tukey's test ($P \leq 0.05$). Bars represent the standard deviation of the means.

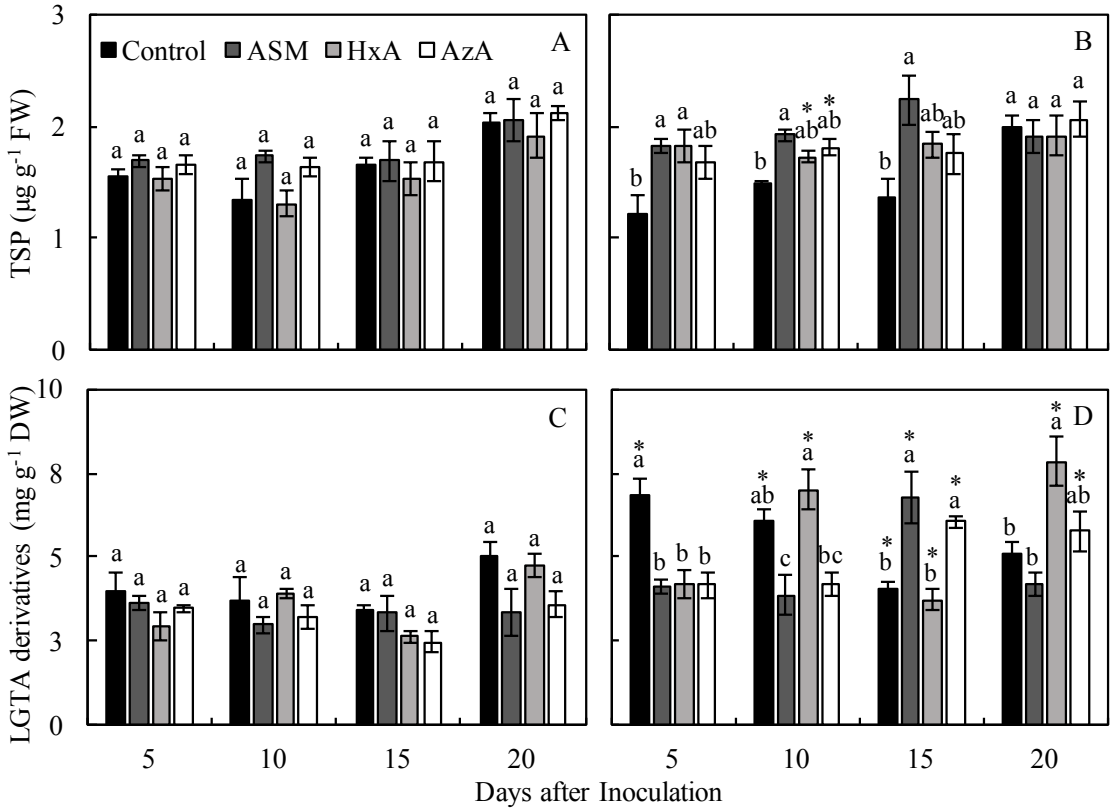

Figure 12. Concentrations of total soluble phenols (TSP) (A and B) and lignin-thioglycolic acid (LTGA) derivatives (C and D) determined on leaves of soybean plants non-inoculated (A and C) or inoculated (B and D) with *Phakopsora pachyrhizi* and sprayed with water (control), Acibenzolar-S-Methyl (ASM), hexanoic acid (HxA), and azelaic acid (AzA). Means from non-inoculated and inoculated plants followed by an asterisk (*), at each evaluation time, are significantly different according to the *F* test ($P \leq 0.05$). Means from control, ASM, HxA, and AzA treatments followed by different letters, at each evaluation time, are significantly different according to the Tukey's test ($P \leq 0.05$). Bars represent the standard deviation of the means. FW and DW = fresh and dry weight, respectively.

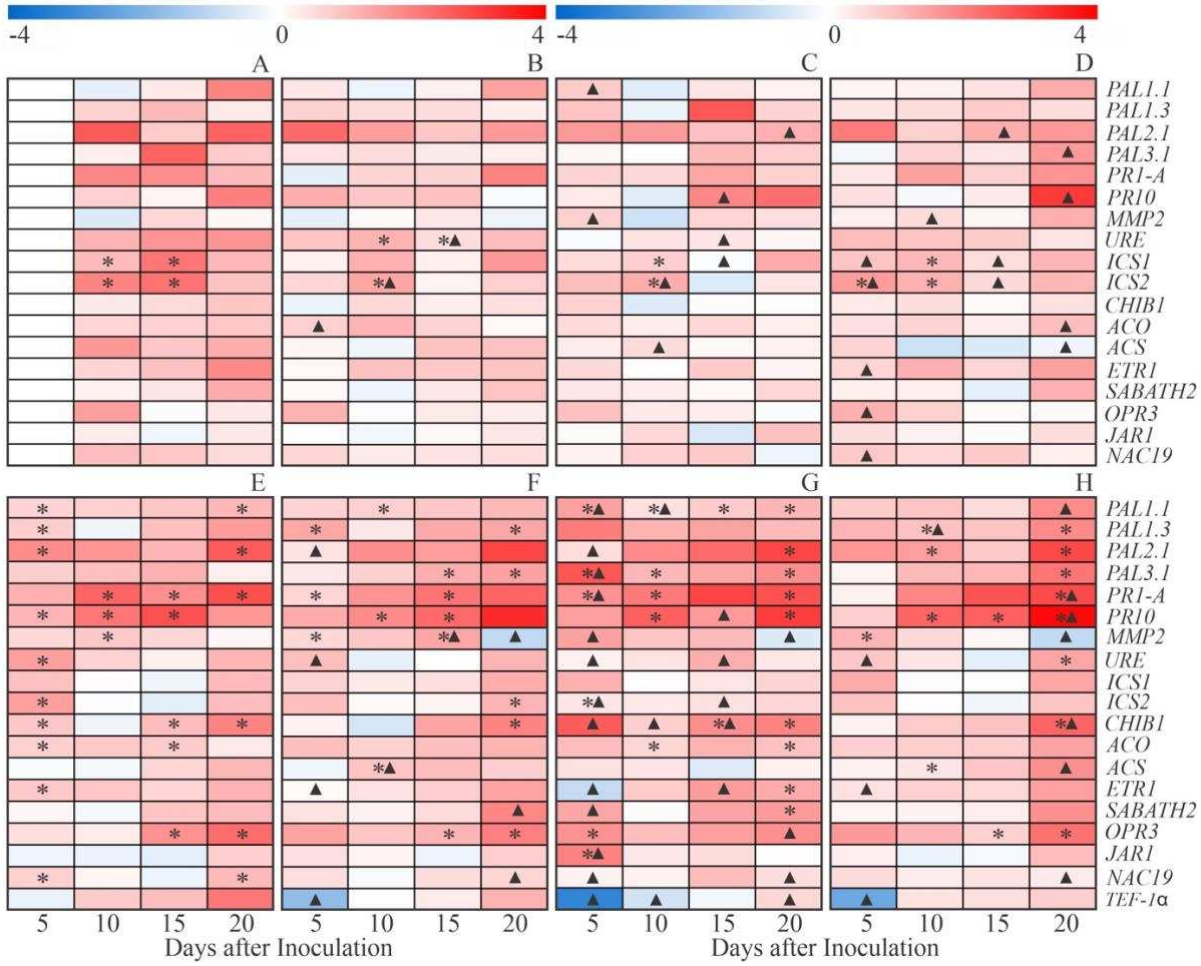

Figure 13. Expression profile of genes determined in the leaves of soybean plants non-inoculated (NI) (A, B, C, and D) or inoculated (I) (E, F, G, and H) with *Phakopsora pachyrhizi* and sprayed with water (control) (A and E), Acibenzolar-S-Methyl (ASM) (B and F), hexanoic acid (HxA) (C and G), and azelaic acid (AzA) (D and H). Color cells represent the relative transcript levels ranging from blue (-4.0) to red (4.0). Amplifications of Ubiquitin-3 (*UBIQ*) and glyceraldehyde 3-phosphate dehydrogenase (*GAPDH*) genes from soybean were used as internal controls for data normalization. Fold changes were calculated based on transcript level for NI plants of the control treatment at 5 days after inoculation (dai). For each leaf sample, four biological replications were used with their respective two technical replicates. Significant difference between NI and I plants, at each evaluation time, is indicated by an asterisk (*) according to the *F* test ($P \leq 0.05$). A triangle (▲) indicates significant difference for ASM, HxA, and AzA treatments, separately, in comparison to control treatment, at each evaluation time, according to the Dunnett's test ($P \leq 0.05$).

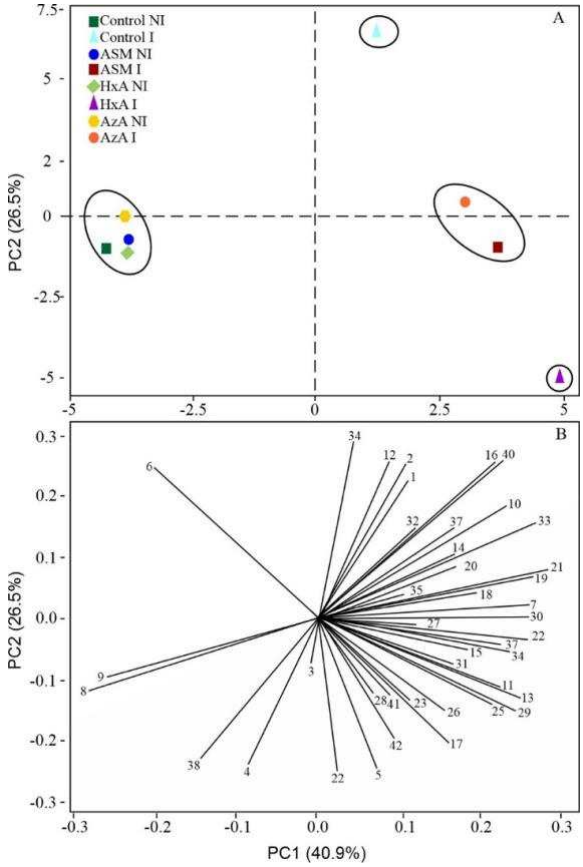

Figure 14. Score plots (A) and loading (B) values in the principal component analysis (PCA) for variables and parameters evaluated in soybean plants non-inoculated (NI) or inoculated (I) with *Phakopsora pachyrhizi* and sprayed with water (control), Acibenzolar-S-Methyl (ASM), hexanoic acid (HxA), and azelaic acid (AzA). Numbers in the loading plot (b) are as follow: severity (1), area under disease progress curve (2), chlorophyll *a* fluorescence parameters (3, 4, 5, 6, and 7, respectively, to F_v/F_m, Y(II), Y(NPQ), Y(NO), and ETR), photosynthetic pigments (8 and 9, respectively, to Chl *a*+*b* and carotenoids), metabolites (10, 11, and 12, respectively, to MDA, H_2O_2, and $O_2^{\bullet-}$), activities of antioxidant (13, 14, 15, 16, and 17, respectively, to SOD, POX, CAT, APX, and GR) and defense-related (18, 19, 20, 21, 22 respectively, to CHI, GLU, PAL, PPO, and LOX) enzymes, TSP (23), LTGA derivatives (24) and genes expression (25, 26, 27, 28, 29, 30, 31, 32, 33, 34, 35, 36, 37, 38, 39, 40, 41, and 42, respectively, to *PAL1.1*, *PAL1.3*, *PAL2.1*, *PAL3.1*, *PR-1A*, *PR10*, *MMP2*, *URE*, *ICS1*, *ICS2*, *CHIB1*, *ACO*, *ACS*, *ETR1*, *SABATH2*, *OPR3*, *JAR1*, and *NAC19*. Groups were generated from cluster analysis with complete linkage and Pearson distance. Data from variables and parameters used in the PCA analysis were obtained for NI and I plants at 15 days.

CHAPTER II

POTENTIATION OF SOYBEAN RESISTANCE AGAINST *Phakopsora pachyrhizi* INFECTION BY A COPPER-POLYPHENOLIC COMPOUND

Abstract

Asian soybean rust (ASR), caused by *Phakopsora pachyrhizi*, is a destructive disease affecting soybean production. The finding of new environmentally-friendly control strategies to minimize fungicide spraying to control ASR must be prioritized. In this scenario, induced resistance using an array of abiotic or biotic inducers of resistance becomes a very promising alternative. This study investigated the potential of using Mantus® (copper (20%) and polyphenolic (10%)) to reduce ASR symptoms by boosting defense responses. A 2 × 2 factorial experiment was arranged in a completely randomized design with four replications per sampling time. The factors studied were plants sprayed with water or Mantus® (referred to as induced resistance (IR) stimulus hereafter) that were non-inoculated or inoculated with *P. pachyrhizi*. Urediniospores germination was reduced by 97% by the IR stimulus *in vitro*. The ASR severity and area under disease progress curve decreased by 68 and 35%, respectively, for IR stimulus-sprayed plants compared to water-sprayed plants. Defense-related genes (*PAL1.1*, *PAL1.3*, *PAL3.1*, *CHIA1*, *CHIB1*, *LOX*, *PR10*, *ICS1*, and *JAR1*) were up-regulated for IR stimulus-sprayed plants compared to water-sprayed plants during the infection process of *P. pachyrhizi*. Infected and IR stimulus-sprayed plants showed less impairment in their photosynthesis (moderate changes on both gas and chlorophyll *a* fluorescence parameters, linked to great concentrations of total chlorophyll *a*+*b* and carotenoids) and a more robust antioxidative metabolism (lower concentrations of hydrogen peroxide and anion superoxide, higher superoxide dismutase activity, and lower ascorbate peroxidase, catalase, peroxidase, and glutathione reductase activities) in contrast to infected and water-sprayed plants. The results reported here highlight the potential of using this IR stimulus for ASR management considering its fungicide effect against urediniospores and by priming soybean resistance more efficiently to cope against *P. pachyrhizi* infection.

Keywords: *Glycine max*, disease management, induced resistance, plant defense mechanisms, photosynthesis, rust.

Introduction

It is an undoubted fact that soybean (*Glycine max* (L.) Merril) ranks as one of the most economically important oilseeds and biodiesel crops grown worldwide for being the main source of protein and oil for both human consumption, animal feed, and biofuel production (Hartman et al., 2011). However, the occurrence of Asian soybean rust (ASR), caused by the biotrophic fungus *Phakopsora pachyrhizi* H. Sydow & P. Sydow, has contributed significantly to reducing yield due to photosynthetic impairment, profound yellowing of leaves and defoliation, and earlier maturation of infected plants (Langenbach et al., 2016; Rios et al., 2018).

The unavailability of soybean cultivars exhibiting race-specific resistance against *P. pachyrhizi* infection places the use of fungicides associated with very few cultural practices (*e.g.*, early-maturing cultivars, early sowing dates, detection of the early development of ASR symptoms and fungal signs, and a period without growing soybean in the off-season to avoid early urediniospores production) as the control strategies available for farmers to manage ASR epidemics and minimize yield losses (Langenbach et al., 2016; Kashiwa et al., 2020). Less efficacy of some fungicides routinely used for ASR control, mainly caused by the emergence of *P. pachyrhizi* populations resistant to fungicides has caused soybean farmers to experience great yield losses (Scherm et al., 2009; Klosowski et al., 2018). ASR control strategies, which contribute to more sustainable agriculture and aim to help farmers depend less on fungicides spraying, deserve to be investigated. The use of inducers of resistance may fit well as an environmentally friendly alternative for ASR management. It is important to fill out the knowledge gaps to better understand how resistance inducers may modulate plant performance at physiological, biochemical, and molecular levels in coping with pathogen infection. This approach will place the new and yet-to-be-discovered resistance inducers closer to the market and be recognized by the farmers as a sustainable option for crop protection.

The fascinating phenomenon of induced resistance (IR) has called the attention of many researchers worldwide caring about more sustainable agriculture. In this regard, plants mainly

from cultivars carrying good agronomic traits but at the same time susceptible to infection by pathogens, previously exposed to IR stimuli of either abiotic or biotic nature, are more prone to activating a diversity of structural and biochemical defense mechanisms (Dixon et al., 1994; Lyon, 2007; Reignault and Walters, 2007; Siah, 2018; Zeier, 2021). Plants in the state of IR are categorized as developing either induced systemic resistance (ISR) or systemic acquired resistance (SAR) (Kesel et al., 2021; Vlot et al., 2021; Zeier, 2021). During ISR, plants rely on the signaling pathway mediated by both jasmonic acid (JA)/ethylene (ET) against infection by necrotrophic pathogens after being challenged with nonpathogenic microorganisms or in contact with a specific type of IR stimulus (Vlot et al., 2021). By contrast, mobile signals (*e.g.*, salicylic acid (SA), glycerol-3-phosphate, azelaic acid, pipecolic acid, and N-hydroxy-pipecolic acid) play a role in the infection caused by biotrophic and hemibiotrophic pathogens during SAR in a faster and long-lasting manner (Spoel and Dong, 2012; Kesel et al., 2021). Regardless of ISR or SAR, synergistic, antagonistic, and even additive interplay between the signaling pathways which are tightly regulated by SA and JA/ET can take place at the pathogen infection site for more robustness of the induced defense mechanisms (Glazebrook, 2005; Pieterse et al., 2012; Kazan and Lyons, 2014; Vlot et al., 2021). It is hoped that sustainable farming practices for plant disease management must include the use of IR stimuli (Vallad and Goodman, 2004; Siah et al., 2018). Considering the soybean-*P. pachyrhizi* pathosystem, the potential of using different types of IR stimuli is very well documented in the literature (*e.g.*, *Bacillus subtilis*, *Metarhizium* spp., cell wall extract of *Saccharomyces cerevisiae*, thaxtomin A from the *Streptomyces scabies*, harpin protein-derived peptides, saccharin, silicon, and nickel) to reduce ASR severity at both greenhouse and field conditions through induction of defense reactions (Paula et al., 2021).

The present study hypothesized that a copper-polyphenolic compound sprayed onto soybean plants could boost their resistance against *P. pachyrhizi* infection rapidly and

efficiently with fine biochemical and physiological adjustments. From a more environmentally friendly perspective, it is postulated that using this type of IR stimulus could avoid great yield losses due to severe ASR epidemics and, at the same time, reduce the number of fungicide applications through a defense-stimulating effect.

Materials and Methods

In vitro assay

The sensitivity of urediniospores of *P. pachyrhizi* to Mantus® (nitrogen (1%) and copper (20%) complexed with plant-derived pool of polyphenols (10%); FertiGlobal, Larderello, Italy) was evaluated *in vitro*. Melted agar-agar (AA) medium was amended with Mantus® (2 mL/L WA medium) and a total of 20 mL was poured into each Petri dish. Petri dishes containing only AA medium served as the control treatment. A total of 100 µl of urediniospores suspension (10^5 urediniospores/mL) was transferred to the center of each Petri dish and homogeneously distributed using a Drigalski glass handle. Petri dishes were transferred to a growth chamber (25°C and photoperiod of 12 h of light and 12 h of dark). After 24 h, 5 µl of lactophenol was added to each dish to stop urediniospores germination. One hundred urediniospores were randomly examined in each Petri dish under a light microscope (Carl Zeiss AxioImager A1) at 40 × magnification. Urediniospore with germ tube larger than its diameter was considered germinated. The percentage of urediniospores germination was calculated for the replication of each treatment.

Plant growth

A total of six soybean seeds from cultivar DS5916IPRO (https://www.brevant.com.br) were sown in each plastic pot containing 2 Kg of a 1:1 mixture of soil and substrate (Tropstrato, Vida Verde, Mogi Mirim, SP, Brazil). After germination, a total of four seedlings were left per pot. Plants in each pot were fertilized weekly with 80 mL of nutrient solution by Clark (1975), with some modifications, which consisted of: 1.04 mM $Ca(NO_3)_2{\cdot}4H_2O$, 1 mM NH_4NO_3, 0.8 mM KNO_3, 0.6 mM $MgSO_4{\cdot}7H_2O$, 0.069 mM KH_2PO_4, 0.931 mM KCl, 19 µM H_3BO_3, 2 µM $ZnSO_4{\cdot}7H_2O$, 7 µM $MnCl_2{\cdot}4H_2O$, 0.6 µM $Na_2MoO_4.4H_2O$, 0.5 µM $CuSO_4{\cdot}5H_2O$, 90 µM $FeSO_4{\cdot}7H_2O$, and 90 mM ethylenediaminetetraacetic acid disodium (EDTA). Plants were

grown in a greenhouse with temperature of 25 ± 2°C, relative humidity of 70 ± 5%, and natural photosynthetically active radiation for 13 h.

Experimental design

For the *in vitro* assay, the experiment was arranged in a completely randomized design with two treatments (control and Mantus®) and ten replications. Each replication corresponded to one Petri dish. A 2 × 2 factorial experiment, consisting of plants sprayed with water (control) and Mantus® and non-inoculated or inoculated with *P. pachyrhizi*, was arranged in a completely randomized design with four replications per evaluation time to assess ASR severity and the parameters related to leaf gas exchange and chlorophyll *a* fluorescence as well to determine photosynthetic pigments concentration. Leaf samples for the biochemical assays and genes expression analysis were obtained from another 2 × 2 factorial experiment with the same factors and arrangement. All experiments were repeated twice.

Application of Mantus®

Soybean plants at the V4 growth stage (≈ 30 days after seedling emergence) were sprayed with 5mL per plant of Mantus® solution (prepared using deionized water) using a VL Airbrush atomizer (Paasche Airbrush Co., Chicago, IL, USA). This treatment will be referred as induced resistance (IR) stimulus thereafter. Plants sprayed with water served as the control treatment.

Plant inoculation with *P. pachyrhizi*

A suspension of 10^5 urediniospores/mL, prepared with gelatin (0.5% w/v), was used to inoculate the plants 24 h after being sprayed with water or IR stimulus using a VL Airbrush atomizer. After inoculation, plants were kept in a mist chamber at 25°C for 16 h under darkness. After this period, plants were transferred to a greenhouse (temperature of 25 ± 2°C, relative humidity of 75 ± 5%, and natural photosynthetically active radiation) until the end of the

experiments. Plants non-inoculated with *P. pachyrhizi* were kept in a different greenhouse under the same environmental conditions.

Evaluation of ASR severity

The leaflets of the second and third leaves of each plant per replication of each treatment (four replications, 16 plants, and 32 leaves) were used to evaluate ASR severity according to the diagrammatic scale proposed by Franceschi et al. (2020) at 5, 10, 15, and 20 days after inoculation (dai). The area under disease progress curve (AUDPC) for each leaflet per leaf of each plant from the replications of each treatment was calculated using the trapezoidal integration of disease progress curves (Shaner and Finney, 1977). At 20 dai, the second and third leaves of each plant per replication of each treatment were collected and scanned at 600 dpi resolution. The images were processed using the software QUANT (Fagundes-Nacarath et al., 2018) to obtain the values of ASR final severity.

Leaf gas exchange measurement

The leaf gas exchange parameters (net CO_2 assimilation rate (A), stomatal conductance to water vapor (g_s), internal CO_2 concentration (C_i), and transpiration rate (E)) were determined on leaflets of the second leaf of each plant per replication of each treatment (four replications, 16 plants, and 16 leaves) by using a portable open-flow gas exchange system (LI-6400XT; Li-Cor Inc., Lincoln, NE) at 10 dai. Leaflets of the second leaf from non-inoculated plants were also evaluated at 10 dai. The measurement occurred from 0900 to 1100 h (solar time) when A was at its maximum under artificial PAR (i.e., 1,000 µmol photons m^{-2} s^{-1} at the leaf level and 400 µmol atmospheric CO_2 mol^{-1}). The measurements were performed at 25°C and the vapor pressure deficit was maintained at approximately 1.0 kPa, while the amount of blue light was set to 10% of the photosynthetic photon flux density (PPFD) to optimize the stomatal aperture.

Imaging and quantification of chlorophyll (Chl) *a* fluorescence parameters

Images and parameters of Chl *a* fluorescence were obtained from leaflets of the second leaf of each plant per replication of each treatment (four replications,16 plants, and 16 leaves) at 10 dai using the Imaging-PAM fluorometer and the Imaging Win software MAXI version (Heinz Walz GmbH, Effeltrich Germany). Leaflets of the second leaf from non-inoculated plants were also evaluated at 10 dai. Plants were adapted to darkness for 30 min and then placed individually in a support at a distance of 18.5 cm from the CCD ("charge-coupled device") camera to obtain images at the resolution of 640 × 480 pixels. The leaflets were exposed to a light pulse intensity of 0.5 μmol m^{-2} s^{-1}, 100 μs, 1 Hz to obtain the initial fluorescence (F_0). Next, a saturating white light pulse of 2,400 μmol m^{-2} s^{-1} (10 Hz) was emitted for 0.8 s to determine the maximum fluorescence emission (F_m). Based on these initial measurements, the maximum PS II photochemical efficiency of dark-adapted leaflets was estimated through the variable-to-maximum Chl *a* fluorescence ratio as follows: $F_v/F_m = [(F_m - F_0)/F_m)]$. Next, the leaflets were exposed to actinic photon irradiance (100 μmol m^{-2} s^{-1}) for 300 s to obtain the steady-state fluorescence yield (F_s), after which a saturating white light pulse (2,400 μmol m^{-2} s^{-1}; 0.8 s) was applied to achieve the light-adapted maximum fluorescence (F_m'). The light-adapted initial fluorescence (F_0') was estimated according to Oxborough and Baker (1997). Based on Kramer et al. (2004), the energy that was absorbed by the PS II for the following three yield components for dissipative processes was calculated as follows: the photochemical yield [$Y(II) = (F_m' - F_s)/F_m')$], the yield for dissipation by down-regulation [$Y(NPQ) = (F_s/F_m') - (F_s/F_m)$], and the yield for other non-photochemical (non-regulated) losses [$Y(NO) = F_s/F_m$]. The apparent electron transport rate was calculated as ETR = Y(II) × PPFD × f × α according to Baker (2008). The parameters of Chl *a* fluorescence were determined on each leaflet (area of ≈ 0.5 cm^2) by selecting the circular option on the Imaging Win software.

Determining photosynthetic pigments concentration

Five leaf discs (1 cm^2 each) were obtained from the leaflets of the second and third leaves of each plant per replication of each treatment (four replications, 16 plants, and 32 leaves) at 5, 8, 11 and 14 dai. The discs were immersed in glass tubes containing 5 ml of saturated dimethyl sulfoxide solution and calcium carbonate (5 g/L), kept in the dark at room temperature for 24 h, and the absorbances of the extracts were read at 480, 649, and 665 nm to determine the concentrations of Chl *a*, Chl *b*, and carotenoids according to Santos et al. (2008).

Histochemical detection of hydrogen peroxide (H_2O_2) and superoxide anion radical ($O_2^{\bullet-}$)

The leaflets of the second leaf of each plant per replication of each treatment (four replications, 8 plants, and 16 leaves) were collected at 15 dai. For H_2O_2 detection, 24 leaflets were randomly placed in glass vials containing 50 mL of a 3,3'-diaminobenzidine tetrahydrochloride (1 mg/mL) solution (Sigma-Aldrich, São Paulo, Brazil) and kept in the darkness at 25°C for 12 h. For $O_2^{\bullet-}$ detection, 24 leaflets were randomly placed in glass vials containing 50 mL of 0.1% solution of nitro blue tetrazolium solution (Sigma-Aldrich, São Paulo, Brazil) in 10 mM potassium phosphate buffer (pH 6.8) and infiltrated for 24 h. Leaflets were cleared in 80% of boiling aqueous ethanol solution for 60 min until brown and blue spots were noticed as an indication of H_2O_2 and $O_2^{\bullet-}$ depositions, respectively.

Biochemical assays and genes expression using quantitative real-time PCR

The second and third leaves of each plant per replication of each treatment (four replications, 16 plants, and 32 leaves) were collected at 2, 3, 5, and 9 dai (for biochemical assays) and at 1, 2, 3, 5, and 9 dai (for analysis of gene expression) from both non-inoculated and inoculated plants. Leaf samples were kept in liquid nitrogen during sampling and stored at -80ºC until further analysis.

Activities of antioxidant enzymes: 0.2 g of leaf tissue was ground into a fine powder with liquid nitrogen using a vibration ball mill (Retsch, Haan, Germany). The fine powder was homogenized in 2 ml of a solution containing 50 mM of potassium phosphate buffer (pH 6.8), 0.1 mM EDTA, 1 mM phenylmethylsulfonyl fluoride (PMSF), and 2% (w/v) polyvinylpyrrolidone (PVP), centrifuged at 12,000 *g* for 15 min at 4°C. The supernatant was used as the crude enzyme extract to determine the activities of ascorbate peroxidase (APX) (EC 1.11.1.11), catalase (CAT) (EC 1.11.1.6), peroxidase (POX) (EC 1.11.1.7), superoxide dismutase (SOD) (EC 1.15.1.1), and glutathione reductase (GR) (EC 1.8.1.7). The SOD activity was determined by measuring its ability to photochemically reduce nitroblue tetrazolium (NBT) as described by Beauchamp and Fridovich (1971). The reaction was initiated by adding the crude enzyme extract to a mixture containing 50 mM potassium phosphate buffer (pH 7.8), 14 mM methionine, 75 µM NBT, 0.1 mM EDTA, and 2 µM riboflavin. Samples were light-exposed for 7 min and the production of formazan blue, resulting from the photoreduction of NBT, was measured at 560 nm with a spectrophotometer (Giannopolitis and Ries, 1977). Samples kept in the dark for 7 min served as a blank. One unit of SOD was defined as the amount of enzyme necessary to inhibit NBT photoreduction by 50%. The CAT activity was determined by adding the crude enzyme extract to a reaction mixture containing 50 mM potassium phosphate buffer (pH 7.0) and 20 mM H_2O_2. The determination of CAT activity was based on the rate of H_2O_2 decomposition measured in the spectrophotometer at 240 nm for 1 min at 25°C (Cakmak and Marschner, 1992). An extinction coefficient of 36 M^{-1} cm^{-1} was used to calculate CAT activity (Anderson et al., 1995). The POX activity was assayed by determining the pyrogallol oxidation as proposed by Kar and Mishra (1976). The reaction was started after adding the crude enzyme extract to a reaction mixture containing 25 mM potassium phosphate (pH 6.8), 20 mM pyrogallol, and 20 mM H_2O_2. The POX activity was determined by the absorbance of colored purpurogallin recorded for 1 min at 420 nm at 25°C. The extinction

coefficient of 2.47 mM^{-1} cm^{-1} (Chance and Maehley, 1955) was used to calculate POX activity. The APX activity assay followed that described by Nakano and Asada (1981). The crude enzyme extract was added to a mixture containing 50 mM phosphate buffer (pH 7.0), 0.5 mM ascorbic acid, and 0.1 mM H_2O_2. The rate of ascorbate oxidation was measured by recording the absorbance at 290 nm for 1 min. The extinction coefficient of 2.8 mM^{-1} cm^{-1} (Nakano and Asada, 1981) was used to calculate APX activity. In order to determine GR activity, the reaction was started after the addition of the crude enzyme extract to a mixture containing 50 mM potassium phosphate (pH 7.8), 1 mM oxidized glutathione (GSSG), and 0.75 mM NADPH prepared in 0.5 mM Tris-HCl buffer (pH 7.5) according to Carlberg and Mannervik (1985). The decrease in absorbance was determined at 340 nm for 1 min at 30°C. The extinction coefficient of 6.22 mM^{-1} cm^{-1} was used to calculate GR activity (Foyer and Halliwell, 1976). The activities of these enzymes were expressed in a protein-basis whose concentration was determined according to Bradford (1976).

Concentrations of total soluble phenolics (TSP) and lignin-thioglycolic acid (LTGA) derivatives: 0.1 g of leaf tissue was ground as described above. The fine powder was homogenized in 1 mL of 80% (v/v) methanol solution. The crude extract was shaken at 300 rpm at 25°C for 2 h and the mixture was centrifuged at 17,000 *g* for 30 min. The TSP concentration was determined in the methanolic extract and the pellet was used to determine the LTGA derivatives concentration according to Tatagiba et al. (2014).

Genes expression: 75 mg of leaf tissue was ground as described above. The RNA was extracted with Trizol (Invitrogen®). DNA contaminations were removed using the RQ1 RNase-Free DNase (Promega). The quality and integrity of the RNA were verified by 1.2% agarose gel electrophoresis and the amount of RNA was measured in a Qubit fluorometer using Qubit RNA HS Assay Kit (Invitrogen, São Paulo, Brazil). Single-stranded cDNAs were synthesized by reverse transcription using 5 μg of total RNA with oligo(dT) primers in a final volume of 20

μL using the SuperScript First Strand Synthesis System for RT-PCR (Invitrogen®). The qRT-PCR was performed on a Bio-Rad CFX Real Time Thermal Cycler using SYBR Green PCR Master Mix according to the manufacturer's recommendations. All reactions were performed in duplicate and the relative expression values for each gene studied were calculated using the $2^{-\Delta\Delta Ct}$ method (Livak and Schmittgen, 2001). Expression analysis of genes encoding for phenylalanine ammonia-lyase (*PAL1.1*, *PAL1.3*, *PAL2.1*, and *PAL3.1*), chitinase (*CHIA1*), chalcone isomerase (*CHI1B1*), lipoxygenase (*LOX*), pathogenesis-related protein 1 (*PR1-A*), pathogenesis-related protein 10 (*PR10*), metalloproteinase (*MMP2*), urease (*URE*), isochorismate synthase (*ICS1* and *ICS2*), and jasmonic acid-amino synthetase (*JAR1*) was performed using specific primers sequences (Table 1). The expression of *TEF-1*α, corresponding to the translation elongation factor 1α of *P. pachyrhizi*, was also quantified to confirm its presence in plant tissues. The Ubiquitin-3 (*UBIQ*) and glyceraldehyde-3-phosphate dehydrogenase (*GAPDH*) genes were used as a reference for normalization as proposed by Mortel et al. (2007).

Data analysis

Data from the variables and parameters evaluated from the repeated experiments were combined following the procedures described by Moore and Dixon (2015). Data from urediniospores germination was submitted to analysis of variance (ANOVA) and means were compared by the *F* test ($P \leq 0.05$). For other variables and parameters, data was subjected to ANOVA and means for control and IR stimulus treatments as well as non-inoculated and inoculated plants were compared by the *F* test ($P \leq 0.05$). Data was checked for normality and homogeneity of variance before ANOVA. Data from variables and parameters from control and IR stimulus treatments for non-inoculated and inoculated plants at 10 dai was used for principal components analysis. The Minitab Statistical software was used for the statistical analysis (Minitab, Inc., 2021).

Results

Analysis of variance

The factor products (P) was significant for germination of urediniospores, AUDPC, severity, *A*, *E*, Y(II), ETR, Chl *a*+*b*, SOD, and GR. The factor plant inoculation (PI) was significant for *A*, g_s, *E*, Y(II), ETR, Chl *a*+*b*, Car, SOD, POX, APX, TSP, LTGA derivatives, *PAL1.1*, *PAL3.1, CHIA, LOX, PR1-A, MMP2, URE,* and *ICS2*. The interaction P × PI was significant for *A*, g_s, *E,* Y(II), Y(NPQ), Y(NO), ETR, Chl *a*+*b*, SOD, and POX (Table 2).

In vitro assay

The germination of urediniospores from *P. pachyrhizi* was significantly reduced by 97% on WA medium amended with IR stimulus compared to control treatment (Fig. 1).

Symptoms, AUDPC, and severity of ASR

On leaflets of water-sprayed plants, there were many necrotic lesions containing several uredinia in contrast to the leaflets from plants sprayed with the IR stimulus which the lesions were much less developed (Fig. 2a and b). The AUDPC significantly decreased by 35% for IR stimulus-sprayed plants compared to plants from the control treatment (Fig. 2c). The severity of ASR estimated by the QUANT software was significantly reduced by 68% for plants sprayed with IR stimulus compared to plants from the control treatment (Fig. 2d).

Leaf gas exchange

The *A*, g_s, and *E* were significantly higher by 28, 40, and 28%, respectively, for inoculated IR stimulus-sprayed plants compared to inoculated plants from the control treatment (Fig. 3a, b, and d). For the control treatment, *A*, g_s, and *E* were significantly higher by 52, 53, and 37%, respectively, for non-inoculated plants compared to inoculated plants (Fig. 3a, b, and d). For the IR stimulus treatment, *A* significantly increased by 30% for non-inoculated plants compared

to inoculated plants, while C_i significantly increased by 3% for inoculated plants compared to non - inoculated plants (Fig. 3a and c).

Imaging and quantification of Chl *a* fluorescence parameters

Notable damage to the photosynthetic apparatus occurred for plants from control treatment compared to those from IR stimulus treatment at 10 dai based on darker areas in the images for F_v/F_m, Y(II), Y(NPQ), and Y(NO) parameters (Fig. 4). For non-inoculated plants, Y(NO) was significantly higher by 23% for IR stimulus treatment compared to control treatment (Fig. 5d). For inoculated plants, Y(II) and ETR were significantly higher by 56 and 51%, respectively, while Y(NPQ) and Y(NO) were significantly lower by 14 and 37%, respectively, for IR stimulus treatment compared to control treatment (Fig. 5b-e). For the control treatment, Y(II) and ETR were significantly higher by 56 and 50%, respectively, for non-inoculated plants compared to inoculated plants, while Y(NO) was significantly lower by 39% for inoculated plants compared to non-inoculated plants (Fig. 5b and d-e). For IR stimulus treatment, Y(NO) was significantly higher by 20% for non-inoculated plants compared to inoculated plants (Fig. 5d).

Concentrations of photosynthetic pigments

For non-inoculated plants, Chl *a*+*b* and carotenoids concentrations significantly increased by 12% for IR stimulus treatment compared to control treatment at 11 dai (Fig. 6a and c). For inoculated plants, concentrations of Chl *a*+*b* (69% at 14 dai) and carotenoids (19 and 27%, respectively, at 8 and 14 dai) were significantly higher for IR stimulus treatment compared to control treatment (Fig 6b and d). In general, Chl *a*+*b* and carotenoids concentrations were significantly higher for non-inoculated plants compared to inoculated plants from control and IR stimulus treatments during the time-course evaluated (Fig. 6a-d).

Histochemical localization of H_2O_2 and $O_2^{\bullet-}$

The leaflets from non-inoculated plants sprayed with the IR stimulus did not show any sign of cellular perturbation based on the absence or weak staining for detection of H_2O_2 and $O_2^{\bullet-}$ compared to the control treatment (Figs. 7a-b and 8a-b). Depositions of H_2O_2 (brown color) and $O_2^{\bullet-}$ (blue color) were less remarkably intense in leaflets of inoculated plants from IR stimulus treatment (Figs. 7d and 8d) compared to control treatment (Figs. 7b and 8b).

Activities of antioxidant enzymes

For non-inoculated plants, SOD and POX activities were significantly higher by 37 and 30% at 3 dai, while CAT and GR activities were significantly lower by 44 and 65% at 2 dai for IR stimulus treatment compared to control treatment (Fig. 9a, c, e, and i). For inoculated plants, SOD (44 and 31%, respectively, at 3 and 5 dai) and POX (51% at 5 dai) activities were significantly higher, while POX (56 and 64%, respectively, at 2 and 9 dai), CAT (70% at 9 dai), APX (60 and 64%, respectively, at 3 and 9 dai), and GR (74% at 9 dai) activities were significantly lower for IR stimulus treatment compared to control treatment (Fig. 9b, d, f, h, and j). Activities of SOD, POX, CAT, APX, and GR were significantly higher for inoculated plants compared to non-inoculated plants for control and IR stimulus treatments, especially for the former, from 2 to 9 dai (Fig. 9a-j).

Concentrations of TSP and LTGA derivatives

The concentrations of TSP and LTGA derivatives concentrations for non-inoculated plants and TSP concentration for inoculated plants were not affected by control and IR stimulus treatments regardless of evaluation time (Fig. 10a-c). For inoculated plants, LTGA derivatives concentration was significantly lower by 9% for IR stimulus treatment compared to control treatment at 9 dai (Fig. 10d). The concentration of LTGA derivatives was significantly higher

for inoculated plants compared to non-inoculated plants for control and IR stimulus treatments for 3 to 9 dai (Fig. 10c-d).

Genes expression

Comparing NI *vs.* I plants for control and IR stimulus treatments

Expressions of *PAL1.1*, *PAL1.3*, *PAL2.1*, *PAL3.1*, *CHIA1*, *CHIB1, PR1-A, PR10*, and MMP2 at 1 dai, *PAL1.1*, *CHIA1, PR1-A*, and *MMP2* at 2 dai, *MMP2* at 3 dai, and *PAL1.1* and *PR10* at 5 dai were significantly up-regulated for inoculated plants compared to non-inoculated plants for control treatment. Expressions of *ICS1* at 1 dai, *LOX* at 2 dai, and *CHIB1* at 5 dai were significantly down-regulated for inoculated plants compared to non-inoculated plants for control treatment (Fig. 11a and c). Expressions of *PAL1.1*, *PAL1.3*, *PAL3.1*, *CHIA1, PR1-A*, *ICS1*, and *JAR1* at 1 dai, *PAL1.1*, *CHIA1,* and *PR1-A* at 2 dai, *PAL1.3*, *PAL3.1, CHIA1, PR1-A*, *PR10*, *ICS1*, and *JAR1* at 3 dai, *PAL3.1*, *CHIA1*, *CHIB1*, and *PR10* at 5 dai were significantly up-regulated for inoculated plants compared to non-inoculated plants for IR stimulus treatment. Expressions of *LOX* at 1 and 5 dai and *URE* at 1 and 2 dai were significantly down-regulated for inoculated plants compared to non-inoculated plants for IR stimulus treatment (Fig. 11b and d).

Comparing IR stimulus and control treatments for NI and I plants

Non-inoculated plants

Expressions of *PAL3.1, CHIB1, PR1-A, PR10*, and *JAR1* were significantly up-regulated at 1 dai, while *PAL1.1*, *CHIB1*, and *LOX* at 1, 5, and 2 dai, respectively, were significantly down-regulated for IR stimulus treatment compared to control treatment (Fig. 11a and b)

Inoculated plants

Expressions of *PAL1.3* and *ICS1* at 1 dai, *PAL1.1*, *PAL1.3*, *PAL3.1*, *CHIA1*, *LOX*, *PR10*, *ICS1*, and *JAR1* at 3 dai, as well as *CHIB1* at 5 dai were significantly up-regulated, while *LOX* and *PR10* at 1 dai, *ICS2* at 3 dai as well as *PAL1.1* and *PAL1.3* at 5 dai were significantly down-regulated for IR stimulus treatment compared to control treatment (Fig. 11c and d). Expression

of *TEF-1α* was significantly down-regulated at 1 and 2 dai for IR stimulus treatment compared to control treatment (Fig. 11c and d).

PCA analysis

One principal component (PC) explained most of data variation (PC1 = 59.4% and PC2 = 28.7%) (Fig. 12a-b). According to cluster analysis with complete linkage and Pearson distance, one cluster was generated for each treatment NI (control and IR stimulus) and I (control and IR stimulus) (Fig. 12a). The first PC resulted in negative scores for photosynthetic parameters (F_v/F_m, Y(II), and ETR), photosynthetic measurements (*A*, *E,* and g_s), MDA, Chl *a+b*, Car*,* and for expression of the following genes: *URE*, *CHIB1*, *PAL1.3*, *PR1-A*, *ICS1*, *ICS2* and *LOX*, and positive scores for other variables and parameters evaluated (Fig. 12b). According to cluster analysis with complete linkage and Pearson distance, four treatments were distinctly separated (Fig. 12a). One principal component (PC) explained most of data variation (PC1 = 59.4% and PC2 = 28.7%) (Fig. 12a-b). The first PC was characterized by negative scores for photosynthetic parameters (*A*, g_s, *E*, F_v/F_m, Y(II), and ETR), photosynthetic pigments (Chl *a+b* and Car), LOX activity, and genes expression (*PAL1.3*, *CHIB1*, *PR1-A*, *ICS1*, *ICS2*, and *URE*). Positive scores were obtained severity, AUDPC, photosynthetic parameters (C_i, Y(NPQ), and Y(NO)), antioxidant enzymes (APX, CAT, POX, SOD, and GR), TSP and LTGA derivatives, genes expression (*PAL1.1*, *PAL2.1*, *PAL3.1*, *PR10*, *MMP2*, and *JAR1*) (Fig. 12a-b).

Discussion

The loss of efficacy of fungicides routinely used for SR control in soybean fields is deeply linked to the strong capacity of *P. pachyrhizi* to develop new resistance mechanisms against them. In this scenario, the use of IR stimuli becomes an eco-friendly and sustainable alternative for integrated SR management. In the present study, SR symptoms were efficiently reduced (smaller necrotic lesions surrounded by discreet chlorosis resulting in lower severity and reduced colonization of leaflets tissues by *P. pachyrhizi* based on lower *TEF-1α* expression from 1 to 2 dai) by the IR stimulus used. Even though the IR stimulus had a direct antifungal activity against germination of *P. pachyrhizi* urediniospores *in vitro*, it showed great potential to trigger soybean defense responses against fungal infection. In fact, some IR stimuli reported in the literature may exert a fungicide effect against some pathogens by inhibiting mycelial growth or spore germination rather than only eliciting or prime host defense reactions (Roberts, 1999; Lyon, 2007; Siah et al., 2018; Mejri et al., 2021; Mohammad et al., 2021; Paula et al., 2021, 2022; Santos et al., 2021).

It is known that increased susceptibility of plants against pathogens of different lifestyles is associated with photosynthetic impairment considering that their capacity for a prompt defense response due to profound alterations in the source-to-sink transport of photoassimilates across plant organs (Dallagnol et al., 2011; Debona et al., 2014; Silveira et al., 2015; Rios et al., 2017; Dias et al., 2018; Aucique-Pérez et al., 2020; Sterling and Melgarejo, 2021). Particularly in soybean leaves, infection by *P. pachyrhizi* seriously compromises photosynthesis as pictured by remarkable changes in values of leaf gas exchange (lower A, g_s, C_i, and E) and Chl *a* fluorescence (lower F_v/F_m, Y(II), and Y(NPQ) accompanied by increases in Y(NO)) parameters associated with lowering the photosynthetic pigment (total Chl *a*+*b* and carotenoids) pool (Rios et al., 2018). The findings of the present study are in agreement with previous studies (Rios et al., 2018; Einhardt et al., 2020a; Picanço et al., 2021), but provide clear shreds of evidence that photosynthesis was greatly preserved in infected leaves of IR

stimulus-sprayed plants. Great *A*, g_s, and *E* values obtained for infected leaves of IR stimulus-sprayed plants reflected a better physiological performance due to less biochemical and diffusional limitations associated with great preservation of stomata functionality as the infection process of *P. pachyrhizi* infection took place. A balance between the electron flow and CO_2 assimilation during photosynthesis occurred for infected leaves of IR stimulus-sprayed plants considering great *A* and ETR values. On top of that, infected leaves of IR stimulus-sprayed plants suffered less photodamage (*e.g.*, higher Y(II) values concomitantly with reductions in Y(NPQ) and Y(NO)) at the photosynthetic machinery level. Linked to that, ETR was higher while Y(NPQ) was lower indicating that heat dissipation to alleviate any damage imposed on PSII was minimal and ensuring even more preservation of the photosynthetic apparatus. Interestingly, damage to the reaction centers associated with the photosystems based on F_v/F_m values was similar between control and IR stimulus treatments regardless of plant inoculation with *P. pachyrhizi*. High photosynthetic pigment (Chl *a*+*b* at 14 dai and carotenoids at 8 and 14 dai) pool was noticed in infected leaves of IR stimulus-sprayed plants due to reduction in SR symptoms denoted that light energy was used more efficiently towards improved photosynthesis. Interestingly, Chl *a*+*b* and carotenoids concentrations were higher for IR-stimulus plants compared to water-sprayed plants not challenged with *P. pachyrhizi* at 11 dai. The literature highlights the potential of different IR stimuli to alleviate the stress imposed by foliar pathogens on the photosynthetic apparatus of their hosts, including the soybean-*P. pachyrhizi* interaction, due to the reduction in disease symptoms (*e.g.*, more leaf area photosynthetically active due to less chlorosis, necrosis, and wilting) mainly as a result of the potentiation of host defense responses than just having a fungistatic effect (Rios et al., 2014; Rodrigues et al., 2017; Fagundes-Nacarath et al., 2018; Aucique-Pérez et al., 2019; Dias et al., 2018, 2020; Einhardt et al., 2020b).

Accumulation of ROS and the associated cellular damage is a well-documented phenomenon occurring in plant tissue facing infection by pathogens (Debona et al., 2012; Huang et al., 2019; Aucique-Pérez et al., 2020). A well-coordinated enzymatic system in the cell wall, plasma membrane, and symplast of leaves infected by pathogens plays a major role to scavenge the excess of ROS (SOD converts $O_2^{\bullet-}$ into H_2O_2 and O_2, whereas H_2O_2 can be subsequently scavenged by APX, CAT, and POX activities) generated for less oxidative damage against DNA, lipids, and proteins (Das and Roychoudhury, 2014). The GR uses NADPH to reduce GSSG to reduced glutathione during redox homeostasis, mainly in chloroplasts (Das and Roychoudhury, 2014). In contrast to IR stimulus-sprayed plants, soybean plants from the control treatment displayed increased POX, CAT, APX, and GR activities in response to *P. pachyrhizi* infection. Interestingly, higher SOD activity in infected leaves of IR stimulus-sprayed plants was higher at 3 and 5 dai helped to decrease the pool of $O_2^{\bullet-}$ which was also histochemically confirmed. Beyond that, the great amount of H_2O_2 generated as a result of increased SOD activity did not seem to exert a harmful effect in infected leaves of IR stimulus sprayed plants considering that SR symptoms were reduced, CAT, APX, and GR (except POX at 5 dai) activities did not increase to scavenge H_2O_2, and foliar H_2O_2 precipitation was minimal. On the other hand, lower GR activity in infected leaves of IR stimulus-sprayed plants was possibly linked to less production of other ROS (*e.g.*, singlet oxygen and hydroxyl radical) during the infection process of *P. pachyrhizi* in contrast to higher activity obtained for infected leaves of water-sprayed plants at 9 hai. It is noteworthy in this context that the IR stimulus used in the present study played a detrimental role in alleviating the oxidative stress imposed by *P. pachyrhizi* infection without imposing a high metabolic cost on soybean plants. More than a possible harmful effect of the transitional pool of H_2O_2, indirectly associated with higher SOD activity, in infected leaves of IR stimulus-sprayed plants, its role as a signaling molecule to trigger defense responses in plants expressing SAR to cope with pathogen infection as reported

in the literature (Low and Merida, 1996; Pitzschke et al., 2006; Camejo et al., 2016) cannot be ruled out. In general, plants exposed to different types of IR stimuli seem to develop a more robust and transient antioxidative metabolism to mitigate the stress occurring at the pathogen infection site (Rios et al., 2014; Rodrigues et al., 2017; Fagundes-Nacarath et al., 2018; Aucique-Pérez et al., 2019; Dias et al., 2018, 2020; Einhardt et al., 2020a; Mohammad et al., 2021; Paula et al., 2021).

The involvement of the IR stimulus in boosting soybean resistance against *P. pachyrhizi* infection was investigated at the molecular level by examining the expression of some defense-related genes. Interestingly, in the absence of *P. pachyrhizi* infection, earlier up-regulation of four genes (*PAL3.1*, *CHIB1*, *PR1-A*, *PR10*, and *JAR1* at 1 dai) in IR stimulus-sprayed plants indicated elicitation of soybean defense responses. Notably, for inoculated plants, the gene expression pattern was strikingly similar but sometimes more remarkable for IR stimulus-sprayed plants compared to water-sprayed plants. In this context, up-regulation of *PAL1.1*, *PAL3.1*, *CHIA1*, *LOX*, *PR10*, and *JAR1* at 3 dai, *PAL1.3* and *ICS1* at 1 and 3 dai, and *CHIB1* at 5 dai for IR stimulus-sprayed plants and closely linked to their increased resistance against SR. The literature is rich with reports highlighting the potential of IR stimuli to elicit or prime plants previously exposed to them to cope with pathogen infection in a faster, more effective, and more extended period due to the involvement of different pathogenesis-related proteins (*e.g.*, chitinases, β-1,3-glucanases, PR1, and PR10), antimicrobial compounds (*e.g.*, phenolics, quinones, phytoalexins, and some peptides), and lignification of plant tissue (van Loon and Pieterse, 2006; Mauch-Mani et al., 2017; Kesel et al., 2021; Vlot et al., 2021).

In the present study, *CHIA1* was up-regulated for IR stimulus-sprayed plants in response to *P. pachyrhizi* infection at 3 dai. Considering that chitinases hydrolyze chitin in the cell walls of different fungal pathogens and the released chitin oligomers can trigger defense reactions

(Rodrigues et al., 2003; Sánchez-Vallet et al., 2014), it can be therefore assumed that the IR stimulus helped to hamper the colonization of soybean leaves by *P. pachyrhizi*.

The PAL is the major enzyme in the phenylpropanoid pathway from which different types of phenolics with antimicrobial activity are formed (Dixon et al., 2002; Daayf et al., 2012). Despite up-regulation of *PAL* for infected plants from control (*PAL1.1* and *PAL3.1* at 5 dai) and IR stimulus (*PAL1.1* and *PAL3.1* at 3dai and *PAL1.3* at 1 and 3 dai) treatments, there was no corresponding increase in the TSP concentration or even their subsequent polymerization towards lignin production (except higher LTGA derivatives concentration for water-sprayed plants compared to IR stimulus-sprayed plants at 9 dai). In some cases, soybean plants counteract *P. pachyrhizi* infection by increasing the production of either phenolics or lignin, but this biochemical type of defense can be greatly affected by the IR stimulus used (Einhardt et al., 2020b; Paula et al., 2021; Picanço et al., 2021; Schulman et al., 2021). In soybean, the enzyme chalcone isomerase, encoded by *CHIB1*, is involved in synthesizing flavonoids (*e.g.*, coumestrol daidzein, genistein, glyceollin, quercetin, and kaempferol) in the flavonoid biosynthesis pathway (Kim and Chung, 2007). Interestingly, *CHIB1* was up-regulated in infected leaves of IR stimulus-sprayed plants at 5 dai and most likely contributed to reducing ASR symptoms. It can be assumed that IR stimulus-sprayed plants seemed to be more dependent on the flavonoid pathway, for which phenolics originating from the phenylpropanoid pathway are also important, to cope with *P. pachyrhizi* infection. Park (2010) reported that transcript for *CHI1*, coding for chalcone isomerase 1, was abundantly produced in soybean leaves infected by *P. pachyrhizi* at 10 hai.

Different IR stimuli have been shown to induce soybean resistance against soilborne and foliar diseases caused by pathogens of different lifestyles through SAR or ISR (Cruz et al., 2020; Paula et al., 2021; Santos et al., 2021). It is reasonable to assume that the IR stimulus used in the present study showed the potential to prime both SA and JA signaling pathways to

cope with the harmful effect of *P. pachyrhizi* infection. Taking into consideration the particularity of symptoms caused by *P. pachyrhizi* on soybean leaves (intense necrosis) in contrast to those caused by other fungi causing rust (*e.g.*, *Uromyces appendiculatus* in common beans with the absence of necrosis and discrete chlorosis at the infection sites) it is expected plants will be prone to develop SAR. However, at some point in the *P. pachyrhizi* infection process, a necrotrophic behavior can take place over the biotrophic lifestyle to manipulate the immune system of soybean plants with effectors released in favor of a successful infection (Barros et al., 2020). The knowledge that signaling pathways mediated by SA and JA/ET are more effective against pathogens of biotrophic/hemibiotrophic and necrotrophic lifestyles, respectively (Vlot et al., 2020; Kesel et al., 2021) will still be a matter of debate for the soybean-*P. pachyrhizi* interaction. In soybean, SA is originated from either phenylpropanoid or isochorismate pathways in which *PAL* and *ICS*, respectively, are involved (Shine et al., 2016) and considered to be one of the most important signals for triggering SAR in infected plants (Kachroo and Kachroo, 2020; Vlot et al., 2021). It is tempting to speculate that SA originated from both phenylpropanoid and isochorismate pathways were important for the increased resistance of IR stimulus-sprayed plants against SR considering the more substantial upregulation of *PAL1.1* (at 3 dai), *PAL1.3* (at 1 and 3 dai), *PAL3.1* (at 3 dai), and *ICS1* (at 1 and 3 dai) most likely through the establishment of SAR. In many plant-pathogen interactions, *JAR1* expression has been used as a molecular marker to check the activation of the JA pathway (Reymond and Farmer, 1998; Feys and Parker, 2000), while *PR1* is often up-regulated in infected plants exhibiting SAR (van Loon and Pieterse, 2006). However, in the present study, increased resistance of IR stimulus-sprayed plants cannot rely exclusively on *PR1-A*, but taking into consideration a holistic role played by other genes (*e.g.*, *PAL* and *ICS*) studied. Indeed, there was no difference between infected plants from control and IR stimulus treatments regarding *PR1-A* expression. Paula et al. (2022) reported that reduction in SR severity by

thaxtomin A had the involvement of ET (up-regulation of *ACC*) and no apparent effect of SA pathway based on down-regulation of *PR1*, *NPR1*, and *MeSA*. The up-regulation of *JAR1* for infected and IR stimulus-sprayed plants at 3 dai shed light on the possible contribution of ISR in soybean resistance against SR. The decision of plants to follow either the SA or the JA/ET pathway, or having their co-participation at some stage of the pathogen infection process, is often linked to the type of IR stimulus (rate and time of application), the genetic background of the cultivar, and the pathogen lifestyle aiming to allocate the metabolic energy as more efficiently as possible (Walters et al., 2005; Lyon et al., 2007; Spoel and Dong, 2012; Siah et al., 2018; Vlot et al., 2021; Zeier, 2021). Great LOX activity in plant tissues is one of the strategies mounted by plants to defend against pathogen infection, especially the necrotrophic (Slusarenko, 1996; Aerts et al., 2021). In this context, LOX acts in the hydroperoxidation of polyunsaturated fatty acids containing cis and cis-1,4-pentadiene moieties to produce oxylipins that are further enzymatically metabolized into JA and methyl jasmonate that are involved in ISR (Feussner and Wasternack, 2002). Curiously, the involvement of *LOX* in water-sprayed plants (early expression, at 1 dai) or even for IR stimulus-sprayed plants (late expression, at 3 dai) for reducing ASR symptoms was barely noticed in the present study.

According to Park (2010), PR10 was one of the 40 proteins differentially expressed in leaves of soybean plants from a susceptible cultivar infected by *P. pachyrhizi* until 10 dai and transcript level of *PR10* was also significantly induced at 10 hai as well as at 6 and 8 days after inoculation. The *PR10* was also up-regulated in soybean leaves infected by *Phytophthora sojae and also previously exposed to SA,* ethylene, abscisic acid, and JA (Jiang et al., 2015). In the present study, *PR10* was expressed earlier (at 1 dai) and late (at 3 dai), respectively, for water- and IR stimulus-sprayed plants infected by *P. pachyrhizi* and its possible implication in soybean resistance against ASR cannot be ruled out. The production of antimicrobial peptides is an important strategy of plant defense against pathogen infection and *MMP2* expression is needed

in this process (Marino and Funk, 2012). In the present study, *MMP2* expression was similar for infected plants from control and IR stimulus treatments. Interestingly, *MMP2* was upregulated only for infected and water-sprayed plants compared to non-inoculated and water-sprayed plants in an ineffective attempt to cope with *P. pachyrhizi* infection. Large amounts of nitrogen are mainly transported in soybean leaves as ureides rather than as amides or amino acids, which are metabolized to urea and subsequently converted to $NH4^+$ (McClure and Israel, 1979). No change in *URE* expression was noticed between plants from control and IR stimulus treatments regardless of inoculation with *P. pachyrhizi* during the evaluation time. Considering the IR stimulus-sprayed treatment in particular, *URE* was up-regulated for non-inoculated plants than for inoculated plants highlighting an enhancement in the conversion of urea to ammonium and its increasing availability for the production of compounds containing nitrogen.

Taken together, the IR stimulus was capable of increasing soybean resistance against ASR based on a body of pieces of evidence at the physiological, biochemical, and molecular levels reported in the present study. The boosted defense reactions taking place in soybean leaves to cope with *P. pachyrhizi* infection occurred through the expression of genes involved in basal host defense as well as in SA and JA signaling pathways, a more operant antioxidative metabolism, and preservation of the photosynthetic apparatus. Interestingly, the separation of the clusters related to inoculated IR stimulus-sprayed plants and inoculated water-sprayed plants based on the PCA analysis highlights the peculiar effect of the IR stimulus on the outcome of variables and parameters investigated. It is tempting to assume that using this IR stimulus associated with available control strategies may become a promising alternative to slow the SR epidemic rate under field conditions and avoid yield losses more sustainably.

References

Aerts N, Mendes MP, Van Wees SC (2021) Multiple levels of crosstalk in hormone networks regulating plant defense. Plant Journal 105:489-504.

Anderson LA, Johnson AK, Simms MD, Willingham TR (1995) Comparative analysis of catalases: spectral evidence against heme-bound water for the solution enzymes. FEBBS Letters 370:97-100.

Aucique-Pérez CE, Resende RS, Martins AO, Silveira PR, Cavalcanti JHF, Vieira NM (2020) How do wheat plants cope with *Pyricularia oryzae* infection? A physiological and metabolic approach. Planta 252:24.

Aucique-Pérez CE, Resende RS, Neto LBC, Dornelas F, DaMatta FM, Rodrigues FA (2019) Picolinic acid spray stimulates the antioxidative metabolism and minimizes impairments on photosynthesis on wheat leaves infected by *Pyricularia oryzae*. Physiologia Plantarum 167:628-644.

Baker NR (2008) Chlorophyll fluorescence: a probe of photosynthesis *in vivo.* Annual Review of Plant Biology 59:89-113.

Barros VA, Fontes PP, Souza GB, Gonçalves AB, Carvalho K, Rincão MP, Lopes ION, Costa MDL, Alves MS, Marcelino-Guimarães FC (2020) *Phakopsora pachyrhizi* triggers the jasmonate signaling pathway during compatible interaction in soybean and *GmbZIP89* plays a role of major component in the pathway. Plant Physiology and Biochemestry 151:526-534.

Beauchamp C, Fridovich I (1971) Superoxide dismutase: improved assays and an assay applicable to acryl amide gels. Analytical Biochemistry 44:276-287.

Bradford MN (1976) A rapid and sensitive method for the quantitation of microgram quantities of protein utilizing the principle of protein-dye binding. Analytical Biochemistry 72:248-254.

Cakmak I, Marschner H (1992) Magnesium deficiency and high light intensity enhance activities of superoxide dismutase, ascorbate peroxidase, and glutathione reductase in bean leaves. Plant Physiology 98:1222-1227.

Camejo D, Guzmán-Cedeño A, Moreno A (2016) Reactive oxygen species, essential molecules, during plant-pathogen interactions. Plant Physiology and Biochemistry 103:10-23.

Carlberg I, Mannervik B (1985) Glutathione reductase. Methods in Enzymology, 113:484-490.

Chance B, Maehley AC (1955) Assay of catalases and peroxidases. Methods in Enzymology 2:764-775.

Clark RB (1975) Characterization of phosphates in intact maize roots. Journal of Agricultural and Food Chemistry 23:458-460.

Cruz MFA, Pinto MO, Barros EG, Rodrigues FA (2020) Differential gene expression in soybean infected by *Phakopsora pachyrhizi* in response to acibenzolar-S-methyl, jasmonic acid and silicon. Journal of Phytopathology 168:571-580.

Daayf F, El Hadrami A, El-Bebany AF, Henriquez MA, Yao Z, Derksen H (2012) Phenolic compounds in plant defense and pathogen counter-defense mechanisms. Recent Advances in Polyphenol Research 3:191-208.

Dallagnol LJ, Rodrigues FA, DaMatta FM, Mielli MV, Pereira SC (2011) Deficiency in silicon uptake affects cytological, physiological, and biochemical events in the rice-*Bipolaris oryzae* interaction. Phytopathology 101:92-104.

Das K, Roychoudhury A (2014) Reactive oxygen species (ROS) and response of antioxidants as ROS-scavengers during environmental stress in plants. Frontiers in Environmental Science 2:53.

Debona D, Rodrigues FA, Rios JA, Martins SCV, Pereira LF, DaMatta FM (2014) Limitations to photosynthesis in leaves of wheat plants infected by *Pyricularia oryzae*. Phytopathology 104:34-39.

Debona D, Rodrigues FA, Rios JA, Nascimento KJT (2012) Biochemical changes in the leaves of wheat plants infected by *Pyricularia oryzae*. Phytopathology 102:1121-1119.

Dias CS, Araujo L, Alves Chaves JA, DaMatta FM, Rodrigues FA (2018) Water relation, leaf gas exchange and chlorophyll *a* fluorescence imaging of soybean leaves infected with *Colletotrichum truncatum*. Plant Physiology and Biochemistry 127:19-128.

Dias CS, Rios JA, Einhardt AM, Chaves JAA, Rodrigues FA (2020) Effect of glutamate on *Pyricularia oryzae* infection of rice monitored by changes in photosynthetic parameters and antioxidant metabolism. Physiologia Plantarum 169:179-193.

Dixon RA, Achnine L, Kota P, Liu CJ, Reddy MS, Wang L (2002) The phenylpropanoid pathway and plant defence - a genomics perspective. Molecular Plant Pathology 3:371-390.

Dixon RA, Harrisson MJ, Lamb CJ (1994) Early events in the activation of plant defence responses. Annual Review of Phytopathology 107:113-119.

Einhardt AM, Ferreira S, Hawerroth C, Valadares SV, Rodrigues FA (2020a) Nickel potentiates soybean resistance against infection by *Phakopsora pachyrhizi*. Plant Pathology 69:849-859.

Einhardt AM, Ferreira S, Souza GMF, Mochko ANR, Rodrigues FA (2020b) Cellular oxidative damage and impairment on the photosynthetic apparatus caused by Asian soybean rust on soybeans are alleviated by nickel. Acta Physiologiae Plantarum 42:115.

Fagundes-Nacarath IRF, Debona D, Rodrigues FA (2018) Oxalic acid-mediated biochemical and physiological changes in the common bean-*Sclerotinia sclerotiorum* interaction. Plant Physiology and Biochemistry 129:109-121.

Feussner I, Wasternack C (2002) The lipoxygenase pathway. Annual Review of Plant Biology 53:275-297.

Feys BJ, Parker JE (2000) Interplay of signaling pathways in plant disease resistance. Trends in Genetics 16:449-455.

Franceschi VT, Alves KS, Mazaro SM, Godoy CV, Duarte HSS, Ponte EMD (2019) A new standard diagram set for assessment of severity of soybean rust improves accuracy of estimates and optimizes resource use. Plant Pathology 69:495-505.

Giannopoilitis CN, Ries SK (1977) Superoxide dismutases: purification and quantitative relationship with water soluble protein in seedlings. Plant Physiology 59:315-318.

Glazebrook J (2005) Contrasting mechanisms of defense against biotrophic and necrotrophic pathogens. Annual Review of Phytopathology 43:205-227.

Hartman GL, West ED, Herman TK (2011) Crops that feed the World 2. Soybean-worldwide production, use, and constraints caused by pathogens and pests. Food Security 3:5-17.

Honglin H, Farhan U, Dao-Xiu Z, Ming Y, Yu Z (2019) Mechanisms of ROS regulation of plant development and stress responses. Frontiers in Plant Science 10:800.

Jiang L, Wu J, Fan S, Li W, Dong L, Cheng Q (2015) Isolation and characterization of a novel pathogenesis-related protein gene (*GmPRP*) with induced expression in soybean (*Glycine max*) during infection with *Phytophthora sojae*. PLoS ONE 10:e0129932.

Kachroo A, Kachroo P (2020) Mobile signals in systemic acquired resistance. Current Opinion in Plant Biology 58:41-47.

Kar M, Miashra D (1976) Catalase, peroxidase and polyphenoloxidase activities during rice leaf senescence. Plant Physiology 57:315-319.

Kashiwa T, Muraki Y, Yamanaka N (2020) Near-isogenic soybean lines carrying Asian soybean rust resistance genes for practical pathogenicity validation. Scientific Reports 10:13270.

Kazan K, Lyons R (2014) Intervention of phytohormone pathways by pathogen effectors. The Plant Cell 26:2285-2309.

Kesel J, Conrath U, Flors V, Luna E, Mageroy MH, Mauch-Mani B, Pastor V, Pozo MJ, Pieterse CMJ, Ton J, Kyndt T (2021) The induced resistance lexicon: do's and don'ts. Trends in Plant Science 26:685-691.

Kim JA, Chung IM (2007) Change in isoflavone concentration of soybean (*Glycine max* L.) seeds at different growth stages. Journal of the Science of Food and Agriculture 87:496-503.

Klosowski AC, Castellar C, Stammler G, May de Mio LL (2018) Fungicide sensitivity and monocyclic parameters related to the *Phakopsora pachyrhizi*-soybean pathosystem from organic and conventional soybean production systems. Plant Pathology 67:1697-1705.

Kramer DM, Johnson G, Kiirats O, Edwards GE (2004) New fluorescence parameters for the determination of Q_A redox state and excitation energy fluxes. Photosynthesis Research 79:209-218.

Langenbach C, Campe R, Beyer SF, Mueller AN, Conrath U (2016) Fighting Asian soybean rust. Frontiers of Plant Science 7:797.

Livak KJ, Schmittgen TD (2001) Analysis of relative gene expression data using real-time quantitative PCR and the $2^{-\Delta\Delta CT}$ method. Methods 25:402-408.

Low PS, Merida JR (1996) The oxidative burst in plant defense: function and signal transduction. Physiologia Plantarum 96:533-542.

Lyon G (2007) Agents that can elicit induced resistance. In: Walters D, Newton A, Lyon G (Eds). Induced resistance for plant defense: A sustainable approach to crop protection. Blackwell Publishing pp. 9-23.

Marino G, Funk C (2012) Matrix metalloproteinases in plants: a brief overview. Physiology Plantarum 145:196-202.

Mauch-Mani B, Baccelli I, Luna E, Flors V (2017) Defense priming: an adaptive part of induced resistance. Annual Review of Plant Biology 68:485-512.

McClure PR, Israel DW (1979) Transport of nitrogen in the xylem of soybean plants. Plant Physiology 64:411-416.

Mejri S, Magnin-Robert M, Randoux B, Ghinet A, Halama P, Siah A, Reignault P (2021) Saccharin provides protection and activates defense mechanisms in wheat against the hemibiotrofic pathogen *Zymoseptoria tritici*. Plant Disease 105:780:786.

Mohammad MA, Cheng Y, Aslam M, Jakada BH, Wai MH, Ye K (2021) ROS and oxidative response systems in plants under biotic and abiotic stresses: revisiting the crucial role of phosphite triggered plants defense response. Frontiers in Microbiology 12:631318.

Moore KJ, Dixon PM (2015) Analysis of combined experiments revisited. Agronomy Journal 107:763-771.

Mortel M, Recknor JC, Graham MA, Nettleton D, Dittman JD, Nelson RT, Godoy CV, Abdelnoor RV, Almeida AMR, Baum TJ, Whitha SA (2007) Distinct biophasic mRNA changes in response to Asian soybean rust infection. Molecular Plant-Microbe Interactions 20:887-899.

Nakano Y, Asada K (1981) Hydrogen peroxide is scavenged by ascorbate specific peroxidase in spinach chloroplasts. Plant and Cell Physiology 22:867-880.

Oxborough K, Baker NR (1997). Resolving chlorophyll *a* fluorescence images of photosynthetic efficiency into photochemical and non-photochemical components - calculation of *qP* and *Fv′*/*Fm′* without measuring *Fo′*. Photosynthesis Research 54:135-142.

Park S (2010) Study of host-fungus interactions between soybean and *Phakopsora pachyrhizi* using proteomics. *Louisiana State University. Doctoral Dissertations* 3217.

Paula S, Dalio RJD, Maximo HJ, Pino LE, Amorim DJ, Paz SMR, Brandão DFR, Demétrio CGB, Pascholati SF (2022) Potential of thaxtomin A for the control of the Asian soybean rust. Canadian Journal of Plant Pathology 44:56-65.

Paula S, Holz S, Souza DHG, Pascholati SF (2021) Potential of resistance inducers for soybean rust management. Canadian Journal of Plant Pathology 43:298-307.

Picanço BBM, Ferreira S, Fontes BA, Oliveira LM, Silva BN, Einhardt AM, Rodrigues FA (2021) Soybean resistance to *Phakopsora pachyrhizi* infection is barely potentiated by boron. Physiological and Molecular Plant Pathology 115:101668.

Pieterse CM, Van der Does D, Zamioudis C, Leon-Reyes A, Van Wees SC (2012) Hormonal modulation of plant immunity. Annual Review of Phytopathology 28:489-521.

Pitzschke A, Forzani C, Hirt H (2006) Reactive oxygen species signaling in plants. Antioxidants & Redox Signaling 8:1757-1764.

Reignault P, Walters D (2007) Topical applications of inducers for disease control. In: Walters D, Newton A, Lyon G (Eds). Induced resistance for plant defense: A sustainable approach to crop protection. Blackwell Publishing, pp.179-200.

Reymond P, Farmer EE (1998) Jasmonate and salicylate as global signals for defense gene expression. Current Opinion in Plant Biology 1:404-411.

Rios JA, Rios VS, Aucique-Pérez CE, Cruz MFA, Morais LE, DaMatta FM, Rodrigues FA (2017) Alteration of photosynthetic performance and source-sink relationships in wheat plants infected by *Pyricularia oryzae*. Plant Pathology 66:1496-1507.

Rios JA, Rodrigues FA, Debona D, Resende RS, Moreira WR, Andrade CCL (2014) Induction of resistance to *Pyricularia oryzae* in wheat by acibenzolar-S-methyl, ethylene and jasmonic acid Tropical Plant Pathology 39:224-233.

Rios VS, Rios JA, Aucique-Pérez CE, Silveira PR, Barros AV, Rodrigues FA (2018) Leaf gas exchange and chlorophyll *a* fluorescence in soybean leaves infected by *Phakopsora pachyrhizi*. Journal of Phytopathology 166:75-85.

Roberts TR (1999) Plant Activators. In: Roberts TR, Hudson DH, Lee PW, Nicholls PH, Plimmer JR (Eds). Metabolic Pathways of Agrochemicals: Insecticides and fungicides. 1st Edition, Royal Society of Chemistry, Cambridge. p. 1453-1462.

Rodrigues FA, Benhamou N, Datnoff LE, Jones JB, Bélanger RR (2003) Ultrastructural and cytochemical aspects of silicon-mediated rice blast resistance. Phytopathology 93:535-546.

Rodrigues FA, Rios JA, Debona D, Aucique-Pérez CE (2017) *Pyricularia oryzae*-wheat interaction: physiological changes and disease management using mineral nutrition and fungicides. Tropical Plant Pathology 42:223-229.

Sánchez-Vallet A, Mesters JR, Thomma BPHJ (2014) The battle for chitin recognition in plant-microbe interactions. FEMS Microbiology Reviews 39:171-183.

Santos IMO, Abe VY, Carvalho K, Barazetti AR, Simionato AS, Pega, GEA, Matis SH, Cano BG, Cely MVT, Marcelino-Guimarães FC, Chryssafidis AL, Andrade G (2021) Secondary metabolites of *Pseudomonas aeruginosa* Iv strain decrease Asian soybean rust severity in experimentally infected plants. *Plants 10*:1495.

Santos RP, Cruz ACF, Iarema L, Kuki KN, Otoni WC (2008) Protocolo para extração de

pigmentos foliares em porta-enxertos de videira micropropagados. Ceres 55:356-364.

Scherm H, Christiano RSC, Esker PD, Del Ponte EM, Godoy CV (2009) Quantitative review of fungicide efficacy trials for managing soybean rust in Brazil. Crop Protection 28:774-782.

Schulman P, Ribeiro THC, Fokar M, Chalfun-Junior A, Lally RD, Paré PW, Medeiros FHV (2021) A microbial fermentation product induces defense-related transcriptional changes and the accumulation of phenolic compounds in *Glycine max.* Phytopathology. In Press.

Shaner G, Finney RE (1977) The effect of nitrogen fertilization on the expression of slow-mildewing resistance in Knox wheat. Phytopathology 67:1051-1056.

Shine MB, Yang JW, El-Habbak M, Nagyabhyru P, Fu DQ, Navarre D, Ghabrial S, Kachroo P, Kachroo A (2016) Cooperative functioning between phenylalanine ammonia lyase and isochorismate synthase activities contributes to salicylic acid biosynthesis in soybean. New Phytologist 212:627-636.

Siah A, Randoux B, Magnin-Robert M, Choma C, Rivière C, Halama P, Reignault P (2018) Natural agents inducing plant resistance against pests and diseases. In: Mérillon JM, Rivière C (Eds). Natural Antimicrobial Agents, Sustainable Development and Biodiversity series. Springer, pp. 121-159.

Silveira PR, Nascimento KJT, Andrade CCL, Bispo WMS, Oliveira JR, Rodrigues FA (2015) Physiological changes in tomato leaves arising from *Xanthomonas gardneri* infection. Physiological and Molecular Plant Pathology 92:130-138.

Slusarenko AJ (1996) The role of lipoxygenase in plant resistance to infection. In: Piazza GJ (Eds). Lipoxygenase and lipoxygenase pathway enzymes. AOCS Press, Champaign, pp. 176-197.

Spoel SH, Dong X (2012) How do plants achieve immunity? Defense without specialized immune cells. Nature Reviews Immunology 12:89-100.

Sterling A, Melgarejo LM (2021) Photosynthetic performance of *Hevea brasiliensis* affected by South American leaf blight under field conditions. European Journal of Plant Pathology 161:953-967.

Tatagiba SD, Rodrigues FA, Filippi MCC, Silva GB, Silva LC (2014) Physiological responses of rice plants supplied with silicon to *Monographella albescens* infection. Journal of Phytopathology 162:596-606.

Vallad GE, Goodman RM (2004) Systemic acquired resistance and induced systemic resistance in conventional agriculture. Crop Science 44:1920-1934.

van Loon LC, Rep M, Pieterse CMJ (2006) Significance of inducible defense-related proteins in infected plants. Annual Review of Phytopathology 44:135-62.

Vlot AC, Sales JH, Lenk M, Bauer K, Brambilla A, Sommer A, Chen Y, Wenig M, Nayem S (2021) Systemic propagation of immunity in plants. New Phytologist 229:1234-1250.

Walters D, Walsh D, Newton A, Lyon G (2005) Induced resistance for plant disease control: maximizing the efficacy of resistance elicitors. Phytopathology 95:1368-1373.

Zeier J (2021) Metabolic regulation of systemic acquired resistance. Current Opinion in Plant Biology 62:102050.

Tables and Figures

Table 1. Primer sequences for the genes phenylalanine ammonia-lyase (*PAL1.1*, *PAL1.3*, *PAL2.1*, and *PAL3.1*), chitinase (*CHIA1*), chalcone isomerase (*CHI1B1*), lipoxygenase (*LOX7*), pathogenesis-related protein 1 (*PR1-A*), pathogenesis-related protein 10 (*PR10*), metalloproteinase (*MMP2*), urease (*URE*), isochorismate synthase (*ICS1* and *ICS2*), jasmonic acid-amino synthetase (*JAR1*), ubiquitin-3(*UBIQ*), glyceraldehyde-3-phosphate dehydrogenase (*GAPDH*), and the translation elongation factor 1α of *Phakopsora pachyrhizi* (*TEF-1α*).

Genes	GenBank Identifications	Primer Sense 5'-3'	Primer Antisense 5'-3'
PAL1.1	Glyma 19G182300	GCAAGTGCAACCATAATCATTT	AACCAAAGCTCCGGCAAA
PAL1.3	Glyma 03g181600	TTTGTACCTATGCAAGAAAAACCA	TGAAGGAACATTGAAATTAGGCT
PAL2.1	Glyma 10G058200	ATCTCCCTCCACTCACCATA	GTTCAAGGGGTCATTAGCAC
PAL3.1	Glyma 02G309300	TGCTCTTCAGAAGGAAATGGT	GTTGCTGATTTAGGCAGTGT
CHIA1	Glyma 02G0425001	TTCTTGGCTCAAACTTCTCATGAA	CCCACGCATATGGACCATCT
LOX7	Glyma 13G347800	ACAAGCTAGGCACAACAAAA	TTGTTTCCTCCGATGATTCCAA
PR1-A	AF 136636.1	GCACTACACACAGGTCGTTTGG	CCTCCGTTATCACATGTCACTTTG
PR10	Glyma 09G040500	AAATCAACTCCCCTGTGGCTC	CCACCATTTCCCTCAACGTTT
MMP2	Glyma 01G0369001	TGGGCTCTTCCCAGTGAAA	TTGCCGCACTCTCCAAGTC
URE	Glyma 11g248700	AGTTAGTCACCATTCATGACCT	CAAGTGAAGGTACTGGAAGAAAA
ICS1	Glyma 01G104100	GAAACAGTACAGTCCCTGCT	TGTGGCTGGGAAAAGAAAAC
ICS2	Glyma 03G070600	GCAACATCCTCGTACCTCTT	CTCTCTGCAACCGTTCATTG
CHIB1	Glyma 20G2416001	GTTTCCCCTGCTTTGAAAGAGA	GGATTGGCCTCTAACTCTTTGAAG
JAR1	LOC 100813492	AGCCGTATGGTTGTGTTGTTC	TGCAGCATTGGGATTGGAGT
UBIQ	Glyma 20g141600	GTGTAATGTTGGATGTGTTCCC	ACACAATTGAGTTCAACACAAACCG
GAPDH	Glyma 04G193500	AAGGGTGGTGCAAAGAAGGT	TCTGGCTTGTACTCGTGCTC
TEF-1α	EF 560586.1	ATTCGAAGCCGGTATTTCTAAAG	CCACTTGGTTGTGTCCATCTTAT

Table 2. Analysis of variance for the effects of products (P), plant inoculation (PI), and the P × PI interaction on urediniospores germination (UG), area under disease progress curve (AUDPC), severity, parameters of leaf gas exchange (net CO_2 assimilation rate (*A*), stomatal conductance to water vapor (g_s), internal CO_2 concentration (C_i), and transpiration rate (*E*)) and chlorophyll *a* fluorescence (maximum PSII quantum efficiency (F_v/F_m), photochemical yield (Y(II)), yield for dissipation by down-regulation (Y(NPQ)), yield for non-regulated dissipation (Y(NO)), and electron transport rate (ETR)), concentrations of chlorophyll *a*+*b* (Chl *a*+*b*) and carotenoids (Car), activities of antioxidant enzymes (superoxide dismutase (SOD), peroxidase (POX), catalase (CAT), ascorbate peroxidase (APX), and glutathione reductase (GR)), concentrations of total soluble phenolics (TSP) and lignin-thioglycolic acid (LTGA) derivatives as well as on gene expression phenylalanine ammonia-lyase (*PAL1.1*, *PAL1.3*, *PAL2.1*, and *PAL3.1*), chitinase (*CHIA1*), chalcone isomerase (*CHI1B1*), lipoxygenase (*LOX7*), pathogenesis-related protein 1 (*PR1-A*), pathogenesis-related protein 10 (*PR10*), metalloproteinase (*MMP2*), urease (*URE*), isochorismate synthase (*ICS1* and *ICS2*), and jasmonic acid-amino synthetase (*JAR1*).

Variables/Parameters	P	PI	P × PI
UG	**<0.001**	-	-
AUDPC	**0.027**	-	-
Severity	**0.001**	-	-
A	**0.050**	**<0.001**	**0.002**
g_s	0.122	**<0.001**	**0.018**
C_i	0.364	0.059	0.280
E	**0.018**	**<0.001**	**0.001**
F_v/F_m	0.187	0.262	0.421
Y(II)	**<0.001**	**<0.001**	**0.001**
Y(NPQ)	0.428	0.254	**<0.001**
Y(NO)	0.115	0.507	**0.043**
ETR	**0.009**	**0.010**	**0.030**
Chl *a*+*b*	**0.005**	**<0.001**	**0.003**
Car	0.065	**<0.001**	0.125
SOD	**0.029**	**0.001**	**0.024**
POX	0.534	**<0.001**	**0.038**

CAT	0.355	0.317	0.107
APX	0.114	**0.003**	0.394
GR	**0.003**	0.877	0.332
TSP	0.911	**0.028**	0.817
LTGA derivatives	0.653	**<0.001**	0.318
PAL1.1	0.992	**<0.001**	0.887
PAL1.3	0.080	0.094	0.195
PAL2.1	0.239	0.508	0.183
PAL3.1	0.215	**<0.001**	0.561
CHIA	0.273	**<0.001**	0.906
CHIB1	0.394	0.269	0.146
LOX7	0.120	**0.019**	0.592
PR1-A	0.714	**0.028**	0.534
PR10	0.917	0.239	0.939
MMP2	0.343	**<0.001**	0.328
URE	0.801	**0.026**	0.741
ICS1	0.218	0.319	0.093
ICS2	0.084	**0.019**	0.212
JAR1	0.507	0.796	0.771

Bold values are significant at $P \leq 0.05$.

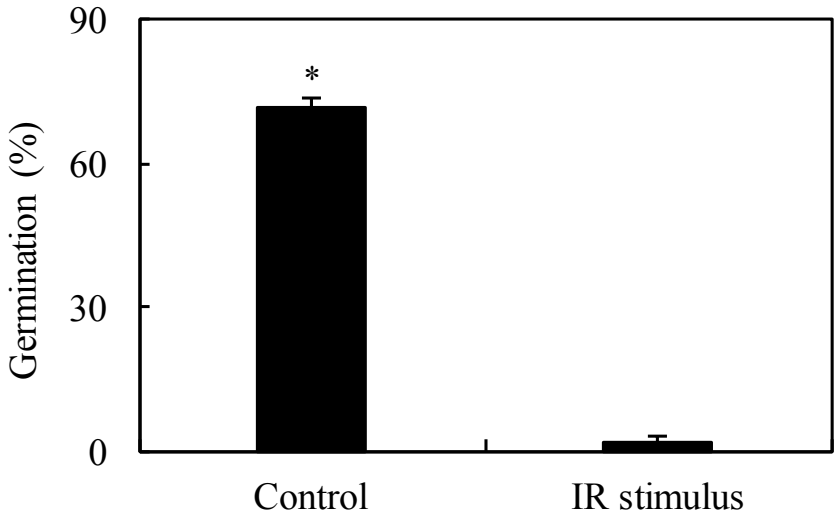

Figure 1. Urediniospores germination of *Phakopsora pachyrhizi* in Petri dishes containing water-agar medium non-amended (control) or amended with induced resistance (IR) stimulus. The asterisk (*) indicates a significant difference between treatments according to the *F* test ($P \leq 0.05$). Bars represent the standard error of the means.

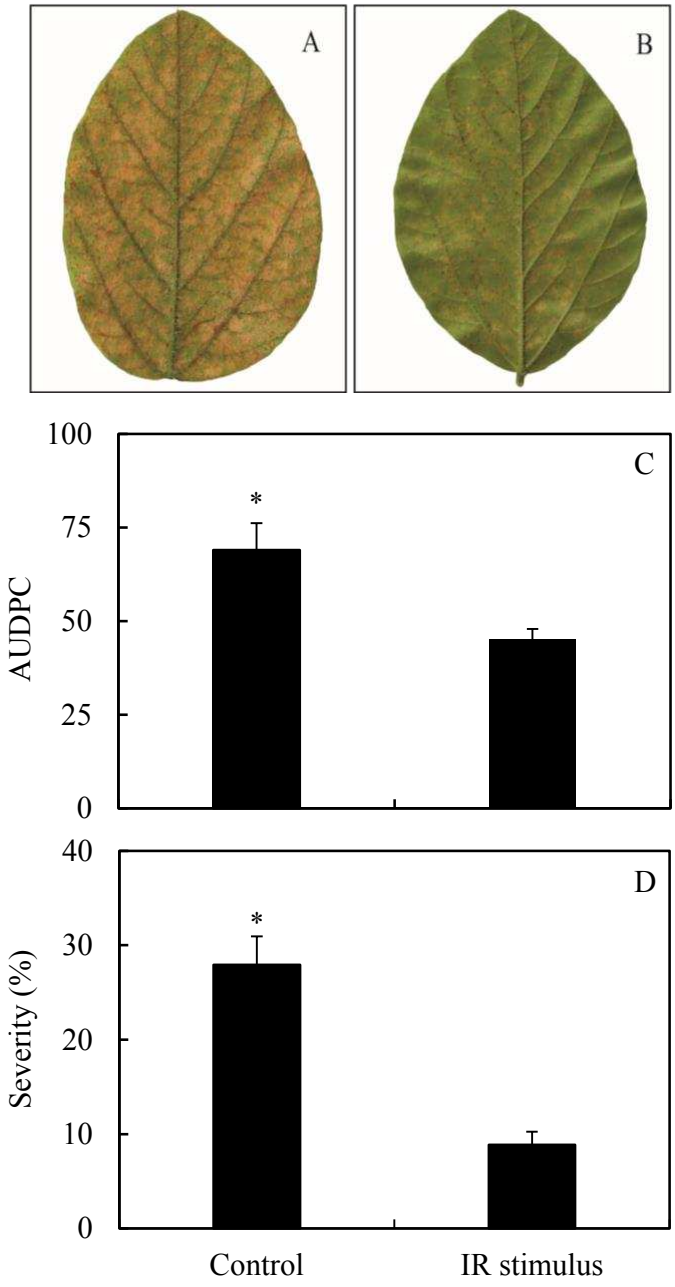

Figure 2. Symptoms (chlorosis and necrosis) of Asian soybean rust and sporulation of *Phakopsora pachyrhizi* in the abaxial surface of leaflets from soybean plants sprayed with water (control) (A) or with induced resistance (IR) stimulus (B). Area under disease progress curve (AUDPC) (C) and severity of Asian soybean rust (D) for soybean plants sprayed with water (control) or with induced resistance (IR) stimulus. The asterisk (*) (C and D) indicates a significant difference between treatments according to the *F* test ($P \leq 0.05$). Bars represent the standard error of the means.

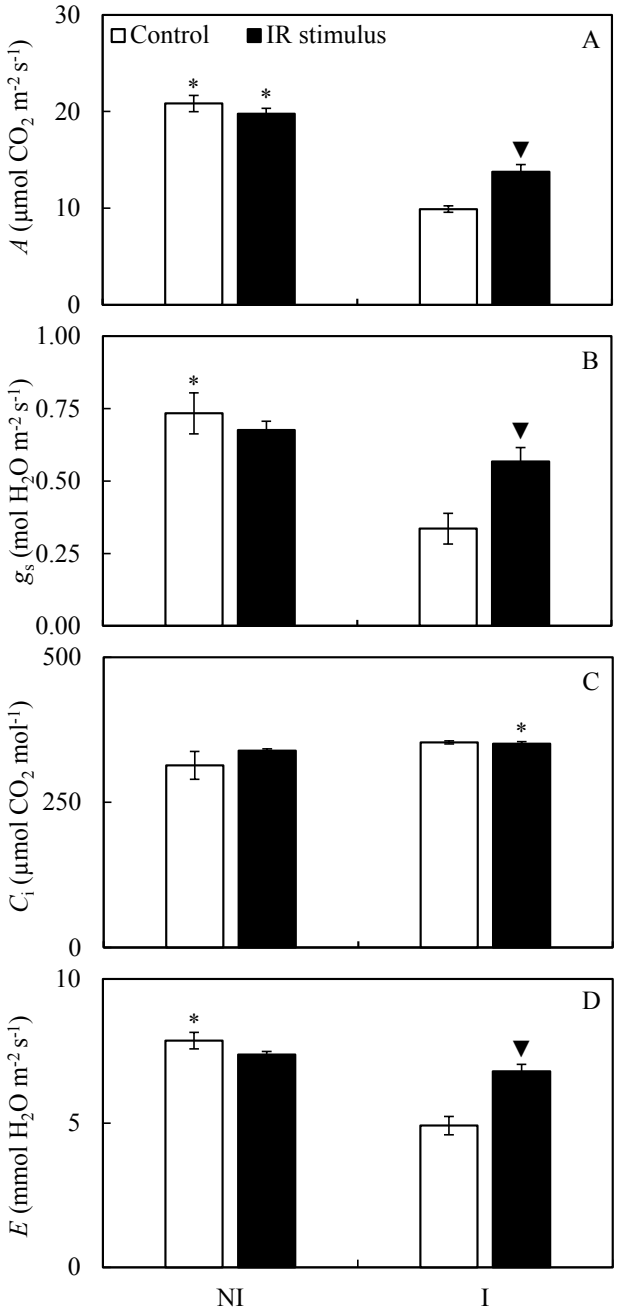

Figure 3. Leaf gas exchange parameters net CO_2 assimilation rate (A) (A), stomatal conductance to water vapor (g_s) (B), internal CO_2 concentration (C_i) (C), and transpiration rate (E) (D) determined on the leaflets of soybean plants non-inoculated (NI) or inoculated (I) with *Phakopsora pachyrhizi* and sprayed with water (control) or with induced resistance (IR) stimulus. Means for NI and I treatments followed by an asterisk (*) and for control and IR stimulus treatments followed by an inverted triangle (▼) are significantly different according to the F test ($P \leq 0.05$). Bars represent the standard deviation of the means. Data shown are from 10 days after non-inoculation or inoculation of plants with *P. pachyrhizi*.

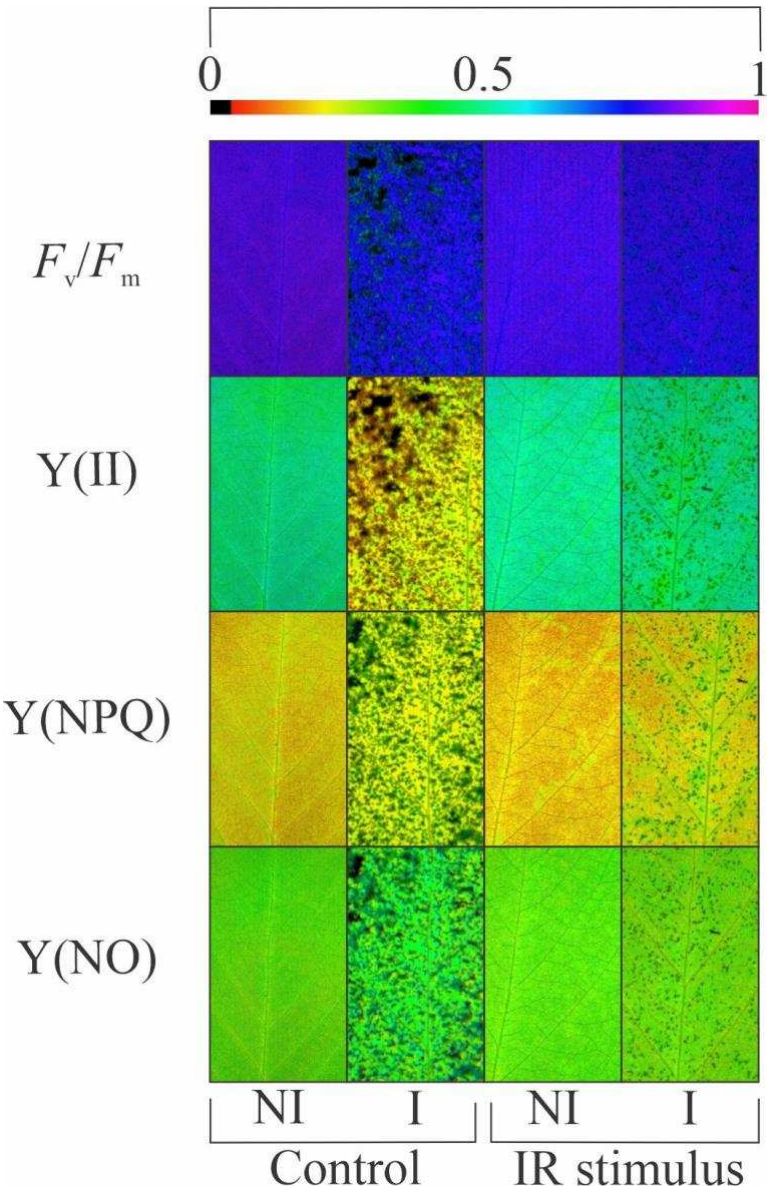

Figure 4. Images of chlorophyll *a* fluorescence parameters: maximum PSII quantum efficiency (F_v/F_m), photochemical yield (Y(II)), yield for dissipation by down-regulation (Y(NPQ)), and yield for non-regulated dissipation (Y(NO)) obtained from leaflets of soybean plants sprayed with water (control) or with induced resistance (IR) stimulus and non-inoculated (NI) or at 10 days after inoculation (I) with *Phakopsora pachyrhizi*.

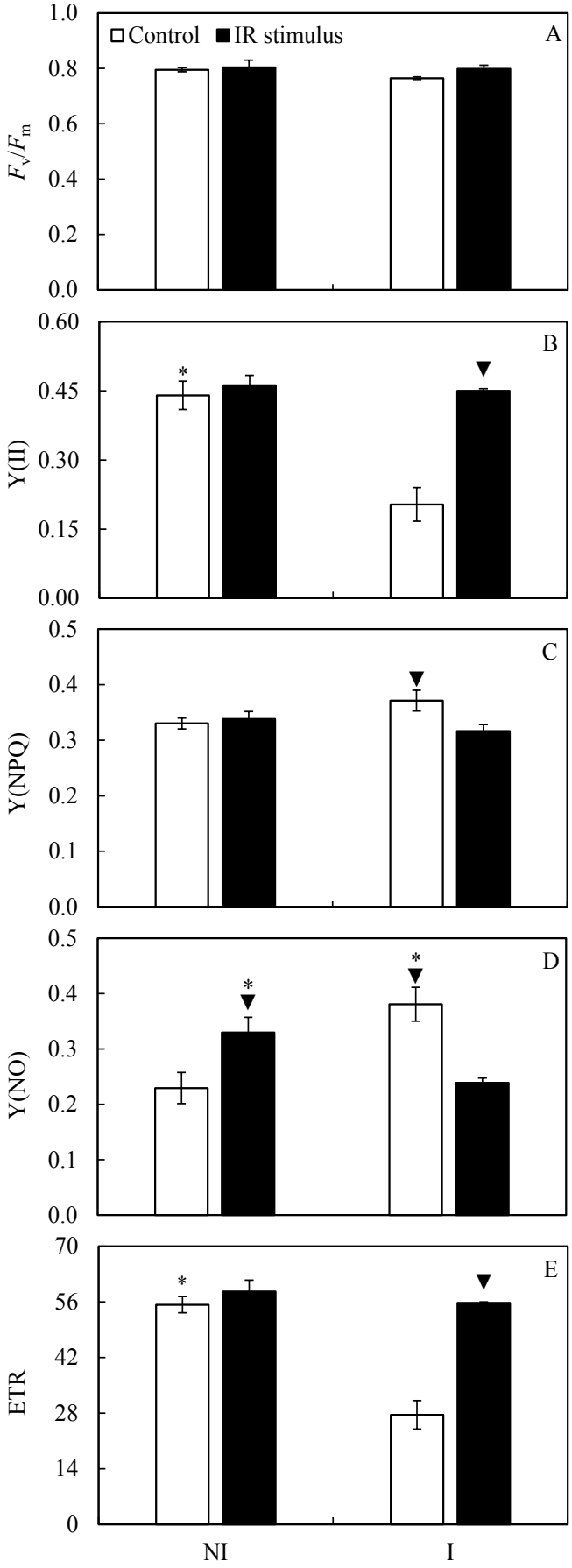
Control
IR stimulus
A
B
C
D
E
F_v/F_m
Y(II)
Y(NPQ)
Y(NO)
ETR
1.0
0.8
0.6
0.4
0.2
0.0
0.60
0.45
0.30
0.15
0.00
0.5
0.4
0.3
0.2
0.1
0.0
70
56
42
28
14
0
*
NI
I

Figure 5. Quantification of chlorophyll *a* fluorescence parameters maximum PSII quantum efficiency (F_v/F_m) (A), photochemical yield (Y(II)) (B), yield for dissipation by down-regulation (Y(NPQ)) (C), yield for non-regulated dissipation (Y(NO)) (D), and electron transport rate (ERT) (E) on the leaflets of soybean plants non-inoculated (NI) or inoculated (I) with *Phakopsora pachyrhizi* and sprayed with water (control) or with induced resistance (IR) stimulus. Means for NI and I treatments followed by an asterisk (*) and for control and IR stimulus treatments followed by an inverted triangle (▼) are significantly different according to the *F* test ($P \leq 0.05$). Bars represent the standard deviation of the means. Data shown are from 10 days after non-inoculation or inoculation of plants with *P. pachyrhizi*.

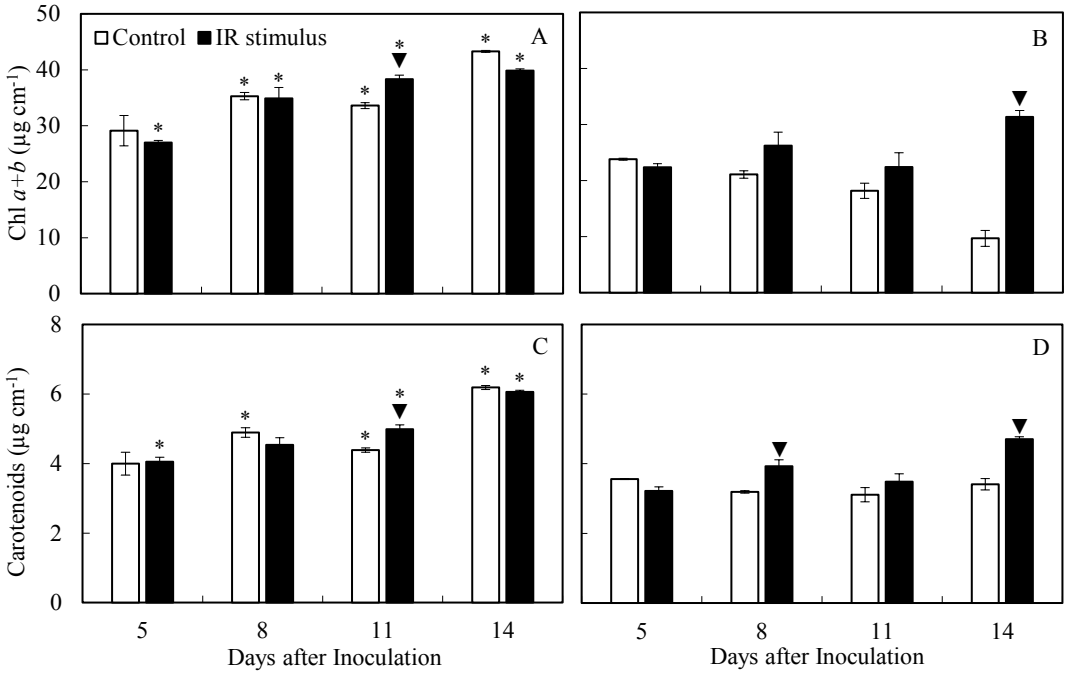

Figure 6. Concentrations of chlorophyll *a*+*b* (Chl *a*+*b*) (A and B) and carotenoids (C and D) determined on the leaflets of soybean plants non-inoculated (A and C) or inoculated (B and D) with *Phakopsora pachyrhizi* and sprayed with water (control) or with induced resistance (IR) stimulus. Means for NI and I treatments followed by an asterisk (*) and for control and IR stimulus treatments followed by an inverted triangle (▼), at each sampling time, are significantly different according to the *F* test ($P \leq 0.05$). Bars represent the standard deviation of the means.

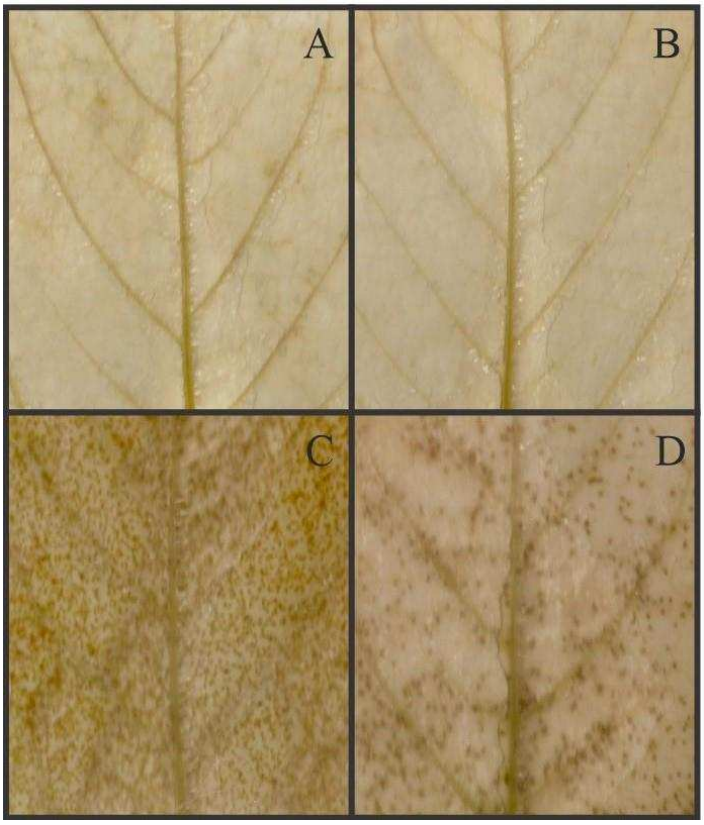

Figure 7. Histochemical detection of hydrogen peroxide on the leaflets of soybean plants non-inoculated (A and B) or inoculated (C and D) with *Phakopsora pachyrhizi* and sprayed with water (control) (A and C) or with induced resistance (IR) stimulus (B and D). The leaflets were sampled 15 days after non-inoculation or inoculation of plants with *P. pachyrhizi*.

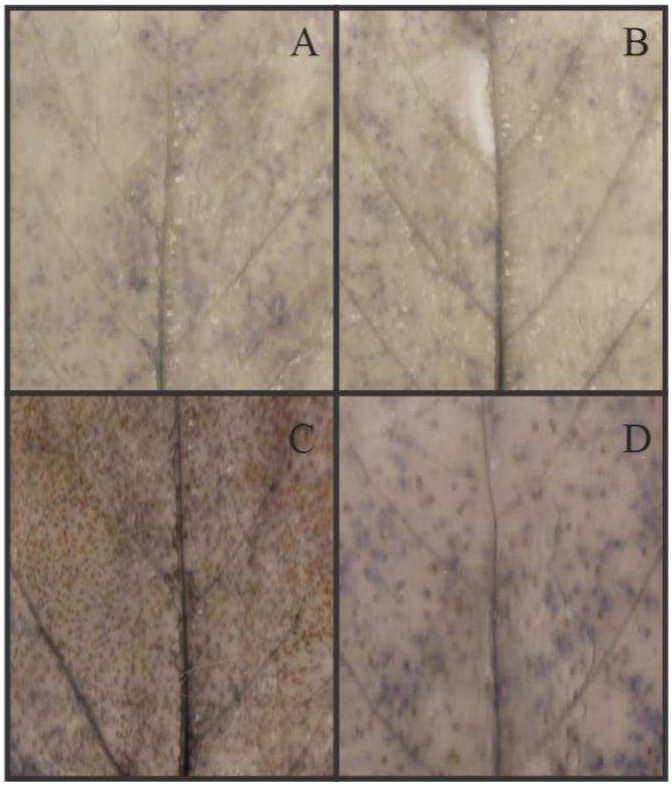

Figure 8. Histochemical detection of superoxide anion radical on the leaflets of soybean plants non-inoculated (A and B) or inoculated (C and D) with *Phakopsora pachyrhizi* and sprayed with water (control) (A and C) or with induced resistance (IR) stimulus (B and D). The leaflets were sampled 15 days after non-inoculation or inoculation of plants with *P. pachyrhizi*.

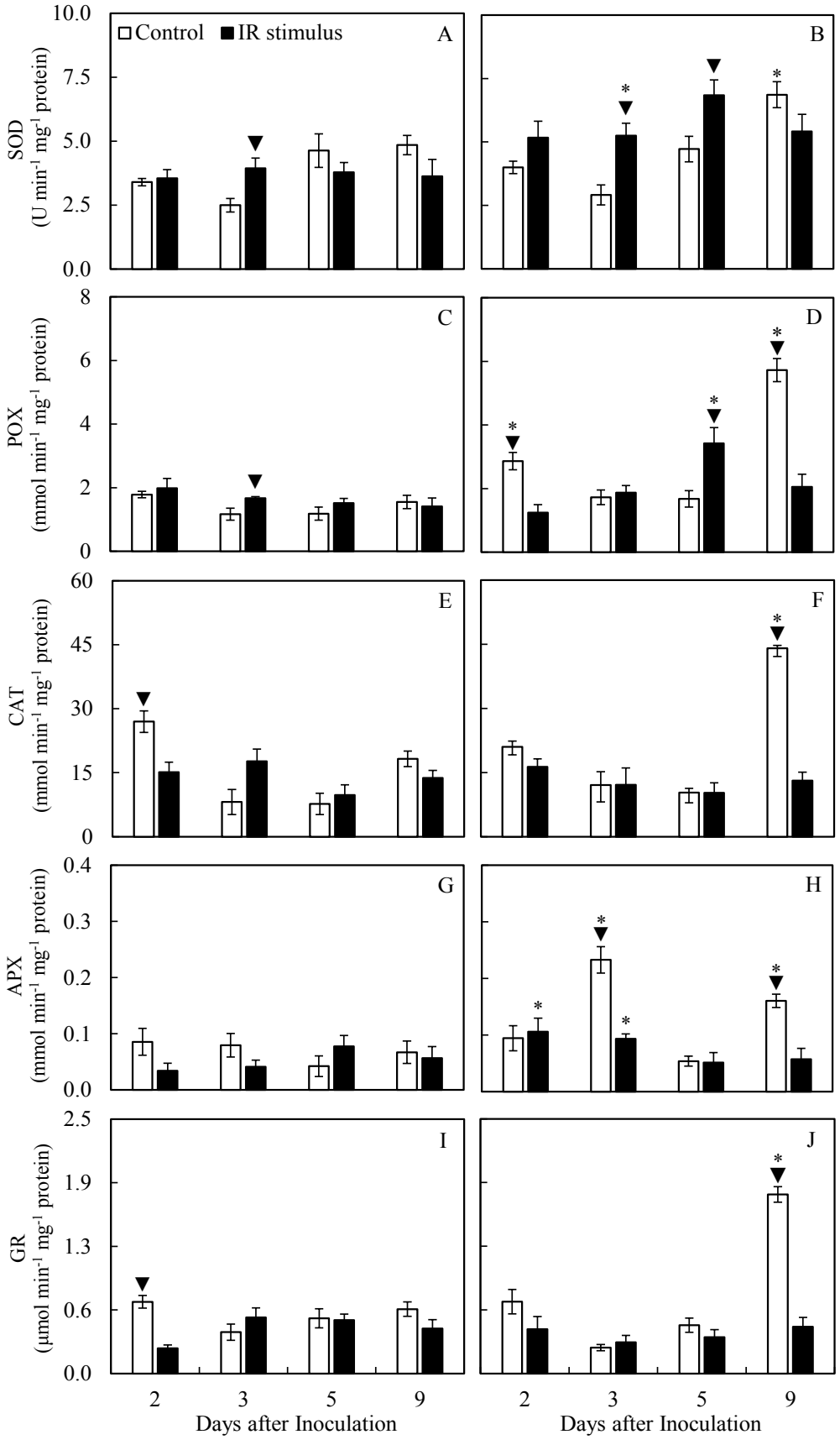
Control
IR stimulus
A
B
C
D
E
F
G
H
I
J
SOD (U min-1 mg-1 protein)
POX (mmol min-1 mg-1 protein)
CAT (mmol min-1 mg-1 protein)
APX (mmol min-1 mg-1 protein)
GR (μmol min-1 mg-1 protein)
10.0
7.5
5.0
2.5
0.0
8
6
4
2
0
60
45
30
15
0
0.4
0.3
0.2
0.1
0.0
2.5
1.9
1.3
0.6
0.0
2
3
5
9
Days after Inoculation
Days after Inoculation

Figure 9. Activities of superoxide dismutase (SOD) (A and B), peroxidase (POX) (C and D), catalase (CAT) (E and F), ascorbate peroxidase (APX) (G and H), and glutathione reductase (GR) (I and J) determined on the leaflets of soybean plants non-inoculated (A, C, E, G, and I) or inoculated (B, D, F, H, and J) with *Phakopsora pachyrhizi* and sprayed with water (control) or with induced resistance (IR) stimulus. Means for NI and I treatments followed by an asterisk (*) and for control and IR stimulus treatments followed by an inverted triangle (▼), at each sampling time, are significantly different according to the *F* test ($P \leq 0.05$). Bars represent the standard deviation of the means.

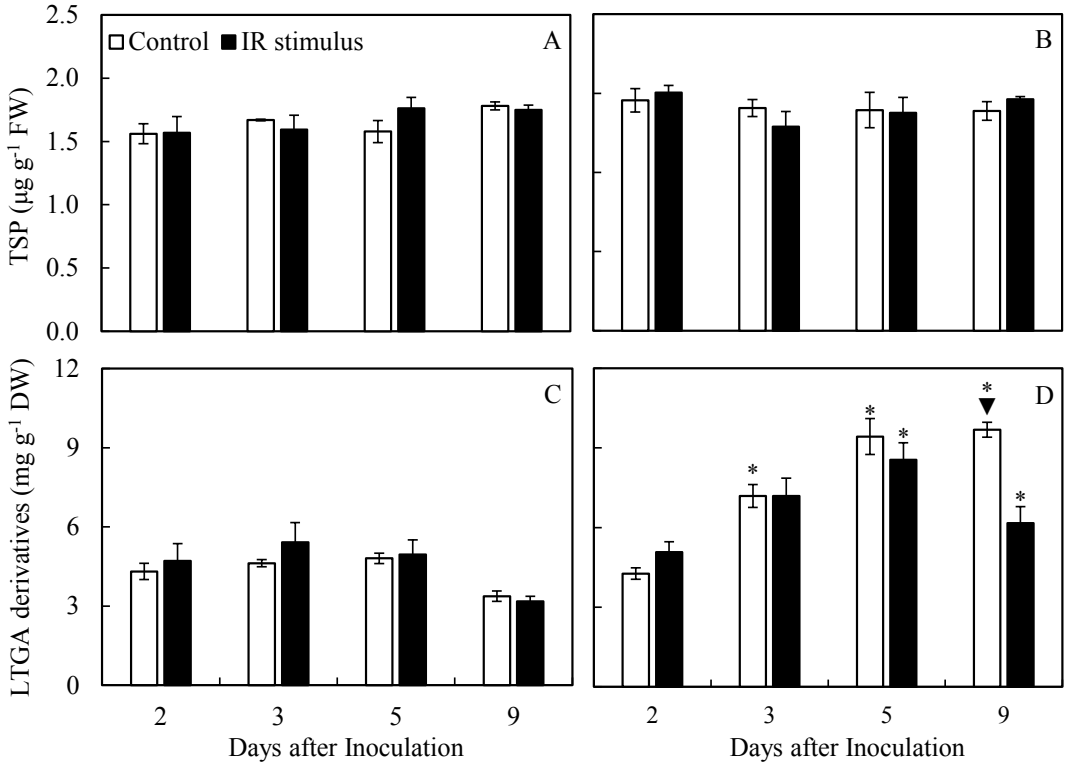

Figure 10. Concentrations of total soluble phenolics (TSP) (A and B) and lignin-thioglycolic acid (LTGA) derivatives (C and D) determined on the leaflets of soybean plants non-inoculated (A and C) or inoculated (B and D) with *Phakopsora pachyrhizi* and sprayed with water (control) or with induced resistance (IR) stimulus. Means for NI and I treatments followed by an asterisk (*) and for control and IR stimulus treatments followed by an inverted triangle (▼), at each sampling time, are significantly different according to the *F* test ($P \leq 0.05$). Bars represent the standard deviation of the means. FW and DW = fresh and dry weight, respectively.

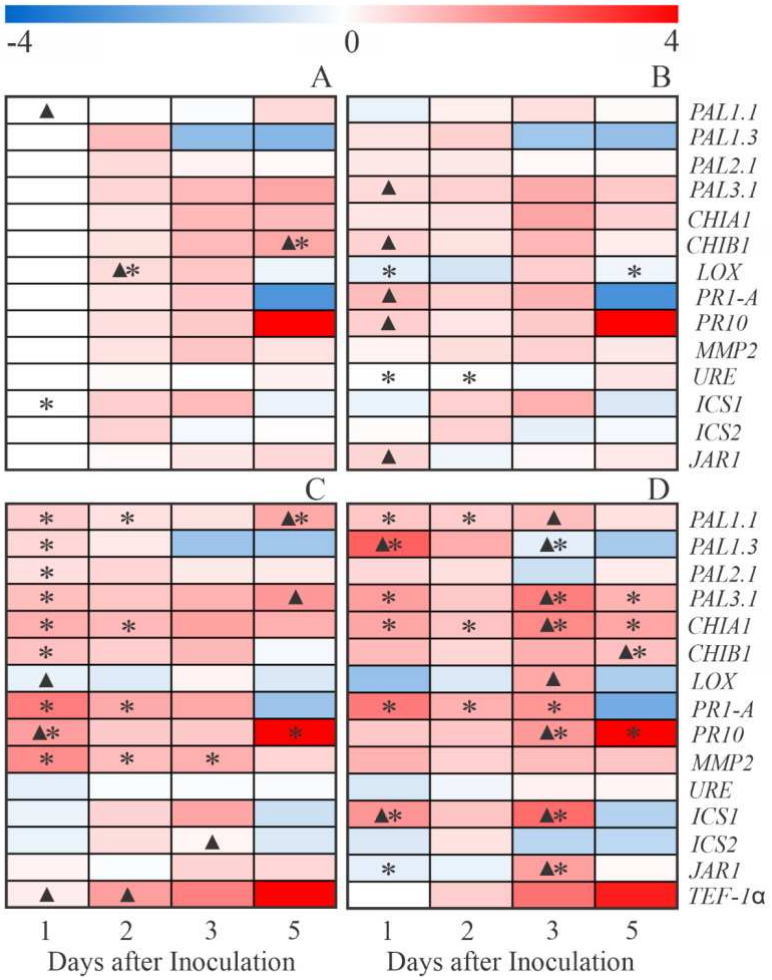

Figure 11. Expression profile of genes determined in leaflets of soybean plants non-inoculated (NI) (A and B) or inoculated (I) (C and D) with *Phakopsora pachyrhizi* and sprayed with water (control) (A and C) or with induced resistance (IR) stimulus (B and D). Color cells ranging from blue (-4.0) to red (4.0) represent the relative transcript levels for the genes studied. Amplifications of Ubiquitin-3 (*UBIQ*) and glyceraldehyde 3-phosphate dehydrogenase (*GAPDH*) genes from soybean were used as internal controls for data normalization. Fold changes were calculated based on the transcript level for NI plants of the control treatment at 1 day after inoculation (dai). For each leaf sample, four biological replications were used with their respective two technical replicates. Means for NI and I plants for control and IR stimulus treatments, at each evaluation time, followed by an asterisk (*) are significantly different ($P \leq 0.05$) according to the *F* test. A triangle (▲) indicates a significant difference between control and IR stimulus treatments for NI and I plants, at each evaluation time, according to the *F* test ($P \leq 0.05$).

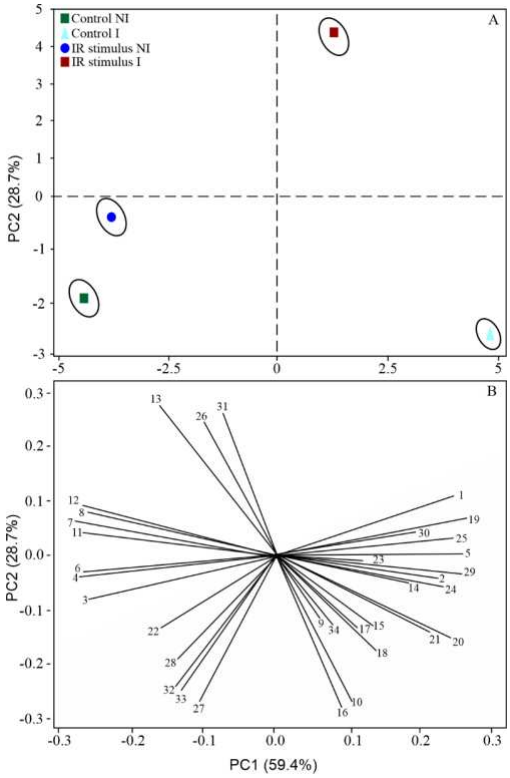

Figure 12. Score plots (a) and loading (b) values in the principal component analysis (PCA) for variables and parameters evaluated in soybean plants non-inoculated (NI) or inoculated (I) with *Phakopsora pachyrhizi* and sprayed with water (control) or with induced resistance (IR) stimulus. Numbers in the loading plot (b) are as follow: severity (1), area under disease progress curve (2), leaf gas exchange parameters (3, 4, 5, and 6, respectively, to net CO_2 assimilation rate, stomatal conductance to water vapor, internal CO_2 concentration, and transpiration rate), chlorophyll *a* fluorescence parameters (7, 8, 9, 10, and 11, respectively, to maximum PSII quantum yield, effective PSII quantum yield, quantum yield of regulated energy dissipation, quantum yield of non-regulated energy dissipation, and electron transport rate), photosynthetic pigments (12 and 13, respectively, to chlorophyll *a*+*b* and carotenoids), activities of antioxidant enzymes (14, 15, 16, 17, and 18, respectively, to superoxide dismutase, peroxidase, catalase, ascorbate peroxidase, and glutathione reductase), total soluble phenolics (19), lignin-thioglycolic acid derivatives (20), and genes expression (21, 22, 23, 24, 25, 26, 27, 28, 29, 30, 31, 32, 33, and 34, respectively, to *PAL1.1*, *PAL1.3*, *PAL2.1*, *PAL3.1*, *CHIA1*, *CHI1B1*, *LOX*, *PR1-A*, *PR10*, *MMP2*, *URE*, *ICS1*, *ICS2*, and *JAR1*). Groups were generated from cluster analysis with complete linkage and Pearson distance. Data from variables and parameters used in the PCA analysis were obtained for NI and I plants at 10 days.